

2010

Equilibrium pricing in electricity markets with wind power

Ofir David Rubin
Iowa State University

Follow this and additional works at: <https://lib.dr.iastate.edu/etd>

 Part of the [Economics Commons](#)

Recommended Citation

Rubin, Ofir David, "Equilibrium pricing in electricity markets with wind power" (2010). *Graduate Theses and Dissertations*. 11323.
<https://lib.dr.iastate.edu/etd/11323>

This Dissertation is brought to you for free and open access by the Iowa State University Capstones, Theses and Dissertations at Iowa State University Digital Repository. It has been accepted for inclusion in Graduate Theses and Dissertations by an authorized administrator of Iowa State University Digital Repository. For more information, please contact digirep@iastate.edu.

Equilibrium pricing in electricity markets with wind power

by

Ofir David Rubin

A dissertation submitted to the graduate faculty
in partial fulfillment of the requirements for the degree of

DOCTOR OF PHILOSOPHY

Major: Agricultural Economics

Program of Study Committee:
Bruce A. Babcock, Major Professor
Dermot J. Hayes
Catherine L. Kling
Sergio H. Lence
James D. McCalley

Iowa State University

Ames, Iowa

2010

Copyright© Ofir David Rubin, 2010. All rights reserved.

Table of contents

| | |
|--|-------------|
| List of tables..... | vii |
| List of figures..... | viii |
| Acknowledgements | xi |
| Abstract..... | xii |
| Chapter 1: Introduction and literature review | 1 |
| Problem statement | 1 |
| Liberalized electricity markets | 2 |
| Wholesale electricity markets | 4 |
| Modeling electricity prices..... | 5 |
| Stochastic approach..... | 6 |
| Diffusion models | 6 |
| Time series models | 8 |
| Fundamental approach | 9 |
| Engineering based models | 9 |
| Equilibrium price models | 10 |
| Modeling oligopoly equilibrium..... | 12 |
| Electricity derivatives..... | 15 |

| | |
|---|-----------|
| Risk management | 16 |
| Electricity from renewable resources | 20 |
| Integrating wind power | 21 |
| Wind forecasting | 23 |
| Previous work and the contribution of this study..... | 26 |
| Organization of this dissertation | 29 |
| Chapter 2: An electricity market model | 31 |
| Characteristics of a desired model | 31 |
| A model developed for this work..... | 31 |
| Load forecasting | 33 |
| Power generation | 35 |
| Spot power and firm entry | 39 |
| Spot market..... | 40 |
| Load Serving Entities and electricity demand..... | 43 |
| Independent Power Producers and electricity supply..... | 48 |
| Solving the model..... | 51 |
| Preliminary results and discussion | 53 |
| Capacity withholding constraint..... | 55 |
| Computational experiments..... | 58 |
| Spot price distribution | 58 |
| Load uncertainty | 60 |

| | |
|--|-----------|
| The number of IPPs and LSEs..... | 63 |
| Cost of generating power..... | 66 |
| Capacity withholding constraint..... | 67 |
| Chapter summary | 68 |
| Chapter 3: Wind power..... | 70 |
| Introduction..... | 70 |
| Overview | 70 |
| Wind speed..... | 74 |
| Wind power density | 83 |
| Usable wind power..... | 85 |
| Regional wind power supply..... | 90 |
| Wind spatial correlation..... | 91 |
| Introduction to a wind-integrated electricity market..... | 95 |
| Chapter 4: Theoretical framework for modeling wind-integrated electricity markets . | 98 |
| Introduction..... | 98 |
| Setup..... | 99 |
| Cournot wind capacity | 101 |
| Fringe wind capacity..... | 111 |
| Chapter summary | 115 |

| | |
|---|------------|
| Chapter 5: A numerical method for simulating the conditional distribution of regional wind power output for modeling trade of short-term electricity forwards..... | 117 |
| Introduction | 117 |
| Simulating wind speed forecasts at one location | 118 |
| Simulating wind power forecasts at one location..... | 120 |
| Simulating wind power forecast errors at one location..... | 120 |
| Calibration and verification | 121 |
| An example of wind power simulation at one location | 122 |
| Aggregate regional wind power output..... | 129 |
| An example of simulating spatially correlated wind | 133 |
| Chapter summary | 141 |
| Chapter 6: Modeling equilibrium in wind-integrated electricity markets | 143 |
| Introduction | 143 |
| Simulation setup..... | 144 |
| Results | 149 |
| Ownership of wind power capacity, generation costs and welfare distribution..... | 156 |
| Chapter summary | 164 |
| Chapter 7: General conclusions..... | 166 |
| Future research | 169 |

| | |
|---|------------|
| Appendix..... | 172 |
| Appendix 1: Contract For Differences | 172 |
| Appendix 2: SOC for the IPPs problem | 175 |
| Appendix 3: Wind turbine used in this study | 178 |
| References | 180 |

List of tables

| | |
|---|-----|
| Table 1: Wind speed classification | 78 |
| Table 2: Estimated July wind speed parameters and moments at selected sites in Iowa, U.S. | 80 |
| Table 3: Estimated monthly wind speed parameters and moments at Osceola County, IA at 50m | 83 |
| Table 4: Moments and parameters of the numerical marginal pdfs of wind speed and wind speed forecast..... | 123 |
| Table 5: Wind speed forecasts: target correlation (top) simulated correlation of wind speed forecast (center) and simulated correlation of wind speed realization (bottom) | 136 |
| Table 6: Simulated wind power correlation; forecasts (top) and realizations (bottom) | 137 |
| Table 7: Wind turbine technical data | 178 |

List of figures

| | |
|---|----|
| Figure 1: U.S. overall wind power capacity | 21 |
| Figure 2: Spot market price densities by expected electricity demand..... | 59 |
| Figure 3: Aggregate demand for electricity forwards as a function of standard deviation of load..... | 60 |
| Figure 4: Equilibrium in the forwards market and the consequence real-time supply curve. Results by standard deviation of load of sizes 5, 15, 25 and 35 are depicted in figures 4a, 4b, 4c and 4d respectively..... | 62 |
| Figure 5: Forward premiums as a function of standard deviation of load | 63 |
| Figure 6: Equilibrium electricity forwards and premiums by number of IPPs in the market (base-case scenario assumptions) | 64 |
| Figure 7: Equilibrium electricity forwards and premium by number of LSEs in the market (base-case scenario assumptions) | 65 |
| Figure 8: Premiums as a function of real-time cost parameter and the number of IPPs..... | 66 |
| Figure 9: Equilibrium forward price and IPPs expected profits by a capacity withholding constraint..... | 68 |
| Figure 10: Illustration of a Weibull pdf with relation to other distributions | 76 |
| Figure 11: Hourly load in 2007 at the Electric Reliability Council of Texas (ERCOT) and the Southwest Power Pool (SPP) which includes the transmissions to Arkansas, Kansas, Louisiana, Missouri, New Mexico, Oklahoma and Texas..... | 79 |

| | |
|---|-----|
| Figure 12: Fitted Weibull pdfs for July wind speed distributions at 50m height for sites at Allamakee and Osceola counties, IA | 82 |
| Figure 13: Month to month mean power density at 50m for Osceola County, IA | 85 |
| Figure 14: Illustration of July and April wind speed distributions at Osceola County, IA and a power curve of a typical modern 1.5 MW wind turbine..... | 88 |
| Figure 15: Monthly numerical capacity factors of a 1.5MW wind turbine sited at Osceola County, IA (disregarding loss factor). | 90 |
| Figure 16: Empirical spatial correlation function of wind speed in Ireland. Source: Haslett and Raftery (1989) | 92 |
| Figure 17: Fitted cross correlation functions of wind power output, various studies..... | 94 |
| Figure 18: Variance of the conditional wind speed in the experiment | 122 |
| Figure 19: Numerical marginal pdf of wind speed forecast (top) and wind speed (bottom)..... | 123 |
| Figure 20: Conditional wind speed, the associated conditional wind power distributions and the distributions of wind power forecasting error given wind speed forecasts of 2, 5, 8, 12, 16 and 25 m/s | 128 |
| Figure 21: The unconditional distribution of wind power forecasting error at one location (kW) | 129 |
| Figure 22: Wind spatial correlation in the experiment | 134 |
| Figure 23: Marginal pdfs of wind power forecast; no correlation (left), some correlation (center) and full correlation (right) | 141 |
| Figure 24: Conditional pdf of wind power, imposing some correlation; low (left), intermediate (center) and high wind power forecasts (right)..... | 141 |

| | |
|---|-----|
| Figure 25: Fitted annual hourly wind speed pdf in Zearing, IA and the power curve of a 1.5 MW turbine employed in the experiment | 148 |
| Figure 26: Forecasted wind power penetration rate and the share of forwards of expected load; full correlation (top) some correlation (middle) and zero correlation (bottom) | 151 |
| Figure 27: Forecasted wind power penetration rate and expected spot price; full correlation (top) some correlation (middle) and zero correlation (bottom) | 152 |
| Figure 28: Forecasted wind power penetration rate and expected forward premium; full correlation (top) some correlation (middle) and zero correlation (bottom)..... | 153 |
| Figure 29: Ratio between total short-run generation costs in the Cournot capacity case and fringe capacity case; full correlation (top) some correlation (middle) and zero correlation (bottom)..... | 160 |
| Figure 30: Ratio between IPPs' profits from non-wind power generation units in the Cournot capacity case and fringe capacity case; full correlation (top) some correlation (middle) and zero correlation (bottom) | 161 |
| Figure 31: Ratio between total short-run generation costs in the Cournot capacity case and fringe capacity case, $\alpha s = 3$; full correlation (top) some correlation (middle) and zero correlation (bottom) | 162 |
| Figure 32: Ratio between IPPs' profits from non-wind power generation units in the Cournot capacity case and fringe capacity case, $\alpha s = 3$; full correlation (top) some correlation (middle) and zero correlation (bottom)..... | 163 |
| Figure 33: The two-settlement process in the case of over-trading forward contracts..... | 174 |
| Figure 34: Fitted power curve of a 1.5MW wind turbine to be used in this study | 179 |

Acknowledgements

I would like to take this opportunity to express my thanks to those who helped me with various aspects of conducting research and writing of this dissertation. First and foremost, I would like to express my deepest gratitude and appreciation to Dr. Bruce Babcock, my major professor for his guidance, commitment and support throughout my graduate studies at Iowa State University. I also would like to thank my committee members Dr. Dermot Hayes, Dr. Catherine Kling, Dr. Sergio Lence and Dr. James McCalley for their valuable insights and comments. Special thanks go to Dr. Harvey Lapan and Dr. Oscar Volij for their helpful advices and friendships.

Finally, I am thankful to my family: My parents, Sandy and Asher, my brothers, Aviad and Amir, and my two children, Eyal and Ariel. Above all, I am grateful to my wife, Anat Rubin for her endless love and support in this long and stimulating journey. Anat, I dedicate this research to you.

Abstract

Estimates from the World Wind Energy Association assert that world total wind power installed capacity climbed from 18 Gigawatt (GW) to 152 GW from 2000 to 2009. Moreover, according to their predictions, by the end of 2010 global wind power capacity will reach 190 GW. Since electricity is a unique commodity, this remarkable expansion brings forward several key economic questions regarding the integration of significant amount of wind power capacity into deregulated electricity markets.

The overall dissertation objective is to develop a comprehensive theoretical framework that enables the modeling of the performance and outcome of wind-integrated electricity markets. This is relevant because the state of knowledge of modeling electricity markets is insufficient for the purpose of wind power considerations. First, there is a need to decide about a consistent representation of deregulated electricity markets. Surprisingly, the related body of literature does not agree on the very economic basics of modeling electricity markets. That is important since we need to capture the fundamentals of electricity markets before we introduce wind power to our study. For example, the structure of the electric industry is a key. If market power is present, the integration of wind power has large consequences on welfare distribution. Since wind power uncertainty changes the dynamics of information it also impacts the ability to manipulate market prices. This is because the quantity supplied by wind energy is not a decision variable. Second, the intermittent spatial nature of wind over a geographical region is important because the market value of wind power capacity is derived

from its statistical properties. Once integrated into the market, the distribution of wind will impact the price of electricity produced from conventional sources of energy. Third, although wind power forecasting has improved in recent years, at the time of trading short-term electricity forwards, forecasting precision is still low. Therefore, it is crucial that the uncertainty in forecasting wind power is considered when modeling trading behavior.

Our theoretical framework is based on finding a symmetric Cournot-Nash equilibrium in double-sided auctions in both forwards and spot electricity markets. The theoretical framework allows for the first time, to the best of our knowledge, a model of electricity markets that explain two main empirical findings; the existence of forwards premium and spot market mark-ups. That is a significant contribution since so far forward premiums have been explained exclusively by the assumption of risk-averse behavior while spot mark-ups are the outcome of the body of literature assuming oligopolistic competition.

In the next step, we extend the theoretical framework to account for deregulated electricity markets with wind power. Modeling a wind-integrated electricity market allows us to analyze market outcomes with respect to three main factors; the introduction of uncertainty from the supply side, ownership of wind power capacity and the geographical diversification of wind power capacity.

For the purpose of modeling trade in electricity forwards one should simulate the information agents have regarding future availability of aggregate wind power. This is particularly important for modeling accurately traders' ability to predict the spot price distribution. We develop a novel numerical methodology for the simulation of the conditional distribution of regional wind power at the time of trading short-term electricity forwards.

Finally, we put the theoretical framework and the numerical methodology developed in this study to work by providing a detailed computational experiment examining electricity market outcomes for a particular expansion path of wind power capacity.

Chapter 1: Introduction and literature review

Problem statement

Wind power has been recently established as a major source of renewable energy. The rapid increase in wind power generation worldwide introduces two central challenges to the electric industry. One is the physical aspect of connecting a large amount of intermittent new power capacity to the grid. The other is how to incorporate trade in wind power and how it will affect the price of electricity from other energy sources in a deregulated market. Technically, transmission system planners seem to be able to identify and to take steps to relieve bottlenecks to integration of wind power such that system reliability is not compromised. In contrast, the impact of wind power on electricity market dynamics and welfare distribution has not yet been studied comprehensively. A better understanding of the new economic environment of wind-integrated electricity markets is essential for future energy policy designs.

Public good aspects such as reducing dependency on fossil fuel and reductions in greenhouse gas emissions are often the grounds for governments to support renewable energy. Yet, when the percentage of renewable energy and particularly that of wind power increases, the impact on electricity markets should be considered as well. Therefore, a fundamental question is how market participants respond to an increasing supply of intermittent energy source. In markets that make use of forward contracts as their primary pricing tool, how does increased

wind power penetration affect trading behavior? It is therefore necessary to investigate how the entire electricity market is affected, rather than just the economics of wind power, in order to analyze the value of wind power to producers, consumers and the subsequent welfare effects.

At present, wholesale electricity markets make use of the uniform price auction mechanism to administer trade in electricity. This mechanism promotes efficiency by encouraging power producers and consumers to bid their marginal costs and marginal willingness to pay respectively. Wind power producers on the other hand, are not obliged to do so, and typically do not participate in these markets. Instead, wind power is utilized whenever it is available in real-time and wind power producers are compensated at the settled uniform auction price. This arrangement may perform well where wind power has a small market share, but for higher penetration rates it may cause market distortions and deviations from efficient allocation of energy resources. Moreover, wind power is unique because its marginal cost is close to zero, thus its revenues are extremely sensitive to how and when electricity is traded. Therefore, investigating the performances of electricity markets in conjunction with the expansion of wind power capacity is a key research question.

Liberalized electricity markets

For over a decade electric industries worldwide have transitioned from a regulated to a more liberalized structure. Under a monopoly regime, vertically integrated companies control the generation, transmission and distribution of electricity in a broad geographical area. A regulator would guaranty the monopoly a fixed rate per unit of service in an attempt to

deduce (and not overestimate) its average cost. For many years electricity generation and distribution have been operated as natural monopolies due to economies of scale. However, recent technological advances in power generation have weakened the belief that the advantages of economies of scale outweigh the potential benefits of a liberalized market.

In a deregulated electricity market, a monopoly utility is replaced by several independent entities, including independent power producers (IPPs), load serving entities (LSEs) and a system operator. IPPs are generation companies that produce and sell power in the deregulated electricity markets. LSEs are a typical buyer in those markets. These firms must purchase electricity to meet real-time demand of their consumers. The system operator's role is to accommodate the unique features of electricity. Two key technical peculiarities of electricity make it a unique commodity. First, it cannot be stored economically. Thus any unconsumed quantity is lost. Second, electricity requires a transmission system which means that some degree of coordination and/or regulation by a system operator needs to be in place. Examples include independent system operators (ISO) or regional transmission organizations (RTO)¹. In addition, electricity is an essential commodity. Thus, there are large welfare losses from any failure in the market from inadequate supplies. Power systems need to operate reliably at all times and timely investments in capacity must be made to meet growing demand. The function of the system operator is a key in any market structure implementation. For that reason, deregulation in electric industries has been limited to power generation and retailing. More about the challenges and experiences related to the transition to liberalized market itself are discussed elsewhere (Griffin and Puller 2005).

¹ ISOs and RTOs are independent and nonprofit organizations which have as their primary role managing power transmissions, reliability and efficiency of the power system.

Wholesale electricity markets

In a liberalized electricity sector a competitive wholesale market is developed and operated by the system operator or some other entity that does not otherwise participate in the market for electricity. The main functions of electricity exchanges are to accommodate trade and balance real-time operations. Short term electricity trade is usually organized as two-settlement processes: the day-ahead market and the real-time or spot markets. Market participants submit their bids and market price is determined according to the type of auction system adopted by the market administrator. In the U.S. and most electricity exchanges a uniform pricing auction is implemented in which the price of the marginal traded unit of electricity determines the market price. This mechanism is considered competitive as long as the number of market participants is large enough to eliminate the possibility of market power and strategic biddings. Under this circumstance the market price represents an efficient allocation of power generator resources. Unfortunately, this is usually not the case. The electric industry is often concentrated and the unique characteristics of electricity commodity contribute to the ability of generators to exercise market power. This is mainly due to an inelastic demand and the fact that electricity cannot be stored economically.

There are several other commodities that are traded in the deregulated electricity markets including financial transmission rights, reserve capacity and ancillary services. We discuss these only briefly because they are not directly related to our research problem. Financial transmission rights are traded to hedge the cost component of electricity prices which is caused by congestion of transmission lines. The market for reserved capacity is where firms

compete for investments in new power generation to accommodate future increase in demand. Ancillary services are traded as complementary commodities to spot power. The purpose of these services is to help maintain the security and the quality of the supply of electricity in real-time. The main categories of ancillary services traded are frequency and voltage control and backup and restoration capacity. Ancillary power that are traded are reserve power of different types, reactive power and backup power. The markets for ancillary services often consist of auctions but are fundamentally different from the spot market. Ancillary services are provided by different generators than those participating in the spot market. Also, most of the time ancillary power is not generated, but when it is, the cost of input fuel is relatively high and efficiency level is extremely low.

The exchanges play a significant role in promoting the competitiveness of the market. As a coordination device, the exchanges publish real-time market information, weather forecasts, load forecasts and recently there is a growing trend to adopt central wind forecast systems as well. These transparencies are crucial for efficient decision making in all traded electricity goods.

Modeling electricity prices

Models of how electricity is priced are used to value generation assets, financial transmission rights, and the pricing of electricity derivatives. This section discusses the different approaches that have been used to model electricity prices and reviews recent quantitative methods. Electricity prices have been modeled as either stochastic processes or as arising from the interaction of fundamental supply and demand curves. The most frequent approach

used is to model electricity prices as a stochastic process. In this approach historical price data are used to infer the properties of future electricity prices. The second class of models attempts to model fundamental attributes of electricity supply and demand to infer future price behavior. This class includes engineering and equilibrium based models.

Stochastic approach

Pure stochastic models include continuous-time diffusion models and discrete-time autoregressive models. While both focus on modeling the movement of prices, time series models may also include some features of the market. Neither offers much insight into the fundamental economic forces and market operation that affect prices. Stochastic models are most valuable for pricing derivatives in electricity markets where the stochastic properties of prices are the main interest.

Diffusion models

A typical approach to modeling prices is to assume that they follow Geometric Brownian Motion process as follows:

$$d(P_t) = \mu P_t dt + \sigma P_t dB_t \quad (1.1)$$

where P_t is the price of electricity at time t , μ is a drift rate, σ is volatility and B_t is a standard Brownian motion process increment.

Taking the natural log of P_t guarantees non-negative prices and implies that price is log normally distributed if the movement in price is normally distributed (Lucia and Schwartz

2002; Tseng and Barz 2002). The price movement is often formulated as a mean reversion processes by defining the drift parameter as:

$$\mu = m(m_t - \ln P_t) \quad (1.2)$$

where m is a mean reversion parameter, often referred as the degree of storability of the commodity under investigation. For a storable commodity, this parameter will be small. But it will be large in the case of electricity because electricity is quite costly to store. The parameter m_t captures the cyclical feature of seasonal fluctuations (Denton, et al. 2003). Although very simple and convenient, these models fail to replicate spikes in electricity spot markets. The simplest way to overcome this weakness is to introduce a jump component within this framework (Clewlow and Strickland 2000; Knittel and Roberts 2005; Cartea and Figueroa 2005). Then the model becomes

$$d(P_t) = m(m_t - \ln P_t)P_t dt + \sigma P_t dB_t + P_t dq_t \quad (1.3)$$

where q_t is a Poisson process.

The extended model generates price spikes but fails to mimic the dynamics of their occurrence successfully. The Poisson component introduces an isolated and independent jump. In reality, jumps in electricity prices behave differently. Spikes tend to occur in a cyclical manner and not as a purely random event with a probability of occurrence. Also, in reality a sudden spike in electricity prices is often followed by a rapid price decrease caused by generators being turned on to meet the temporary shortage. Excess supply often follows immediately.

The Markov regime switching model is an approach that replicates spikes in a more realistic fashion (Elliott, Sick and Stein 2003; Huisman and Mahieu 2003). In this model price movements are separated into ‘normal’ periods as in equation (1.1) and ‘spiky’ periods described by

$$d(P_t) = \zeta_t P_t dt + \sigma P_t dB_t . \quad (1.4)$$

While equation (1.1) characterizes the price movement in ‘normal’ periods, equation (1.4) employs ζ_t as oppose to μ_t to describe the drift in ‘spiky’ periods. The switch in this case is governed by a standard 2 by 2 conditional probability matrix.

Other diffusion models were constructed specifically to accommodate the particular nature of electricity. These are more mathematically involved and go beyond ordinary commodity price modeling (e.g. Deng 2000, and Geman and Roncoroni 2006). Their mathematical description is superior and offer a better fit for electricity price behavior.

Time series models

Generalized Autoregressive Conditional Heteroskedastic (GARCH) models are the workhorse of discrete time models of electricity prices (Byström 2005; Garcia, et al. 2005; Goto and Karolyi 2004; Longstaff and Wang 2004; Mount, Ning and Cai 2006). The classic model is defined as

$$P_t = c + \sum_{i=1}^n \phi_i P_{t-i} + \sum_{j=1}^m \vartheta_j \varepsilon_{t-j} + \varepsilon_t \quad (1.5)$$

where

$$\varepsilon_t = h_t^{1/2} v_t, \quad v_t \sim iid(0,1) \quad (1.6)$$

and $h_t = \eta + \sum_{j=1}^m \delta_j \varepsilon_{t-j}^2 + \sum_{i=1}^n \gamma_i h_{t-i}$.

Imposing the required stationarity and non-negativity conditions guaranty mean reversion in electricity prices. Volatility persistence is generated by the structure of the error term ε_t ; current volatility is explained partially by past volatility. Applications of the model often incorporate variables for seasonal effects, weekend/weekday and holiday's effects, time of the day effects, jumps in variance and variance clustering.

Fundamental approach

The fundamental approach for modeling electricity prices accounts for the costs of supplying electricity, the demand for electricity and the behavior of electricity market participants. While both engineers and economists use this approach, their purpose and thereby the focus and methodology is quite different.

Engineering based models

The engineering approach attempts to include all relevant forces in power generation to estimate the nominal cost of electricity production. Major input data considered are characteristics of technologies, input prices, physical and power security constraints, transmission system operation, congestion issues, and energy demand. Then, particular figures are utilized in different scenarios to assign the computed cost of production for given conditions. This approach refers mainly to the algorithm developed and implemented by a

system operator (i.e. ISO or RTO) but may also be employed for studying the aggregate industry profile (Huang and Wu 2008) or adoption of new technology (Bakos 2002).

Equilibrium price models

Equilibrium models examine the relationship among economic drivers in market operation to describe market equilibrium and prices in particular. Behavior of market participants such as IPPs and LSEs are crucial for understanding the evolution of market prices. Here, the models describe the main properties of the market instead of stating the actual engineering figures explicitly. For instance, representing production cost as a convex function can incorporate the fundamental cost structure faced by power generators. Assuming N identical producers, Bessembinder and Lemmon (2002) introduced the following cost function:

$$TC_i = F + \frac{a}{c} (Q_{Pi})^c, i = 1 \dots N \quad (1.7)$$

where F represents a fixed cost, Q_{Pi} is the volume produced by producer i , c is a constant greater or equal to two and a is a parameter. This simple representation implies that the industry is characterized by increasing marginal cost. It is realistic because producers employ different technologies types according to Q_{Pi} and the need to meet demand. Employing economic theory and market data (to calibrate parameters) provides a transparent framework for further economic analysis. An extension of the above cost function was proposed by Suenaga and Williams (2005). They replaced the parameter a with stochastic fuel prices which enabled them to explore the input-output price relationships in power generating. Finding equilibrium electricity prices requires consideration of demand (Barlow 2002;

Vehviläinen and Pyykkönen 2005). In these models demand is characterized as stochastic while supply is not. In Barlow (2002) prices are determined by the interaction of consumers' willingness to pay and an unspecified, fully responsive, supply side. In Vehviläinen and Pyykkönen (2005) demand is completely inelastic and prices are determined by the marginal production cost of the marginal generating unit.

A recent study explains the evolution of prices by defining both demand and capacity (D and C , respectively) as state variables (Cartea and Villaplana 2008). The chosen spot price formula is

$$P_t = \beta e^{\gamma C + \alpha D} \text{ and } \alpha, \beta > 0, \gamma < 0. \quad (1.8)$$

Imposing the signs of the parameters guarantees that prices increase with demand and decrease with capacity. The state variables are composed from deterministic and stochastic components:

$$J_t = g^j(t) + \chi_t^j, j = C, D. \quad (1.9)$$

The diffusion process is described as mean reverting and follows standard Brownian motion:

$$d\chi_t^j = -k^j \chi_t^j dt + \sigma^j dZ_t^j. \quad (1.10)$$

The model links demand and capacity with spot prices in a technical way and does not offer any fundamental economic interpretation. The model assumes that the stochastic parts of the state variables are independent which implies that traders do not respond to price changes. This assumption contradicts the basis of a competitive market operation. LSEs are contracted to supply any realized demand. Thus they are not price responsive. However, IPPs are able to respond to market prices by making capacity adjustments. For example, in the long run

investments are made to meet anticipated electricity demand growth. The short run response is characterized by frequent startups and shut downs of peaking plants to accommodate load spikes.

Modeling oligopoly equilibrium

Empirical studies examining the performances of deregulated electricity markets find high price-cost margins, which suggest the presence of market power in these markets (e.g. Borenstein and Bushnell 1999, Borenstein, Bushnell and Wolak 2002, Green 1999, Mansur 2008, Puller 2007 and Wolfram 1999). If power producers are able to exercise market power, models of oligopoly pricing should be employed instead of those assuming perfectly competitive behavior. Natural candidates for a non-cooperative game are the Cournot and the Bertrand models. In the former firms compete in quantities while the latter describes competition in prices. In the Bertrand equilibrium the firm that prices its output below its rival's will be the only supplier of the good in the market. This framework is not suitable for modeling electricity market since the supposition that a single firm in a deregulated electricity market can supply overall load is unlikely. In addition, the cost function of generating power is known to be convex thus negating the equilibrium characterized by a Bertrand model.

An IPP acting as a Cournot competitor chooses its own quantity taking the quantities of its rivals as given. In doing so, each IPP is aware of the impact of its own production level on the market price. Nash equilibrium in this game is reached where all IPPs simultaneously choose profit maximizing quantities. In the case of electricity markets the outcome of

applying a standard Cournot model usually tends to overestimate market power. First, the Cournot is essentially a static short-run model which does not consider entry and exit of firms. Yet, electricity markets are characterized by repeated games at which in each hour spot market is being cleared. Since supernormal profits encourage the entry of new firms, incumbents may not be able to exercise market power up to the Cournot equilibrium. Secondly, the standard Cournot framework does not consider forward contracts. This is limiting since forward contracts are the main pricing tool in electricity markets. Moreover, Allaz and Vila (1993) show that the presence of contracts in a Cournot setting drives suppliers to act more competitively in the spot market and move away from the Cournot equilibrium.

Supply Function Equilibrium (SFE) is another oligopolistic modeling approach that is frequently being used in studying electricity markets. This is a theoretical framework developed by Klemperer and Meyer (1989) and employed for modeling electricity market in Green and Newbery (1992) and others. In this single settlement model suppliers bid supply curves rather than price-quantity pairs. Since most deregulated markets are governed by uniform price auctions, the SFE setting describes actual IPP behavior more closely than the Cournot and other models. Unfortunately, the solution of a SFE approach is characterized by multiple equilibria. Interestingly, the range of solutions of SFE is bounded between the Bertrand outcome from below (the competitive solution) and the static Cournot outcome from above. The range of possible equilibrium may be narrowed down by capacity constraints, entry and market for contracts (Green 1999; Green and Newbery 1992; Newbery 1998). Under extreme conditions the SFE model may produce unique equilibrium; this

however is very limiting and almost impractical from an applied point of view². For example, as pointed out by Newbery (1998) incorporating an SFE model to account for both forward and spot markets will generate double infinity number of equilibria. Similar to the Cournot model, this is a considerable downside since spot power is being traded in the two-settlement process (day-ahead and a spot market) in most deregulated electricity markets.

Another shortcoming of the oligopolistic modeling approach is the lack of a realistic representation of consumers' behavior. Both Cournot and SFE models employ a demand curve (usually linear) to represent real-time load. Doing so, they fail to describe the optimization problem of LSEs. Since LSEs aggregate large number of consumers and participate in forward markets, the evolution of demand in each of these markets should be accounted for as well. Kian, Cruz and Thomas (2005) proposed a model of double-sided auctions for spot power. They develop bidding strategies for IPPs and LSEs in a dynamic system. Their study suggests that a double sided auction is a more realistic modeling approach. That is because it accounts for the demand side responses to the strategies employed by the supply side. As a result, the outcome of the double-sided auction is more efficient than a single sided auction.

An alternative approach to the oligopoly framework is to assume that agents have learning capabilities. Sun and Tesfatsion (2007) developed a computational model to examine the performance of a wholesale power market. The model is based on strictly buyers and strictly sellers of power (i.e. LSEs and IPPs respectively) and a system operator. A dynamic 5-node

² Sufficient conditions for uniqueness in SFE model are symmetry, unbounded upper support of uncertainty, linear demand and marginal costs

transmission grid is assumed for concrete illustration. Unlike other economic models, by incorporating the power system, Sun and Tesfatsion are able to model locational marginal prices. These prices reflect the least cost of meeting additional megawatt demand at a certain node. Electricity trading is assumed to take place at the two-settlement process of day-ahead and real-time markets. However, the demand side is not studied in Sun and Tesfatsion (2007). Instead, it is assumed that LSEs submit electricity demand which is identical to load forecasts thus no optimization from their side is considered. The IPPs predict the state of the power system to develop strategic biddings. Under this setup, the model shows that if power generators have learning capabilities they may exercise their potential market power and bid strategically. As a result they obtain higher profits.

Electricity derivatives

Uncertain demand, non-storability and a time sensitive cost structure of power generation are the main sources of the volatility in electricity spot market. The exposure to sometimes-extreme price volatility can be costly to both LSEs (buyers) and IPPs (sellers). Various financial and physical instruments for hedging price risk in electricity markets have been developed and implemented. Among these, forwards and futures contracts are the simplest and the most popular. Both contracts are an agreement to buy or sell electricity at a specified price for a particular delivery period. They differ however in the way they are traded, their volume, and in their specificity. Futures contracts are traded in the organized exchanges while forwards are traded bilaterally over the counter. Futures are highly standardized contracts traded in low volume. Forward contracts are sold as blocks tailored to fit on/off

peak load time of any future period at any predetermined location. In the U.S., electricity futures contracts are traded currently only in the Minnesota Grain Exchange. Other exchanges decided to delist them due to low interest. In Europe, electricity futures contracts are traded more frequently.

Typically, LSEs and IPPs manage a portfolio of electricity derivatives which are being traded in different occasions prior to the delivery period in question and according to market conditions and updated demand forecasts. Taking a forward position decreases the exposure of buyers and sellers to spot market volatility. The next section discusses the role of futures and forward contracts in electricity market risk management. A detailed review of a variety of electricity derivatives is given by Deng and Oren (2006).

Risk management

Electricity demand in wholesale electricity markets is represented by LSEs. These firms are contractually obligated to meet any volumetric demand of their end-consumers' at all times. Coupled with spot price volatility this demand-fulfillment requirement makes them extremely exposed to short run losses. Electricity is a non-storable commodity and as such the convenient no-arbitrage approach cannot be applied for hedging its price risk in futures markets. Instead, the distribution of electricity prices may be inferred, and then the prices of futures contracts (and other electricity derivatives) can be computed to comply with a no-arbitrage in expectations principle.

Power producers would be interested in revenue certainty to allow steady cash flow, enable timely investments and preserve firm credit rating and reputation. These circumstances make forwards and futures contracts essential devices to control risk for both LSEs and IPPs. The demand for future contracts and the evolution of their prices have been studied extensively. A conventional starting point for these studies is based on two key assumptions; one is related to the behavior of agents in this market and the other is about the stochastic linkage between electricity prices and demand. First, the demand for hedging instruments is motivated by Markowitz's portfolio model in that buyers and sellers want to diversify their procurements/sales to achieve higher expected utility by trading off mean profits for reductions in variance. Then, an assumption about the particular joint distribution of price and load follows, and is used to optimize a portfolio. For example, both Woo, Horowitz and Karimov (2004), and Oum, Oren and Deng (2006) assume a concave LSE objective function and derive an optimal frontier of futures holding. Employing constant absolute risk aversion and mean-variance functions, the portfolios represent the optimal tradeoff between procurement cost expectation and cost variance. Woo, Horowitz and Karimov exemplified an efficient portfolio for the case that overall procurement cost is assumed to be normally distributed. Oum, Oren and Deng investigated cases which price and load demonstrate bivariate normal or log-normal distributions. Mean-variance objective have been employed to construct the corresponding efficient frontier for power producers (Bjorgan, Liu and Lawarree 1999). Acknowledging that variance of profits penalizes realizations of over and under expected value at the same rate, Paravan, Sheble and Golob (2004) solve the power portfolio optimization problem where the variance of profits is replaced by the conditional value at risk. That is the expected value of loss given a realization of a certain outcome. A

parallel approach for an LSE firm is presented in Woo, Karimov and Horowitz (2004) where the objective is to minimize expected procurement cost subject to a cost exposure constraint.

By imposing exogenous price distributions, the studies above can be viewed as a partial equilibrium approach for risk. A general equilibrium modeling of electricity market is rare due to the intricate feature of this market. Bessembinder and Lemmon (2002) developed a general equilibrium model where both quantity and price of forwards are determined endogenously. This study is unique in its effort to describe the complexity of electricity market essentials based on classic economic theory. It is considered to be a benchmark for economic-based modeling under the assumption of perfectly competitive electricity markets. Bessembinder and Lemmon assume that the settled price of a forward contract is based mainly on the expectations of the spot market price. Storage and risk related to the nature of the traded commodity are generally determinants in forwards markets as well. In the case of electricity, storage is economically irrelevant (excluding hydroelectricity), but risk may play an important role.

Start by assuming that both LSEs and IPPs decision making is based on the following mean-variance objective functions

$$v[E(\pi), Var(\pi)] = E(\pi) - \frac{A}{2} Var(\pi) \quad (1.11)$$

where π is profits and the parameter A is the coefficient of absolute risk aversion. Note that this representation is equivalent to assuming that utility is exponential and profits are normally distributed.

The non-hedged profits of a representative IPP and LSE respectively are

$$\pi_{IPP} = PQ - TC(Q) \text{ and } \pi_{LSE} = Q(P_R - P) \quad (1.12)$$

where TC is the total cost defined in equation (1.7), P and Q are the spot price and realized demand respectively. P_R is the predetermined fixed retail price per unit of electricity.

One can show that the optimal forward position for the mean-variance objective function of both LSE and IPP can be written as

$$Q_{\{IPP,LSE\}}^F = \frac{P_F - E(P)}{AVar(P)} + \frac{Cov(\pi_{\{IPP,LSE\}}, P)}{Var(P)}. \quad (1.13)$$

The first term is driven by the bias of the forward price P_F compare to the expected spot price. The second term is the optimal condition for minimizing the variance of profits.

Solving the model, Bessembinder and Lemmon show that the equilibrium volume and the forward price can be written as functions of the first, second and third moments of the distribution of the spot price. Next, they establish the result that in general the forward price is a biased forecast of the spot price. The risk premium which is defined as the forward contract price minus the expected spot price is increasing in the skewness and decreasing in the variance of spot price. That is, in peak load periods that are characterized by high expected demand and a high variance in demand, the risk premium will be high due to the convex nature of generating cost. In lower demand periods, lower skewness pushes risk premiums down.

Another study provides an empirical analysis based on the theory presented above (Longstaff and Wang 2004). Data from the PJM³ electricity market support the predictions of Bessembinder and Lemmon and implies that an economic-based model is capable of explaining the formation of electricity markets prices.

Electricity from renewable resources

Diversification of energy sources and climate change mitigation have been the major grounds for the growing interest in energy from renewable resources. Higher energy prices coupled with technological advances in harvesting renewable energy enhanced this interest. Renewable energy resources include wind, solar, geothermal, biomass, hydro⁴, landfill gas, and others. Many countries have introduced mandates for renewable energy. For instance, the European Union set an overall binding target of 20% by 2020, though the percentage varies greatly within union members. Australia set 20% by the year 2020 as well. In the U.S. Renewable Portfolio Standards (RPS) have been established by 25 states and the District of Columbia but no national policy has been set. Targets, percentages, timetables, and the energy resources to be used vary among states. Targets are specified as percentages of overall power generation capacity or as annual energy volumes produced⁵. Another support for renewable energy is given in a form of a tax credit and renewable energy certificates, which are granted for generating energy from qualified renewable resources. They are traded

³ PJM Interconnection is a regional transmission organization (RTO) in the U.S. that coordinates the movement of wholesale electricity in all or parts of 13 states and the District of Columbia.

⁴ Hydroelectric power produced in a pumped-storage facility is usually considered as a non-renewable resource as pumping requires energy that comes mainly from fossil fuel generators.

⁵ U.S. state level RPS can be accessed at the American Wind Energy Association website at: <http://www.awea.org/legislative/pdf/State%20RPS%20factsheet%20Nov%202007.pdf>

separately from electricity and can provide a supplementary source of income to producers of renewable energy.

Integrating wind power

Integrating renewable energy into the wholesale electricity market is a challenging task. Unlike conventional power units, renewable energy can fluctuate over time because output depends on precipitation, radiant energy and air flows which are uncertain by nature. Their variable nature means that renewable energy cannot be marketed in the same way that conventional power is marketed. We focus here on wind power as its variability makes it the most difficult energy resource to integrate into the power system (IRC 2007). In addition, U.S. wind power capacity has been rapidly growing as shown in figure 1.

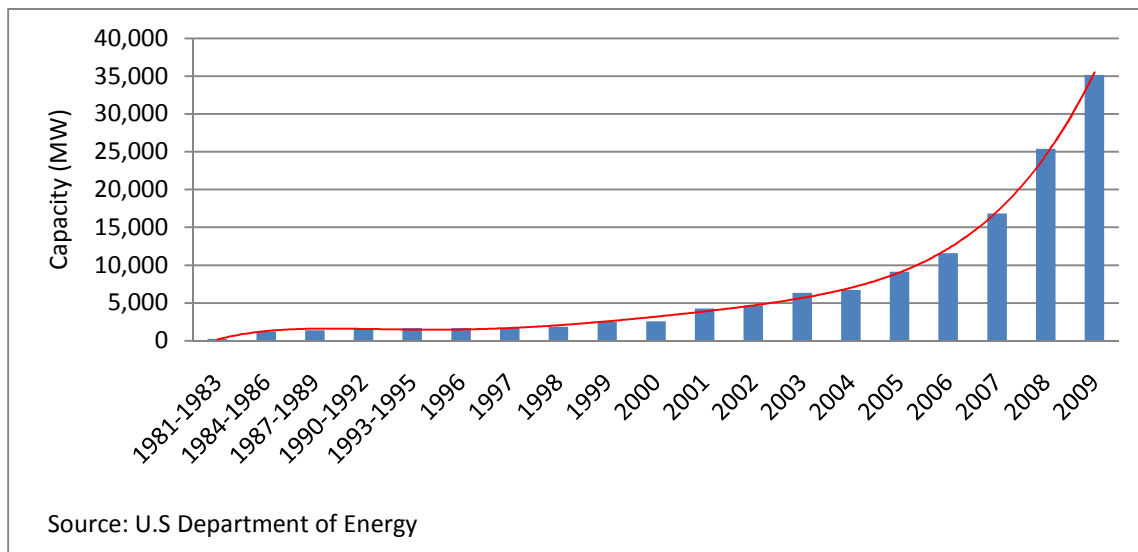


Figure 1: U.S. overall wind power capacity

The large increase in wind power shown in figure 1 suggests that it will be useful to better understand how wind power will impact the power generation industry. The engineering implications of grid connection and reliable transmission of wind power are being studied, discussed and improved on an ongoing basis (Jauch, et al. 2005; Söder, et al. 2006). In particular, both short run and long run reserve requirements need to be re-evaluated because an increasing share of wind power makes quantification of system reserves more complex. Short run reserves are used to account for real-time load forecasting errors and generator outages. Long run reserve refers to the adequacy of overall power capacity of a region to meet demand⁶. When the share of wind power is small, the overall amount of variability that is added to a power system is small. Hence both types of reserve requirements are not significantly altered. When wind has a 10% share, the increase in short term reserve is estimated in the range of 2-8% of total installed wind power capacity (Holtinen and Hirvonen 2005). In terms of overall installed capacity, the capacity credit for wind in low penetration rates is equivalent to that of conventional power units but diminishes at higher rates. The reason for this is that in low penetration rates the variability of wind power production is within the range that short run reserves can handle without further adjustments. As wind power share increases, the ability of these reserves to account for possible sudden drops of wind power is reduced thus long run reserves have to be added. Moreover, at a certain point, capacity credit does not increase with the addition of more wind turbines to the region.

⁶ Capacity calculation of wind power for planning reserve varies greatly. In some regions a fixed proportion of 15% -20% of turbine's rated power is used. When applicable, historical data is utilized to compute empirical capacity factor based on performances. In other regions the capacity evaluation is based only on peak load periods.

A study by Doherty and O'Malley (2005) introduce a novel method to compute reserve requirements for high shares of wind power capacity regime. The study shows that long term capacity adjustments are more substantial relative to the short term requirements. Short term reserve requirements are increasing, but they are fairly low because intra hour wind variation is small relative to overall load variation. However, categories of reserve that act over longer periods of time have to expand with the introduction of more wind power.

Wind forecasting

Wind power value is strongly influenced by the precision of wind speed forecasting. A high quality forecast enables a system operator to schedule wind power to displace conventional generators and minimize ancillary services costs. With regard to the operation of electricity markets, accurate information about wind power availability promotes efficiency in trade. Unfortunately, small wind speed prediction errors are translated into large ones when it comes to wind power predictions, as will be explained in detail in chapter three. Thus, wind energy prediction is not a simple task and still produces relatively inaccurate predictions when predictions are made for more than several hours ahead.

Wind speed predictions for more than several days ahead are performed by numerical weather prediction (NWP) models. These are developed by meteorologists and generate predictions in low resolutions for large areas. Predictions for up to two days-ahead are commonly governed by physical, statistical or combinations of these two methods. Physical methods utilize the predictions of NWP models as inputs and consider the physical local wind conditions of smaller areas to enhance predictions. For short term predictions (hours to

one day-ahead), statistical models are more suitable. In particular, time series models have been developed to improve predictions (El-Fouly, El-Saadany and Salama 2008; Sánchez 2006; Torres, et al. 2005).

The short term prediction of wind speed for power generation purposes is being improved over time. Yet, according to a recent study absolute mean error in the case of day-ahead prediction is still 25%-30% of actual output. An hour-ahead prediction of a single site incorporates an approximately 10%-15% absolute mean error (Smith 2008).

When forecasting aggregate wind power in a region, prediction errors are reduced because of aggregation of forecast errors. Smith (2008) reports that the day-ahead forecasting errors in a region are 15%-18% and the hour figures fall to 6%-11%. Forecasting aggregate wind power has to take into account the spatial correlation of wind speed in the region. If wind speed is strongly correlated over space, reductions in prediction errors would be limited compared to the case of weak correlation. Employing spatial statistics models, it was shown that the decrease in prediction error is related to the size of the geographical area considered rather than the number of wind farm sites in a region (Focken, et al. 2002; Holttinen 2005). Because spatial correlation limits the smoothing effects proposed by a large area, the reduction in the errors of aggregate prediction are not unbounded.

Central wind forecasting systems have been developed and adopted on an ongoing basis in some regions. Some of these systems are still experimental or in a pilot stage while others are

already being practiced⁷. Besides offering the most accurate predictions to market participants, central systems support the competitiveness of electricity markets. The presence of central forecasting system in a market makes the frontier of wind power predictions common knowledge and promotes market coordination.

In most deregulated electricity markets in the U.S. bidding wind power in the day-ahead markets is allowed. But in practice, wind power producers usually do not participate in this market. Instead, their energy is taken into the system and transmitted whenever it is available. Since the marginal cost of wind power generation is zero, it is most efficient to utilize all applicable wind energy before dispatching other generators. Introducing wind power to the system only in real-time minimizes the short term reserve requirements for wind power integration. By doing that, power systems operators avoid the errors involved in forecasting wind power for more than an hour-ahead. Then, wind power producers are compensated at the equilibrium price determined by conventional supply units and demand forces.

Imprecise day-ahead forecasting of wind power and financial penalties levied on deviation from supply commitments discourage wind producers from participating as players in the day-ahead markets⁸. In cases in which the wind power producer is defined as a capacity resource in a region, he receives capacity market revenues but has an obligation to schedule its capacity value in the day-ahead market.

⁷ Some operating forecasting systems are in Alberta Electronic SO, California ISO and ERCOT. NY ISO uses persistence forecasting.

⁸ In the U.S. energy imbalance charges may apply if energy deliveries differ by more than +/- 1.5% from their day-ahead schedule.

Previous work and the contribution of this study

Price modeling has been studied extensively in the deregulated electricity markets era. Stochastic based approaches have generated models of high precision. Advanced models have been developed to reproduce successfully the unique dynamics of electricity prices. These models however are limited by their strong dependency on past observations. The stochastic approach is extremely sensitive to realizations of black-swan events⁹. Focusing only on price dynamics could have never predicted or explain the causes for an improbable event such as the electricity market crisis in California in 2000/2001.

The ability of stochastic approaches to capture ex-post statistical properties depends heavily on the structure of industry, design and market operation from which price realizations are drawn. Significant developments or changes in electricity markets cannot be examined properly by stochastic models. In fact, the focus of my research question - the increasing penetration rate of a new intermittent energy resource – is a good illustration of such a dramatic change.

The fundamental approach is the one that is suitable for our needs. The introduction of wind power not only affects the cost structure and aggregate power supply but also changes the financial risk involved in electricity market operations. For that reason, a model which emphasizes firm behavior needs to be developed. As more producers adopt the technology

⁹ Nassim Nicholas Taleb, the author of the book *The Black Swan: The Impact of the Highly Improbable* (2007), summarizes a black-swan event as “*First, it is an outlier, as it lies outside the realm of regular expectations, because nothing in the past can convincingly point to its possibility. Second, it carries an extreme impact. Third, in spite of its outlier status, human nature makes us concoct explanations for its occurrence after the fact, making it explainable and predictable.*”, *The New York Times*, April 22, 2007.

(i.e. market penetration rate increases), the need for economic analysis to understand market dynamics is strengthened. However, our short review shows that models of electricity markets that are based on classic economic theory are very diverse in their behavioral assumptions, market structure and technical specificity of the power system.

The current state of knowledge of the economic framework of electricity markets is insufficient for our purposes for several reasons. First, all studies regarding risk management reviewed here share the same simplifying assumption that electricity market participants are risk averse. This simplification of the role of risk is to say basically that firms dislike risk simply because they dislike variability in income. Objective functions with a risk aversion component collapse in most studies into a mean-variance formation (to favor higher return and lower variability). By making this assumption, researches presume that objective functions of electricity market participants should treat load prediction error in a symmetric manner. However, the financial and economic consequences of over-prediction and under-prediction of load in the case of electricity trading are not symmetric. Thus the effect of risk in a market that faces a perfectly inelastic demand in real-time needs to be more carefully modeled.

Electricity is a commodity that cannot be stored economically. For that reason holding a quantity that will not be consumed results in an immediate loss equal to the expenditure associated with the excess units bought in advance. In liberalized markets, this loss is not inevitable because excess volume may be resold at the day-ahead, spot markets or settled by a financial instrument. However, since load forecasts are published and known to all, it is not

uncommon that many LSEs within a region make the same error. For this reason, reselling electricity under these circumstances is not a desirable outcome for its holder.

The under-purchase of electricity on the other hand exposes LSEs to spot market price volatility. The extreme volatility of wholesale electricity prices proved to be devastating for LSEs in extreme cases such as the California crisis mentioned above. Even if the probability of a catastrophe is low, its outcome can be very costly. In line with the above, we suggest an alternative approach for modeling firms' objective functions in chapter two. Our approach let agents analyze the possible consequences of price volatility in the case of under or over-purchase as opposed to taking risk as a loss factor *per se*.

Secondly, most power generators are not able to supply electricity instantaneously. Due to ramp-up time the electricity supply curve is not stationary. In fact it corresponds to the generation capacity, which is applicable if needed, to supply electricity for a particular delivery period in the future. This is important for wind power integration because ramp-up time determines the feasibility and the cost of generating power in case of a sudden drop in wind power supply.

Lastly, studies of wind power integration have concentrated mostly on the physical aspects of integration. While electricity demand provided the main uncertainty in electricity markets, the integration of wind power introduces uncertainty from the supply side. Electricity markets are usually organized as a two-settlement process with one market for short-term forward contracts (e.g. day-ahead or hour-ahead) and a spot market. At the time of trading forwards, firms have expectations about real-time load and price, which will be resolved at the spot market. Because wind power forecasting has particular statistical properties,

forecasting spot market outcome in a region with significant amounts of wind power capacity requires particular consideration. For this purpose one should model the statistics of regional wind power and the dynamics of wind power forecasting. In this study I develop a novel numerical methodology for simulating the probability distribution functions (pdf) of regional wind power and wind power forecasting associated with a prospective expansion of wind power capacity. Constructing these pdfs is essential for understanding the uncertainties and risk involved in wind-integrated electricity markets.

Market uncertainties impact the decision making in deregulated electricity markets and thereby equilibrium quantities and prices. To my knowledge, no economic framework has yet been proposed to analyze the adjustments in the behavior of electricity market participants in response to the introduction of an intermittent energy resource. In this dissertation I introduce a theoretical framework and a numerical methodology that enable the analyses of electricity markets in general, and these which face a new economic environment created by an increasing share of wind energy.

Organization of this dissertation

The dissertation is organized as follows: Chapter 1 provided details about the research question, the fundamentals of deregulated electricity markets and a literature review. In chapter 2 a new theoretical framework for modeling the two-settlement process in electricity markets is introduced. Then, numerical experiments and sensitivity analyses demonstrate the qualities of the proposed model. Principles of wind power are explained in chapter 3. In this chapter we make use of wind speed data in Iowa to exemplify and study statistical and other

features of wind power generation. Chapter 4 provides an extension of the theoretical framework developed in chapter 2 to account for deregulated electricity markets with wind power. In doing so, we also expand the theoretical foundations to compare electricity market outcomes and welfare distributions with regard to the ownership of wind power capacity. A novel numerical methodology for the simulations of the conditional pdf of wind power is developed in Chapter 5. The goal in this chapter is to mimic the dynamics of information regarding the availability of future wind power at the time of trading short-term electricity forwards. In chapter 6 we couple the theoretical framework and the numerical methodology to generate predictions regarding the possible market outcomes implied by selected scenarios of wind power expansion. Chapter 7 concludes the findings of this study and makes some suggestions regarding future research.

Chapter 2: An electricity market model

Characteristics of a desired model

Studying our research question requires an economic-based modeling approach. The following are the qualities that such a model should demonstrate:

- Capture the main economic drivers in electricity markets, including the evolution of load, characteristics of supply and risks associated with electricity market operation
- Describe the behavior of market participants in a realistic manner
- May be calibrated easily to fit the characteristics of load in different periods
- Flexible to accommodate various scenarios of integrating wind power with no added complexity
- Generate equilibrium measures of prices and quantities that follow statistical properties of real-world realizations

To our knowledge such a model does not exist.

A model developed for this work

We propose an oligopolistic equilibrium model of a deregulated electricity market. The theoretical framework is developed to model the dynamics of electricity trading patterns toward a specific delivery period in the future. We adopt the current market design of a two-

settlement process, where short-term electricity forwards are being traded and scheduled for delivery at the day-ahead market, and then power is balanced in the delivery period. Electricity is not storable thus the delivery period is also the period that power is generated, transmitted and consumed. For that reason, we denote the delivery period as *real-time*. The day-ahead market will be referred to as *market for forward contracts*.

The model consists on an Independent System Operator (ISO), Load Service Entities (LSEs) and Independent Power Producers (IPPs). The ISO manages the power system and administrates wholesale electricity markets. In addition, the ISO makes predictions regarding electricity demand and available wind power (if applicable) at the beginning of the trading period. These predictions are accessible to all market participants. LSE firms are the natural buyers of power in the model. They are committed to deliver any realized load to their end-users for a fixed short run retail price. Since LSEs face inelastic demand in real-time, they have an incentive to trade power via forward contracts and by that reduce their exposure to upward spikes in the spot price. IPP firms generate and supply power in real-time; they are strictly sellers in forwards markets but may buy back contracts in the event of excess supply in the spot market. IPPs have a time-sensitive convex cost function which characterizes the various types of power generators and a range of fuel inputs in use. The model is based on a double-sided auction where both LSEs and IPPs engage in a Cournot competition. We assume that all players have perfect information about the distribution of the spot price and do not impose any risk preferences on their behavior (i.e. risk neutrality).

The model does not attempt to examine electricity commodities other than spot power. The outcomes of wind power integration on subsequent markets (e.g. ancillary services, reserve capacity and others) may be added to the model in the future.

Load forecasting

Electricity demand varies by season, holiday, day of the week, hour of the day and other factors. Our model addresses one particular future delivery period at a time but may be parameterized easily to accommodate any load characteristics of any particular period. Since both load and wind speed data are usually reported on an hourly basis, we construct the model such that a period in the model corresponds to one hour. We focus on the statistics of the day-ahead forecasts for the rest of this study since this is the time that electricity forwards are being traded in nearly all deregulated electricity markets. Although not treated in this study, we provide in this section a more generalized framework to explain how to go about examining alternative timings for trading forwards. This may be useful for considerations of market design.

First we construct a synthetic time series of loads, which will be used to simulate the short-term evolution of electricity demand. Focusing on a specific period at a time, load is commonly considered to be normally distributed (Bessembinder and Lemmon 2002; Loutan and Hawkins 2007; Oum, Oren and Deng 2006). The dynamics of electricity demand may be fitted by several Gaussian time series models; we employ here a fairly simple model that accounts for the fundamental characteristics of load dynamics.

Let electricity demand at time t follow an exogenous stochastic process of $MA(q)$ type:

$$X_t = \mu + \theta_0 \varepsilon_t + \theta_1 \varepsilon_{t-1} + \cdots + \theta_q \varepsilon_{t-q} \quad (2.1)$$

where μ is the expected value of load when taking into consideration the characteristics of the period in question. The error terms follow the standard distribution

$$\varepsilon_t \stackrel{iid}{\sim} N(0, \sigma_\varepsilon^2) . \quad (2.2)$$

Assume also that $\theta_0 = 1$ and the θ s satisfy stationarity conditions.

Knowing the distribution of load and prior realizations, one could infer easily the distribution of the prediction at each period according to how far apart that period is from real-time. That is, the distribution of the prediction of load in period T , based on information at time t is given by

$$X_T | \Omega_t \sim \begin{cases} N(\mu, (\theta_0^2 + \theta_1^2 + \cdots + \theta_q^2) \sigma_\varepsilon^2) & \text{if } T > q \\ N(\mu + \theta_T \varepsilon_{t-T} + \cdots + \theta_q \varepsilon_{t-q}, (\theta_0^2 + \cdots + \theta_{T-1}^2) \sigma_\varepsilon^2) & \text{if } T \leq q \end{cases} \quad (2.3)$$

where Ω_t is the information observed up to time t . Notice that a prediction precision is non-decreasing with the number of innovations (q) and non-increasing with the prediction horizon (T). For example, a long horizon prediction has an expected value μ and a variance that is composed from the number of innovations which have not occurred. Such a prediction would be vague compared to predictions of shorter horizons. The expected value of a one period ahead prediction is composed of innovations which are already known. The variance of this predictive is of size σ_ε^2 only.

This simple representation of load provides the short-term dynamics and the statistics of load prediction. The choice of a $MA(q)$ model is convenient for applications in numerical

simulations (illustrations are provided later in this chapter). For empirical purposes, load data in time series format conform better to a $AR(p)$ model (the lags of load are observed while the innovations of MA process are not). Provided that standard assumptions are met, the lagged coefficients of load can be estimated and used for calibration in future work.

Power generation

Typically, an electric industry is characterized by various types of power generators and a range of fuel inputs. For example, nuclear and coal plants are large, are costly to build, and generate power at the lowest heat rate levels¹⁰. Smaller generators which run usually on natural gas and oil have lower fixed costs. They are characterized by higher marginal costs because they run at lower efficiency levels and utilize energy sources which are historically more costly than these used by larger plants. The portfolio of generators owned by an IPP firm may be ordered in terms of their marginal cost to obtain a cost curve, which is increasing and convex. Another fundamental feature of this curve is that it is non-stationary. It is time-sensitive since turning on generators is constrained by ramp-up time and the associated start up and shut down costs. Next, we give some more details about power generation technology to demonstrate the importance of this feature in electricity market modeling.

Power plants are classified by their purpose to serve base, intermediate or peak load periods. This classification refers to the flexibility of a generator to adjust to sudden changes of load

¹⁰ Heat rate is used to measure how efficiently a generator converts BTUs of heat to kWh of electricity.

and the associated tradeoffs in the efficiency of power production. Base load plants are in use continuously except for maintenance shut down periods. These large plants use mainly steam turbine technologies powered by coal or nuclear fission. Generators that serve base load require a long ramp-up time and may need many hours or days before they can provide a stable flow of electricity and achieve their full efficiency potential. Thus they are seldom responsive to errors of load predictions. Peak load plants are the most flexible generator units because they are the least costly to turn on. In general, smaller units have a shorter ramp-up time and higher marginal cost. Gas turbines are regularly used to adjust for periods of peak load fluctuations. Their response time is normally between one and four hours according to size and type. For periods of intermediate load, combined cycle gas turbine (CCGT) plants are usually turned on. A CCGT technology combines steam turbine with a gas turbine to enhance the efficiency of power generation. Using a heat recovery steam generator, the waste heat from gas combustion is utilized in a steam cycle. While gas turbines efficiency level is in the range of 10% to 30%, a modern CCGT unit may reach efficiency level of about 60%. However, since their ramp-up time is longer, CCGT units are typically used during periods of intermediate load. To generate power immediately, internal combustion engines may be used. These are small generators which usually produce electricity from oil almost instantaneously. Since they generate power in very low efficiency levels, they are used mainly for peak load periods and for ancillary power.

In line with the above, we consider a time-sensitive supply curve. The curve accounts only for the generation capacity which if needed, is applicable to supply power in a particular delivery period in the future. The set of applicable generators characterizes the IPP's supply

curve at each period prior to real-time. Clearly, this cost formation has some significant financial applications. For example, if producers turn on some of their generators just if they are able to sell their output in advance (e.g. forward contracts) power would be less costly to generate because the capacity which has relatively longer ramp-up time is characterized by lower heat rate. More specifically, the day-ahead supply curve (corresponding to a day-ahead forward market) includes more generators that are able to respond to changes in load at lower cost than the applicable generators in real-time. Therefore load prediction error a day before the delivery period has different financial consequences than the same error made just a few hours before the delivery.

We assume that IPPs have an identical set of generating technologies and that capacity of peaking power plants is large enough to accommodate any possible load realization. Essentially, this is equivalent to the supposition that the system operator manages capacity and ancillary services adequately.

Start by denoting q_F as the amount of electricity that is pre-scheduled by a particular IPP for delivery in real-time. Then, the costs of power generation are governed by two possible states of the world. If production (denoted by q) is lower than q_F then there is no need to turn on additional generators in real-time. In this event power is being generated efficiently and at a relatively low cost. In contrast, if realized production is higher than q_F , generators have to be turned on. In this state of the world, costs of generating power are higher for two main reasons. First, most idle generators cannot produce power instantly. Those that can are characterized by very high operating heat rate. Second, startup costs during ramp-up time

drive marginal costs up. Those startup costs account for the time which generators are turned on but their output level is still low.

We assume the following function to model IPP's marginal cost of power production¹¹

$$C'(q, q_F) = \begin{cases} \alpha_t q & \text{if } q_F \geq q > 0 \\ \alpha_t q + \alpha_s (q - q_F) & \text{if } \bar{q} > q \geq q_F \end{cases} \quad (2.4)$$

where $\alpha_t, \alpha_s \geq 0$ are parameters and \bar{q} is the upper bound for the output of generation capacity owned by each IPP firm.

The parameter α_t characterizes the marginal cost of generating power, which is related only to the quantity produced. In the state of the world where the marginal unit is produced by a generator which was scheduled to deliver power in advance, that is the overall marginal cost. If IPP's production level happens to be higher than the prescheduled capacity, an incremental cost α_s is involved in turning on additional generators toward the delivery period. In this event the marginal cost is higher and thus constructs a spot power supply curve which is steeper. The t subscript is used to differentiate between the time of pre-scheduling power and the delivery period (spot), denoted by subscript s .

The assumed linear marginal costs are a direct derivative of quadratic cost function. The total variable costs of power production are expressed as

$$C(q, q_F) = \begin{cases} 0.5\alpha_t q^2 & \text{if } q_F \geq q > 0 \\ 0.5\alpha_t q^2 + 0.5\alpha_s (q - q_F)^2 & \text{if } \bar{q} > q \geq q_F \end{cases} . \quad (2.5)$$

¹¹ Linear marginal cost functions are being used commonly for modeling the costs of generating power. For example, the supply function equilibrium model (SFE) introduced by Klemperer and Meyer (1989) has been applied in numerous studies of electricity markets. Other examples can be found in Bjorgan, Liu and Lawarree (1999), Sun and Tesfatsion (2007) and Tseng and Barz (2002).

Incorporating a two-state of the world cost function has a significant advantage because it allows for the modeling of spikes in production costs which are not entirely explained by high realizations of load. Sudden increase in generation costs can also be caused by scheduling insufficient generating capacity in advance. This may be the outcome of profit-maximizing behavior or errors in load predictions. In both cases, in real-time the economy cannot avoid startup costs which may drive marginal generating cost up rapidly.

Spot power and firm entry

Markets for spot power (day-ahead, real time and others) are generally administrated by uniform price auctions. IPP and LSE firms submit their bids to the market administrator (usually the ISO itself) and generators are dispatched by their lowest bids until system demand is met. The bid of the marginal unit clears the market and determines the market price. This method is commonly adopted on the ground of the efficiencies associated with the competitive behavior of market participants. If sellers and buyers bid their marginal costs and maximum willingness to pay respectively, economic theory tells us that the allocation of resources will be efficient. In electricity markets however, empirical evidence (see chapter 1) suggest that the assumption of competitive behavior is not always suitable since each LSE firm represents large numbers of consumers and the number of IPP firms in a region is small.

If IPPs exercise market power, the degree to which they are able to manipulate market prices depends on the timing of market operation. Although the same homogeneous commodity is traded in both forwards and spot markets, the cost structure is very different. Due to ramp-up time and fuel costs, peaking plants are turned on mainly for balancing power in real-time,

where base and intermediate load plants are the core supply of power in forward contracting. Moreover, peaking plants are relatively small and do not require high construction costs. Hence supernormal profits in spot market may encourage the entry of new peaking generators (e.g. Newbery 1998). Base and intermediate load plants on the other hand are more expensive and require more time to build. Therefore construction of these plants may be considered only in the long run. Consequently, unlike peaking plants, the strategy for trading the energy output of these plants is less threatened by entry. This environment gives rise to the claim that the degree of competitiveness of electricity markets governed by uniform auctions is negatively linked to the time of trade. In other words, markets which trade power closer to the time of delivery are expected to be more competitive and cannot sustain high mark-ups. Based on the motivation of preventing entry, IPPs behavior in spot and forwards market may diverge greatly. First, we will focus on the spot market; assuming zero construction costs of peaking plants motivates perfect competition behavior in real time¹². On the other hand, market power may be exercised in markets for forward contracts. We will present a static model of oligopoly and analyze separately LSEs' and IPPs' forwards positions to characterize a symmetric Cournot-Nash equilibrium.

Spot market

If the threat of entry motivates IPPs' to bid competitively in the spot market then we know that the realized spot price reflects true marginal costs. That is

¹² The zero construction cost assumption is made for convenient presentation of the concept. In the case of positive construction costs of small generators, IPPs may price their output up to their average costs to prevent entry.

$$P_s = C'(q^1, q_F^1) = \dots = C'(q^M, q_F^M) \quad (2.6)$$

where P_s is the spot price and M is the number of IPPs in the electric industry.

Given the number of forward contracts offered by each firm and the fact that power must be balanced in all times (i.e. $\sum_1^M q^m = X$) one can solve for the spot market outcome. For example, for $M = 2$ and assume without loss of generality that $q_F^2 > q_F^1$ the spot price is

$$P_s(X, q_F^1, q_F^2) = \begin{cases} \frac{\alpha_t}{2} X & \text{if } 2q_F^1 \geq X \geq 0 \\ \alpha_t \frac{(\alpha_t + \alpha_s)X - \alpha_s q_F^1}{2\alpha_t + \alpha_s} & \text{if } \frac{\alpha_s(q_F^1 + q_F^2) + 2\alpha_t q_F^2}{\alpha_t + \alpha_s} \geq X > 2q_F^1 \\ \frac{\alpha_t}{2} X + \frac{\alpha_s}{2} (X - q_F^1 - q_F^2) & \text{if } X > \frac{\alpha_s(q_F^1 + q_F^2) + 2\alpha_t q_F^2}{\alpha_t + \alpha_s} \end{cases} \quad (2.7)$$

and firms' production levels are

$$\{q^1, q^2\} = \begin{cases} \left\{ \frac{X}{2}, \frac{X}{2} \right\} & \text{if } 2q_F^1 \geq X \geq 0 \\ \left\{ \frac{\alpha_s q_F^1 + \alpha_t X}{2\alpha_t + \alpha_s}, \frac{(\alpha_t + \alpha_s)X - \alpha_s q_F^1}{2\alpha_t + \alpha_s} \right\} & \text{if } \frac{\alpha_s(q_F^1 + q_F^2) + 2\alpha_t q_F^2}{\alpha_t + \alpha_s} \geq X > 2q_F^1 \\ \left\{ \frac{X}{2} + \frac{\alpha_s(q_F^1 - q_F^2)}{2(\alpha_t + \alpha_s)}, \frac{X}{2} + \frac{\alpha_s(q_F^2 - q_F^1)}{2(\alpha_t + \alpha_s)} \right\} & \text{if } X > \frac{\alpha_s(q_F^1 + q_F^2) + 2\alpha_t q_F^2}{\alpha_t + \alpha_s} \end{cases} \quad (2.8)$$

The first parts in (2.7) and (2.8) describe the case that capacity traded via forwards is sufficient to meet realized demand. The second is where only firm 1 adds capacity in real-time and the third part is where both firms startup generators in real-time.

Next, and for the rest of this study, we focus on the existence and the characteristics of a symmetric forward position case. That is the case of M identical IPP firms where the Cournot-Nash equilibrium is $q_F^1 = \dots = q_F^M$. Focusing on the symmetric case simplifies the analysis since we need to examine only two states of the world. One is where no generators

are being turned on in real-time and the other is where all firms turn on generators in real-time. For these two states it can be verified that the spot price is

$$P_s(X, \vec{q}_F^m) = \begin{cases} \frac{\alpha_t}{M} X & \text{if } \sum_1^M q_F^m \geq X \geq 0 \\ \frac{\alpha_t}{M} X + \frac{\alpha_s}{M} (X - \sum_1^M q_F^m) & \text{if } X > \sum_1^M q_F^m \end{cases} \quad (2.9)$$

where $\vec{q}_F^m = \{q_F^1, \dots, q_F^M\}$, and production level of firm i is

$$q^i(X, \vec{q}_F^m) = \begin{cases} \frac{X}{M} & \text{if } \sum_1^M q_F^m \geq X \geq 0 \\ \frac{X}{M} + \frac{\alpha_s}{M(\alpha_t + \alpha_s)} \left((M-1)q_F^i - \sum_{1, m \neq i}^M q_F^m \right) & \text{if } X > \sum_1^M q_F^m \end{cases} \quad (2.10)$$

Assuming symmetric forward positions, we can examine the changes in production levels and price caused by deviation of one producer. In the event that power traded via forwards is larger than realized load, deviation in the forward position has no significance on the spot market. That is because no additional generators are needed in real-time. On the other hand, in the event that all firms generate additional power in real-time a deviation has an impact on generation cost and thereby market outcome. Suppose firm i chooses to deviate, the change in the level of output with respect to own forward position is¹³

$$\frac{\partial q^i(X, \vec{q}_F^m)}{\partial q_F^i} = \frac{M-1}{M} \times \frac{\alpha_s}{\alpha_t + \alpha_s} \quad (2.11)$$

and with respect to m 's position it is

¹³ Employing a Cournot approach implies that $\frac{\partial q_F^m(\cdot)}{\partial q_F^i} = 0, m = 1, \dots, M, m \neq i$.

$$\frac{\partial q^i(X, \vec{q}_F^m)}{\partial q_F^m} = -\frac{1}{M} \times \frac{\alpha_s}{\alpha_t + \alpha_s}, \quad m = 1, \dots, M, m \neq i. \quad (2.12)$$

Notice that since demand must be met at all times we get $\sum_{m=1}^M \frac{dq^m(X, \vec{q}_F^m)}{dq_F^i} = 0$.

Finally, a Cournot firm that chooses to deviate from the symmetric position expects (in the case of turning on generators in real-time) a spot price change of

$$\frac{\partial P_s(X, \vec{q}_F^m)}{\partial q_F^i} = -\frac{\alpha_s}{M}. \quad (2.13)$$

These derivatives become useful when we analyze the IPPs maximization problem.

The Cournot players (both IPPs and LSEs) observe both load predictions and forwards offers made by other firms¹⁴. Therefore we may treat the distribution of load and thereby the conditional distribution of spot price and expected production levels as common knowledge in our model.

Load Serving Entities and electricity demand

The objective of this section is to construct the aggregate demand curve for electricity forwards. Assume N identical LSE Cournot firms where each is committed to deliver $1/N$

¹⁴ Conceivably, participating and observing the outcome of 24 day-ahead and 24 real-time electricity markets being cleared on a daily basis may be considered as having complete information about the distribution of spot price. In addition, electricity markets, unlike any other commodity markets, are unique due to the presence of an ISO. As system operator and in most times the market administrator, the ISO reports the conditions of the power system continuously and make predictions accessible to all. The ISOs' reports also include supply and demand bids; volume of forwards traded and market prices. Doing so, the ISOs act as coordinators and diminish the value of private information. In addition to these transparencies, electric industries are typically more concentrated than other industries thereby making strategic modeling approach most relevant.

portion of the realized amount of electricity demand. In the short run (a year or more in the context of building a new large generator) LSEs are compensated by a fixed electricity retail price P_R . In every period the ISO announces a load prediction which is superior to any private forecast. Since this forecast is adopted by all market participants, information about prediction is symmetric. When overall load prediction is \hat{X} , each LSE's expected demand is \hat{X}/N . Armed with this information and taking its rivals' bids as given, LSE j maximizes profits by choosing a forward position x_F^j . That is

$$\begin{aligned} \mathbb{N} &\equiv \max_{x_F^j} E \left(\pi_{LSE}^j \left| \hat{X}, \sum_{n=1, n \neq j}^N \bar{x}_F^n \right. \right) \\ &= [P_R - P_F] x_F^j + \\ &\quad \int_0^{\infty} \left[P_R - P_s \left(X, \sum_{n=1, n \neq j}^N \bar{x}_F^n + x_F^j \right) \right] \times \left(\frac{X}{N} - x_F^j \right) f_x(X | \hat{X}) dX \end{aligned} \quad (2.14)$$

where \bar{x}_F^n is the quantity bid of player n , P_F is the market price of a forward contract and $f_x(X | \hat{X})$ is the conditional probability distribution function of load at the time of trading forwards.

LSE's expected profit has two payoff components; the first component in equation (2.14) stands for the payoff in trading forward contracts while the second component is the expected payoff associated with balancing power in the spot market. Substitute for the expected spot price in the symmetric case (2.9), the profits may be written as

$$\begin{aligned}
\mathbb{N} &= [P_R - P_F]x_F^j \\
&+ \int_0^{\sum_{1,n \neq j}^N \bar{x}_F^n + x_F^j} \left[P_R - \frac{\alpha_t}{M} X \right] \times \left(\frac{X}{N} - x_F^j \right) f_X(X|\hat{X}) dX \\
&+ \int_{\sum_{1,n \neq j}^N \bar{x}_F^n + x_F^j}^{\infty} \left[P_R - \frac{\alpha_t}{M} X - \frac{\alpha_s}{M} \left(X - \sum_{n=1, n \neq j}^N \bar{x}_F^n - x_F^j \right) \right] \\
&\quad \times \left(\frac{X}{N} - x_F^j \right) f_X(X|\hat{X}) dX.
\end{aligned} \tag{2.15}$$

The two integrals in equation (2.15) account for the two cases of need to balance power in real-time. The first integral is the expected spot payoff when the LSE has over-purchased power via forward contracts while the second stands for under-purchase of power. In the former, Contract for Differences (CFD) is put into effect. A typical CFD states that any deviation between forward power and spot power may be traded for the realized spot price. Essentially, CFD is a financial settlement that helps LSEs to hedge against volumetric risk on one hand and on the other helps IPPs avoid the cost and transmission problems associated with spot power surplus. The importance of a CFD settlement is discussed in detail in appendix 1.

Taking the derivative of \mathbb{N} with respect to the decision variable and employing the *Leibniz integral rule*, we get

$$\begin{aligned}
\frac{\partial \mathbb{N}}{\partial x_F^j} = & [P_R - P_F] - \int_0^{\Sigma_{1,n \neq j}^N \bar{x}_F^n + x_F^j} \left[P_R - \frac{\alpha_t}{M} X \right] f_X(X|\hat{X}) dX \\
& - \int_{\Sigma_{1,n \neq j}^N \bar{x}_F^n + x_F^j}^{\infty} \left[P_R - \frac{\alpha_t}{M} X - \frac{\alpha_s}{M} \left(X - \sum_{n=1, n \neq j}^N \bar{x}_F^n + x_F^j \right) \right. \\
& \left. - \frac{\alpha_s}{M} \left(\frac{X}{N} - x_F^j \right) \right] f_X(X|\hat{X}) dX .
\end{aligned} \tag{2.16}$$

The first order condition (FOC) for interior profit maximization is

$$\begin{aligned}
P_F = & \int_0^{\Sigma_{1,n \neq j}^N \bar{x}_F^n + x_F^j} \frac{\alpha_t}{M} X f_X(X|\hat{X}) dX + \\
& \int_{\Sigma_{1,n \neq j}^N \bar{x}_F^n + x_F^j}^{\infty} \left[\frac{\alpha_t}{M} X + \frac{\alpha_s}{M} \left(X - \sum_{n=1, n \neq j}^N \bar{x}_F^n - x_F^j \right) \right. \\
& \left. + \frac{\alpha_s}{M} \left(\frac{X}{N} - x_F^j \right) \right] f_X(X|\hat{X}) dX
\end{aligned} \tag{2.17}$$

or

$$P_F = E[P_S(\cdot)] + \frac{\alpha_s}{M} \int_{\Sigma_{1,n \neq j}^N \bar{x}_F^n + x_F^j}^{\infty} \left(\frac{X}{N} - x_F^j \right) f_X(X|\hat{X}) dX . \tag{2.18}$$

Notice that the second order condition (SOC) is clearly satisfied here as

$$\frac{\partial^2 \mathbb{N}}{\partial x_F^{j2}} = -\frac{2\alpha_s}{M} \int_{\Sigma_{1,n \neq j}^N \bar{x}_F^n + x_F^j}^{\infty} f_X(X|\hat{X}) dX < 0 . \tag{2.19}$$

Condition (2.18) describes the firm's inverse demand function for forward contracts. It is interesting to see that an LSE's willingness to pay for a forward contract exceeds the expected spot power price. Assuming risk neutrality generally drives the price of forward contracts to the commodity's expected spot price (storage is irrelevant for electricity). However, this result need not hold for the case of electricity. Since electricity has to be consumed at the time of production there is an economic value for pre-scheduling power for production (e.g. forward contracting). While for most commodities the time of production does not impact production cost, it does affect electricity generation cost. For that reason, according to condition (2.18) the LSE maximizes profits by choosing a forward position such that the marginal contract bought for price P_F is higher than the expected spot price. The wedge can be explained simply by the financial consequences of not contracting the marginal unit. In this case the marginal unit is not scheduled in advance, therefore its price also includes the expected cost of starting up additional generators. The expected additional cost of not scheduling the marginal unit is expressed by the RHS term in equation (2.18).

Since LSEs are identical all arrive to the same FOC. Considering the symmetric Cournot-Nash equilibrium where $x_F^1 = x_F^2 = \dots = x_F^N \equiv x_F$, the aggregate demand is

$$P_F = E[P_S(\cdot)] + \frac{\alpha_s}{MN} \int_{X_F}^{\infty} (X - X_F) f_X(X|\hat{X}) dX \quad (2.20)$$

where $X_F \equiv Nx_F$.

Corner solutions may arise where at optimum (1) $x_F = 0$; the price of a forward contract is too high to enhance LSE's expected profits or (2) $x_F \rightarrow \infty$; which is the case of a fully

hedged position. i.e. the forward price is lower than the expected spot price for any amount of forward bought.

Independent Power Producers and electricity supply

We start analyzing IPPs' behavior in a fully deregulated wholesale electricity market. That is to assume that IPPs' actions are not constrained by the ISO and therefore are motivated solely by profit maximization. Next, acknowledging IPPs' potential market power we will incorporate a lower bound on IPPs' output. This will be a more realistic examination since in principle IPPs can withhold a significant amount of capacity to raise prices and profits.

The optimization problem of each IPP is similar to that of a monopoly which faces an inverse demand function (equation 2.20) and takes its rivals output as given. Formally, IPP i chooses forward position q_F^i to maximize its expected profits

$$\begin{aligned}
\mathcal{M} &\equiv \max_{q_F^i} E \left(\pi_{IPP}^i \middle| \hat{X}, \sum_{m=1, m \neq i}^M \bar{q}_F^m \right) \\
&= P_F \left(\hat{X}, q_F^i + \sum_{m=1, m \neq i}^M \bar{q}_F^m \right) \times q_F^i \\
&+ \int_0^\infty \left[P_S \left(X, q_F^i + \sum_{m=1, m \neq i}^M \bar{q}_F^m \right) \times (q^i - q_F^i) - C(q^i, q_F^i) \right] f_X(X|\hat{X}) dX.
\end{aligned} \tag{2.21}$$

where \bar{q}_F^m is the quantity offered by rival m taken by i as given.

Express \mathcal{M} with respect to the two states of the world

$$\begin{aligned}
\mathcal{M} &= P_F \left(\hat{X}, q_F^i + \sum_{m=1, m \neq i}^M \bar{q}_F^m \right) q_F^i \\
&+ \int_0^{\sum_{m=1, m \neq i}^M \bar{q}_F^m + q_F^i} [P_S(X) - C(q^i)] f_X(X|\hat{X}) dX \\
&+ \int_{\sum_{m=1, m \neq i}^M \bar{q}_F^m + q_F^i}^{\infty} \left[P_S \left(X, q_F^i + \sum_{m=1, m \neq i}^M \bar{q}_F^m \right) \times (q^i - q_F^i) \right. \\
&\quad \left. - C(q^i, q_F^i) \right] f_X(X|\hat{X}) dX .
\end{aligned} \tag{2.22}$$

Taking the first derivative

$$\begin{aligned}
\frac{\partial \mathcal{M}}{\partial q_F^i} &= \frac{\partial P_F(\cdot)}{\partial q_F^i} q_F^i + P_F(\cdot) - \int_0^{\sum_{m=1, m \neq i}^M \bar{q}_F^m + q_F^i} P_S(\cdot) f_X(X|\hat{X}) dX \\
&+ \int_{\sum_{m=1, m \neq i}^M \bar{q}_F^m + q_F^i}^{\infty} \left[\frac{\partial P_S(\cdot)}{\partial q_F^i} \times (q^i - q_F^i) + P_S(\cdot) \times \left(\frac{\partial q^i}{\partial q_F^i} - 1 \right) \right. \\
&\quad \left. - C'(q^i, q_F^i) \right] f_X(X|\hat{X}) dX .
\end{aligned} \tag{2.23}$$

Writing explicitly the derivatives of the spot price and the cost function

$$\begin{aligned}
\frac{\partial \mathcal{M}}{\partial q_F^i} &= \frac{\partial P_F(\cdot)}{\partial q_F^i} q_F^i + P_F(\cdot) - \int_0^{\sum_{m=1, m \neq i}^M \bar{q}_F^m + q_F^i} P_s(\cdot) f_X(X|\hat{X}) dX \\
&+ \int_{\sum_{m=1, m \neq i}^M \bar{q}_F^m + q_F^i}^{\infty} \left[-\frac{\alpha_s}{M} \times (q^i - q_F^i) + P_s(\cdot) \times \left(\frac{\partial q^i}{\partial q_F^i} - 1 \right) \right. \\
&\quad \left. - \alpha_t q^i \frac{\partial q^i}{\partial q_F^i} - \alpha_s (q^i - q_F^i) \left(\frac{\partial q^i}{\partial q_F^i} - 1 \right) \right] f_X(X|\hat{X}) dX.
\end{aligned} \tag{2.24}$$

Employing symmetry and collecting terms

$$\begin{aligned}
\frac{\partial \mathcal{M}}{\partial q_F^i} &= \frac{\partial P_F(\cdot)}{\partial q_F^i} q_F^i + P_F(\cdot) - E[P_s(\cdot)] \\
&+ \alpha_s \left(1 - \frac{1}{M} \right) \int_{\sum_{m=1, m \neq i}^M \bar{q}_F^m + q_F^i}^{\infty} (q^i - q_F^i) f_X(X|\hat{X}) dX.
\end{aligned} \tag{2.25}$$

The FOC is

$$\begin{aligned}
P_F(\cdot) &= E[P_s(\cdot)] - \frac{\partial P_F(\cdot)}{\partial q_F^i} q_F^i \\
&- \alpha_s \left(1 - \frac{1}{M} \right) \int_{\sum_{m=1, m \neq i}^M \bar{q}_F^m + q_F^i}^{\infty} (q^i - q_F^i) f_X(X|\hat{X}) dX.
\end{aligned} \tag{2.26}$$

The first derivative of the forward price with respect to quantity is

$$\frac{\partial P_F(\cdot)}{\partial q_F^i} = -\frac{\alpha_s}{M} \left(1 + \frac{1}{N} \right) \int_{\sum_{m=1, m \neq i}^M \bar{q}_F^m + q_F^i}^{\infty} f_X(X|\hat{X}) dX. \tag{2.27}$$

Solving for the symmetric Cournot-Nash equilibrium where $q_F^1 = q_F^2 = \dots = q_F^M \equiv q_F$ gives the following optimality condition

$$\begin{aligned}
P_F(\hat{X}, Mq_F) = E[P_S(\cdot)] + \frac{\alpha_S}{M} \left(1 + \frac{1}{N}\right) q_F \int_{Mq_F}^{\infty} f_X(X|\hat{X}) dX \\
- \alpha_S \left(1 - \frac{1}{M}\right) \int_{Mq_F}^{\infty} (q - q_F) f_X(X|\hat{X}) dX.
\end{aligned} \tag{2.28}$$

The willingness to sell forward contracts may be higher or lower than the expected spot price. Withholding capacity has two effects. On the one hand it maintains high prices in both spot and forwards markets. On the other hand, an IPP firm that chooses to offer more forward contracts sells more power in the spot market as well.

We show in appendix 2 that the IPP's profit function is strictly concave in q_F^i . This confirms that if a symmetric Cournot-Nash equilibrium exists it is a unique symmetric solution for the IPP's problem.

Solving the model

If there is a forward price P_F^* at which the market clearing condition $q_F^* M = X_F^*$ holds, then we say that the market for forward contracts has an interior symmetric solution. Equating aggregate demand with aggregate supply (equations 2.20 and 2.28) the following must hold

$$\begin{aligned}
P_F^*(X_F^*) &= E[P_S(\cdot)] + \frac{\alpha_S}{MN} \int_{X_F^*}^{\infty} (X - X_F^*) f_X(X|\hat{X}) dX \\
&= E[P_S(\cdot)] + \frac{\alpha_S}{M} \left(1 + \frac{1}{N}\right) q_F^* \int_{X_F^*}^{\infty} f_X(X|\hat{X}) dX \\
&\quad - \alpha_S \left(1 - \frac{1}{M}\right) \int_{X_F^*}^{\infty} (q - q_F^*) f_X(X|\hat{X}) dX
\end{aligned} \tag{2.29}$$

which solves for the equilibrium quantity of aggregate forward contracts

$$X_F^* = \left(\frac{MN + M - N}{MN + M + 1} \right) \times \frac{\int_{X_F^*}^{\infty} X f_X(X|\hat{X}) dX}{\int_{X_F^*}^{\infty} f_X(X|\hat{X}) dX} . \tag{2.30}$$

Substituting this result back into (2.20) the equilibrium forward price is

$$\begin{aligned}
P_F(X_F^*) &= E[P_S(\cdot)] + \left(1 - \frac{MN + M - N}{MN + M + 1}\right) \times \frac{\alpha_S}{MN} \int_{X_F^*}^{\infty} X f_X(X|\hat{X}) dX \\
\Rightarrow P_F(X_F^*) &= E[P_S(\cdot)] + \frac{\alpha_S(N+1)}{MN(MN+M+1)} \int_{X_F^*}^{\infty} X f_X(X|\hat{X}) dX .
\end{aligned} \tag{2.31}$$

Then, the forward price can be expressed by summing the expected spot price and the forward premium

$$P_F = E[P_S(\cdot)] + R_F \tag{2.32}$$

where

$$R_F = \frac{\alpha_S(N+1)}{MN(MN+M+1)} \int_{X_F^*}^{\infty} X f_X(X|\hat{X}) dX .$$

Preliminary results and discussion

At this point we can make some statements about the equilibrium volume and price of forward contracts. The equilibrium volume of forwards depends on the number of IPPs and LSEs in the market and the stochastic nature and precision of load forecasting. It is easy to see that the equilibrium volume of forward contracts increases in the number of power producers. As the number of IPPs increases, it is less effective for these firms to maximize profits by withholding production. It is not a surprising result seeing that power producers engage in an oligopoly game and the demand side in the model is completely inelastic in real-time. Furthermore, expression (2.30) shows that the equilibrium number of forwards increases in M at a decreasing rate. This reflects the rate at which market power diminishes in the number of producers.

In the contrast, the equilibrium number of forwards decreases in the number of LSE firms. The explanation for this result is quite intuitive and related to the public good aspect of electricity forwards. LSEs share the responsibility to deliver any realized amount of load in real-time. Similar to the familiar *free-rider problem* each LSE firm would prefer that other firms purchase forward contracts which would then lower the expected spot price for all buyers. But with a relatively large number of firms, the ability of each firm to manipulate the spot price is relatively small. Accordingly, the aggregate willingness to purchase forward contracts decreases in the number of LSEs (illustrated and further discussed in the next section).

The absence of the cost parameters α_t and α_s from the expression describing the equilibrium amount of forwards is a noteworthy result. It means that the level of forwards in equilibrium

is fixed over the range of positive cost parameters. Since LSEs demand in spot market is inelastic, IPPs decision on the amount of forwards is contingent on the distribution of load only. Accordingly, the impact of the cost parameters on welfare distribution in equilibrium is captured only by the forward price.

The wedge between the price of forwards and the spot price is rooted in the dynamic nature of the supply curve. Since the cost of generating power is increasing in the time of trade (due to ramp-up time), the link between expected spot price and the forward price is not one to one. In particular, the forward premium is proportional to the incremental startup cost of generation units (α_s). This result expresses our assertion that the premium is driven by the dynamic nature of production cost. LSEs desire to avoid this cost in the spot market and the ability of producers to exercise market power in the forward market determines the size of the forward premium. Notice that the premium R_F is positive in expectations and decreases in both the number of IPP and LSE firms.

Still, there are two cases where the spot and forward prices may coincide and reproduce the familiar competitive solution under risk neutrality assumption. First, consider the case of omitting ramping costs from the analysis. This can be expressed by imposing $\alpha_s = 0$; zero incremental cost between the two periods of trade t and s . Then, aggregate demand for forward contracts would be characterized by¹⁵

$$X_F^* = \begin{cases} 0 & \text{if } P_F > E[P_S] \\ [0, \infty) & \text{if } P_F = E[P_S] \\ \infty & \text{if } P_F < E[P_S] \end{cases} . \quad (2.33)$$

¹⁵ To arrive to this result simply maximize equation (2.15) and impose $\alpha_s = 0$.

In this case the Nash equilibrium is characterized by any non-negative amount of forward contracts as IPPs cannot enhance their expected profits by withholding capacity.

Secondly, there would be no wedge in expectations if the number of IPP or LSE firms is sufficiently large. In particular, the forward price converges to the competitive price in the limit as $M \rightarrow \infty$ or $N \rightarrow \infty$. In any of these cases the forwards premium goes to zero and the forward equilibrium price would reflect the expected spot price.

To conclude this part, the model is able to explain the positive forwards premiums reported by many empirical studies (e.g. Benth, Cartea and Kiesel 2008, Bessembinder and Lemmon 2002, Cartea and Villaplana 2008, Douglas and Popova 2008, and Longstaff and Wang 2004). Yet, it is important to perceive a fundamental difference between our work and the related body of literature in this area. The results presented by this model are not driven by a risk preferences assumption but by the basic properties of power generation cost structure, the number of sellers, buyers, and the commonly adopted design of deregulated electricity markets.

Capacity withholding constraint

The equilibrium volume and price of forward contracts developed in previous sections characterize the solution in a fully deregulated electricity market. Our results make it clear that IPPs have an incentive to manipulate market prices by withholding generation capacity in the forward market to maximize the joint profits from the spot and forward markets. While welfare loss is typically expected in a Cournot competition, the loss in electricity markets is

more severe than in other markets in which market power is present. That is because spot power demand is inelastic; the power is being generated eventually in spite of any capacity withholding behavior. Consequently, the production of power in real-time may be inefficient and cause misuse of energy resources. Policy makers and administrators of deregulated electricity markets are aware of this problem. Yet, in practice it is not an easy task to measure when market power is exercised. Overall operating costs and production constraints are not transparent. Operating costs includes the incremental cost involves in shifting to power plants of higher heat rates, start up and shut down costs and others¹⁶. Those as well as a physical withholding due to outages and periods of maintenance are essentially private information and therefore precise mark-ups are complicated to estimate.

Although there is an ongoing debate about what is the effective way to measure and monitor the degree of competitiveness of wholesale electricity markets, some provisions are commonly implemented. For example, the Hirschmann-Herfindahl Index (HHI) is used as a first screening tool for market power by governmental agencies. Price caps are used frequently as an upper bound for spot price. The price cap is useful in stabilizing the volatility of spot markets and limiting LSEs' exposure to spot prices. Finally, and maybe the most effective and frequently used tool to deal with uncompetitive behavior is to impose a *must-offer* provision. Doing so, ISOs limit the ability of large producers to exercise market power by forcing them to participate and offer their capacity in forward and spot markets. In addition, the ISOs examine regularly whether the prices offered by IPPs enable them to schedule considerable volume in advance, bilaterally and via forward markets.

¹⁶ Mansur (2008) shows that by ignoring production constraints such as ramping costs, several studies overestimated the exercise of market power in electricity markets.

In some markets the expected load is used to determine producers' responsibilities for forward contracting. In the California ISO for example, if the amount of power cleared by the forward markets is insufficient, a secondary auction takes place. The Residual Unit Commitment (RUC) is an auction designed to force IPPs to supply the expected missing amount based on their incremental cost. In the case that IPPs are able to demonstrate market power while trading forwards, the RUC as a more regulated mechanism, is not a favorable alternative for them.

Back to our model, a binding constraint on the offered capacity in forwards markets forces IPPs to move away from their optimal forwards positions. Since IPPs are identical it is reasonable to look at the case where the ISO imposes a symmetric constraint on the minimum amount of power that each IPP is held responsible to offer. In this case, IPPs do not have any incentive to offer more than their own constraint because that will increase their distance from the unconstrained (optimal) solution thus decreasing their profits further. Therefore, the aggregate volume of forwards imposed by the firm-level constraints can be mapped to a particular point on the demand curve.

Frequently, ISOs sets a volumetric constraint which is a function of the moments of the forecasted load. A straightforward example is the one mentioned above, where IPPs are required to offer at least the expected load. In this case the forward price mapped from the demand curve is simply

$$P_F = E[P_S(\cdot)] + \frac{\alpha_S}{MN} \int_{X_F}^{\infty} (X - X_F) f_X(X|\hat{X}) dX \quad (2.34)$$

which can be simplified further assuming a particular conditional probability distribution function.

Computational experiments

We conducted many simulations to evaluate the effectiveness of the model in capturing the economic determinants in electricity markets. We present and discuss in this section the model predictions and the sensitivity of the results to the parameters employed in the analysis. We consider the following figures for the base-case scenario in the numerical analysis. Assume that there are 5 IPP and 5 LSE firms, the cost parameters of generating power are $\alpha_t = 1$, $\alpha_s = 2$ and load is distributed normally and expected to be 100 at real-time. Also, the standard deviation of load prediction is 5 (mean absolute error of 4% of the expected value) when forecasting demand at the day-ahead.¹⁷ All the numerical results consist of 5,000 draws.

Spot price distribution

The model focuses on one particular delivery period at a time. Since there is a great variability in the seasonal, diurnal, hourly and other temporal characteristic of electricity demand we start by evaluating the flexibility of the model to accommodate analyses of different delivery periods.

¹⁷ Various sources indicate a MAE of overall load prediction in the range of 3%-5%, depends on the season and the size of the region.

We consider periods that are characterized by expected loads in the range of 50 to 150. The variance is computed as $\sigma^2 = \frac{1}{n} \sum_{i=1}^n (x_i - \bar{x})^2$. Doing so, we normalize the variance with respect to the expected load of the period in question.

Figure 2 displays the densities of spot market prices by expected electricity demand. In particular, the middle density is the one that illustrates the base-case scenario. The densities are skewed as implied by the two-state cost function. For periods of higher than average expected load the spot price density is shifted right and its variation is higher. In reality, even hourly prices in a single day are drawn from very different distributions. Demand (and thereby prices) at 2am would fit a density in the left side of figure 2. Spot price at 5pm of the same day would be characterized by a density on the right side of the same figure as this is usually the peak load hour of the day.

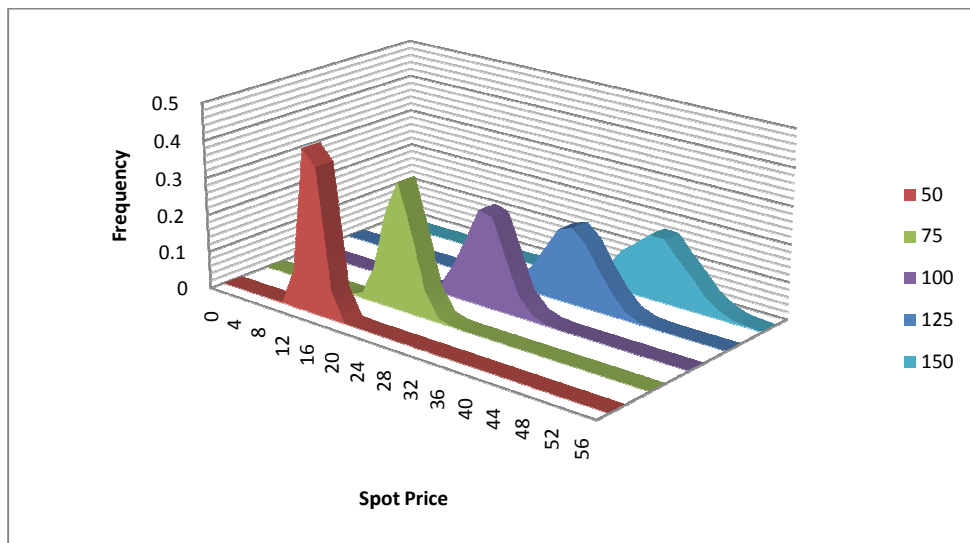


Figure 2: Spot market price densities by expected electricity demand

Load uncertainty

We let standard deviation of load to vary between 5 and 35 to explore the impact of load uncertainty on market equilibrium. Given spot price expectations, the demand for electricity forwards is illustrated in figure 3. As we increase the uncertainty regarding real-time load, demand for forwards shifts upward and becomes smoother. This reflects the higher probability of making errors in load forecasting and therefore increases LSEs willingness to pay for forward contracts.

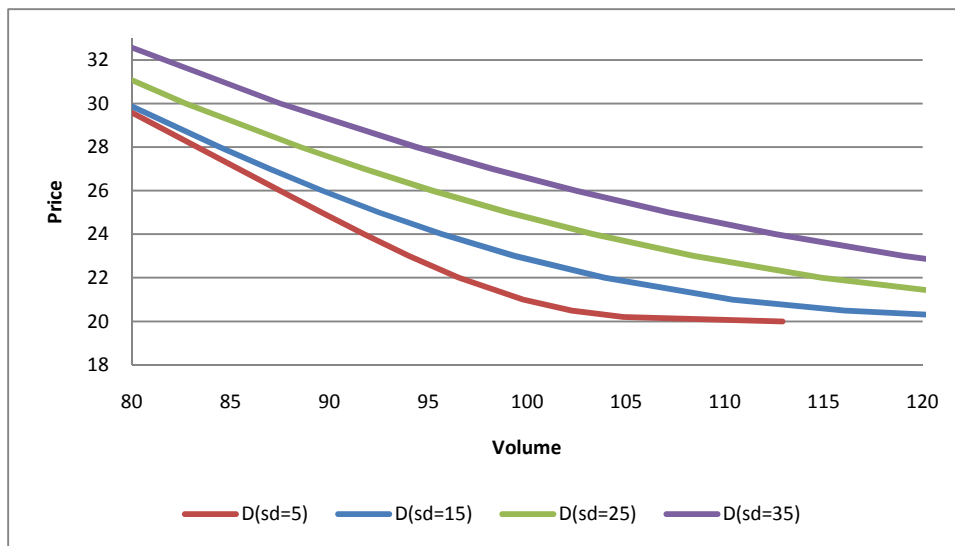


Figure 3: Aggregate demand for electricity forwards as a function of standard deviation of load

Given demand for forwards, each IPP chooses how much electricity to offer in forward markets which then determines the aggregate supply curve in the spot market. Equilibrium in the forwards market is described in figure 4 for various levels of standard deviation of load. The intersections of the dashed vertical line and the demand curve for forwards in the graphs

in figure 4 describe the equilibrium price and quantity of forward contracts in each. Once the forward market is cleared, production cost of any possible realization of load and thereby spot price is determined. The equilibrium is characterized by a capacity withholding as one would expect in an oligopoly modeling. The kink on the supply curve at the equilibrium quantity of forwards describes the shift into a less efficient power production scheme in the event that real-time load is higher than the prescheduled amount. Then, the equilibrium at the spot market may be depicted as the intersection of the illustrated supply curve and an inelastic demand curve created by any given realization of load.

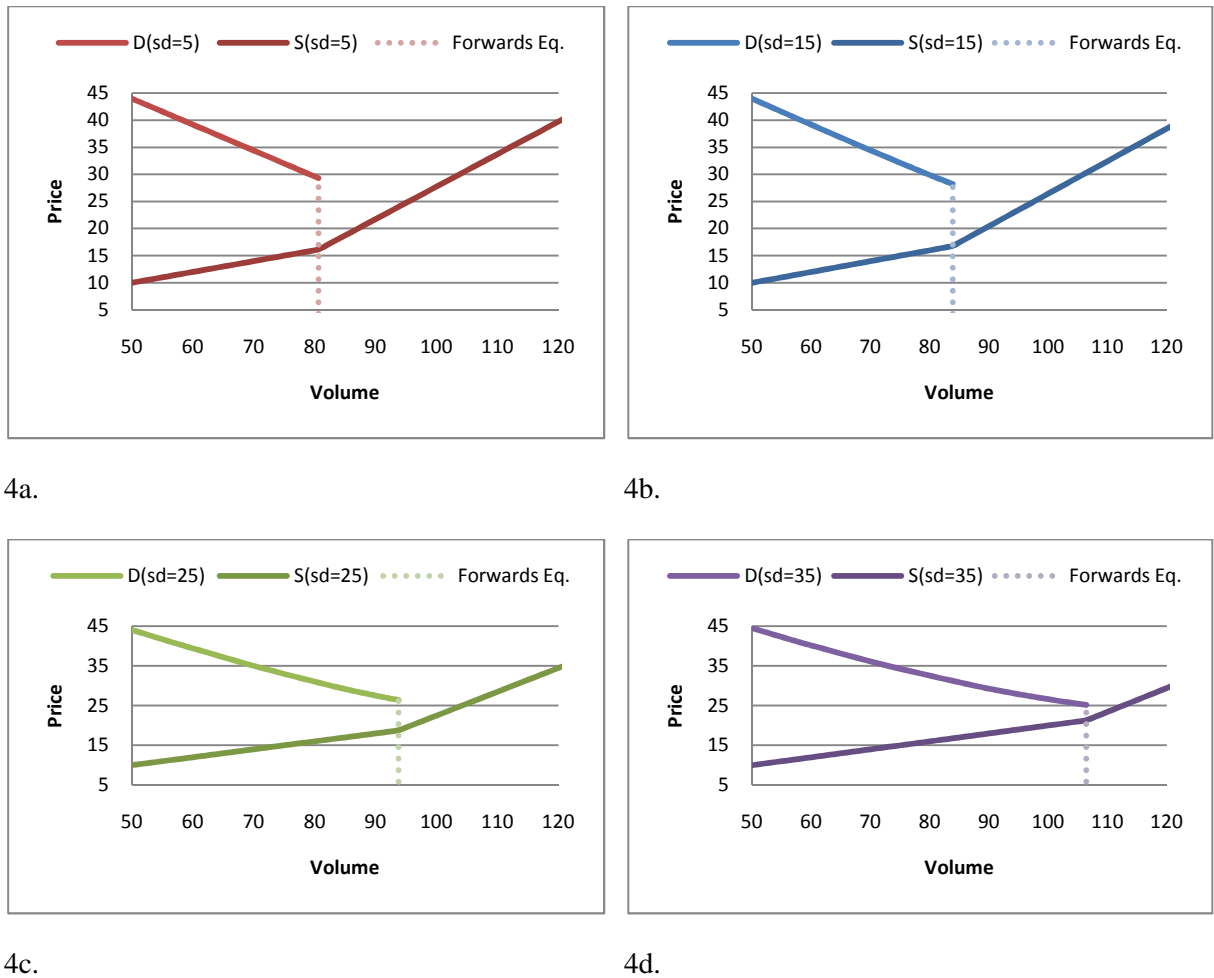


Figure 4: Equilibrium in the forwards market and the consequence real-time supply curve. Results by standard deviation of load of sizes 5, 15, 25 and 35 are depicted in figures 4a, 4b, 4c and 4d respectively

The numerical experiments show that the equilibrium amount of forwards increases in load uncertainty. Demand for forwards increases in standard deviation but demand is also more elastic. Consequently, IPPs maximize profits by offering more forward contracts. Doing so, forward premiums decrease in load uncertainty since more power is scheduled in advance (figure 5).

In the base-case scenario, the expected forward premium is about 5.6% and decreasing with load uncertainty. Similarly to real-world observations, the model generates higher (lower) premiums for peak (base) load periods.

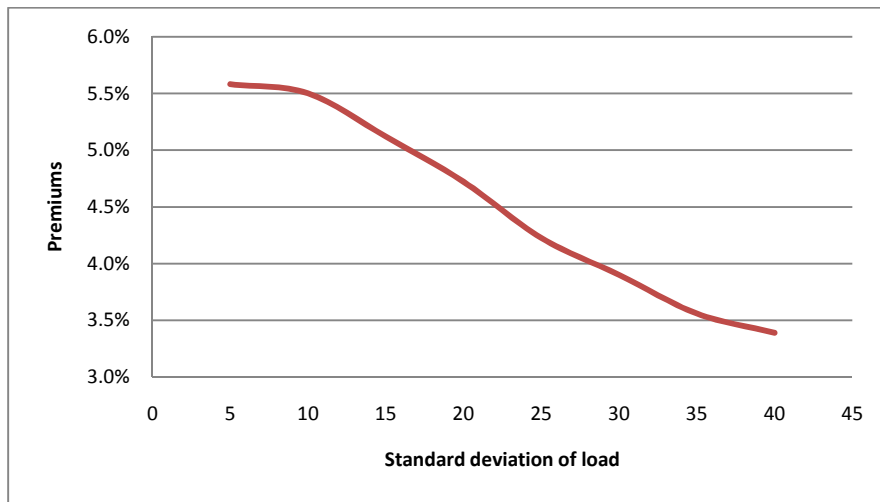


Figure 5: Forward premiums as a function of standard deviation of load

The number of IPPs and LSEs

In a standard Cournot competition the degree to which market power can be exercised is captured essentially by the number of oligopoly players. For example, in the case of a single producer the model outcome coincides with the solution for the monopoly's profit maximization problem. In the case of a duopoly, aggregate profits will be less than the situation of two producers acting as monopolies, and lastly, for a sufficient number of producers the profits would be similar to those generated under perfect competition. On this aspect, the model developed here generates market power dynamics which is similar to the results described by a standard Cournot model.

In figure 6 we examine the results for the simulations of the base-case scenario varying the number of power producers. As the number of IPPs increases, more electricity is settled via forward contracts. This is due to the decrease in IPPs ability to exercise market power by withholding capacity. For example, the particular parameters employed here shows that without any regulation a single IPP would offer less than 15% of the expected load for forward contracting. The amount increases at a decreasing rate; one half in a duopoly electric industry and so on.

The equilibrium prices and profits generated by different numbers of producers are not comparable since the cost function of generating power is convex. Yet, we may evaluate the sensitivity of forward premiums to the number of IPPs. Similar to the equilibrium amount of forwards, the change in premiums also reflect the change in the ability to exercise market power (figure 6). Interestingly, the illustration shows that the model predicts positive premiums even when the amount of electricity traded via forwards exceed the predicted load.

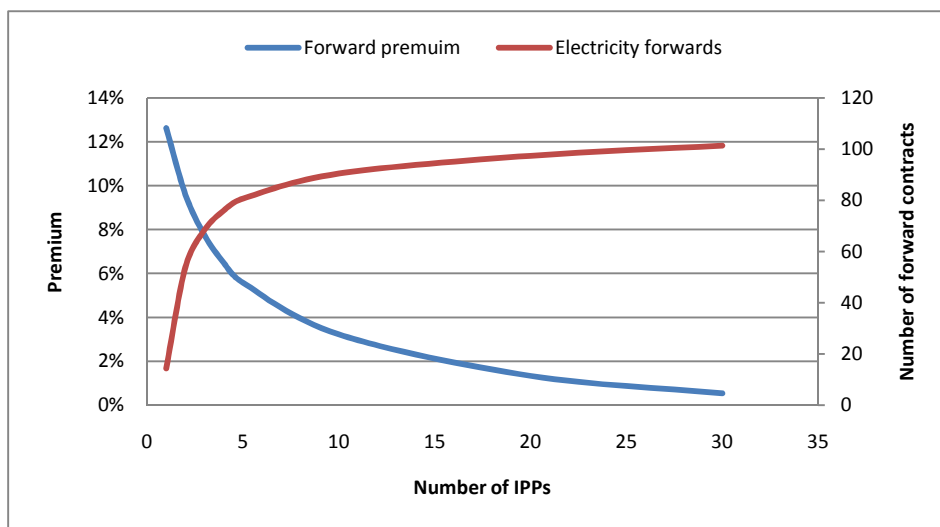


Figure 6: Equilibrium electricity forwards and premiums by number of IPPs in the market (base-case scenario assumptions)

Looking at the number of LSE firms reveals a very similar trend in the forward premiums. Except that the premium decreases here are not due to an increase in the number of forwards. LSEs' incentive to purchase forward contracts is for the purpose of decreasing the expected spot price. Although the decision on the procurement of forwards is taken on the firm level, it has a public good aspect for all LSEs; a lower expected spot price.

When the number of LSEs is relatively small, the quantity purchased by an individual firm has a greater impact on the spot price hence the willingness to pay is higher. As the number of LSEs increases, each firm's ability to influence the spot price is smaller and that encourages a free-rider behavior. As a result, when we increase the number of LSEs the volume of trade is almost constant but the premium reflects the diminishing interest in hedging spot market risk by forward contracting (figure 7).

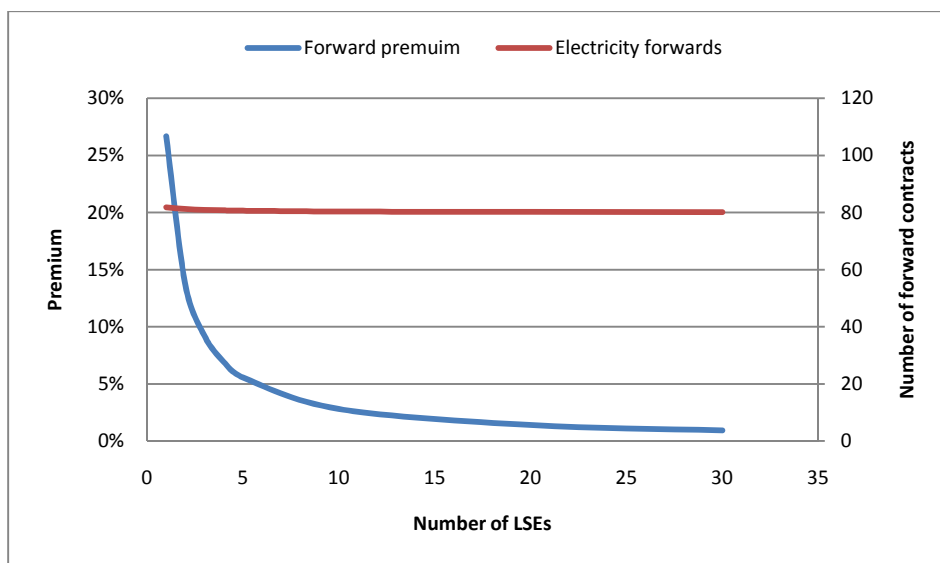


Figure 7: Equilibrium electricity forwards and premium by number of LSEs in the market (base-case scenario assumptions)

Cost of generating power

Our analytical results from previous sections show that the forward price depends linearly on the cost parameters α_t and α_s . This result holds whether the market is fully deregulated (eq. 2.32) or whether capacity constraint is being imposed (eq. 2.34). When we look at the forward premium we see that the wedge between the spot price and the forwards price is fixed for any positive value of α_t . The reason for that is the fact that α_t is an essential cost which cannot be avoided in any state of the world. That is an expected result since the demand for hedging power is created by the fact that generating power by starting up generators is more costly. On the other hand, the forward premium divided by the expected spot price is increasing approximately linearly in α_s (figure 8).

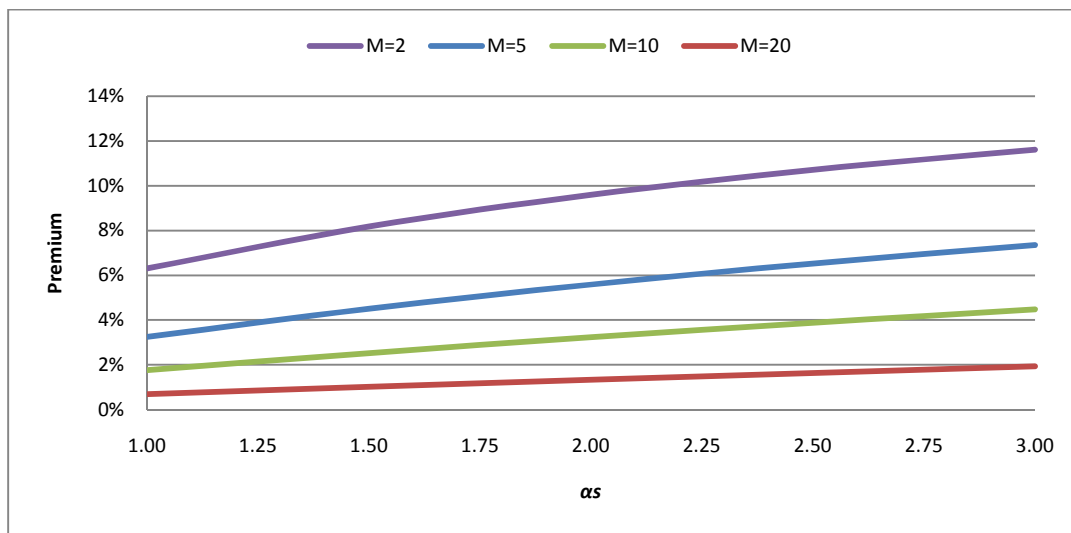


Figure 8: Premiums as a function of real-time cost parameter and the number of IPPs

Capacity withholding constraint

The base-case scenario provides solution for a fully deregulated electricity market for a given set of assumptions. Keeping the same set of assumptions we compare this unconstrained solution with particular levels of capacity constraints the ISO may impose on IPPs to offer in forward markets.

The results are presented in figure 9. The model emphasizes the effectiveness of imposing a capacity constraint in electricity forwards markets. In this example the unconstrained aggregate amount offered by 5 power producers is 80.6, which is in the order of four standard deviations lower than the expected load. The illustration shows that the forward price and IPPs profits decrease in the magnitude of the must-offer constraint. Notice that the constraint is much more effective in the range which it is lower than the expected load. This is due to the asymmetric financial consequences that all market participants experience if realized load is lower or higher than expected.

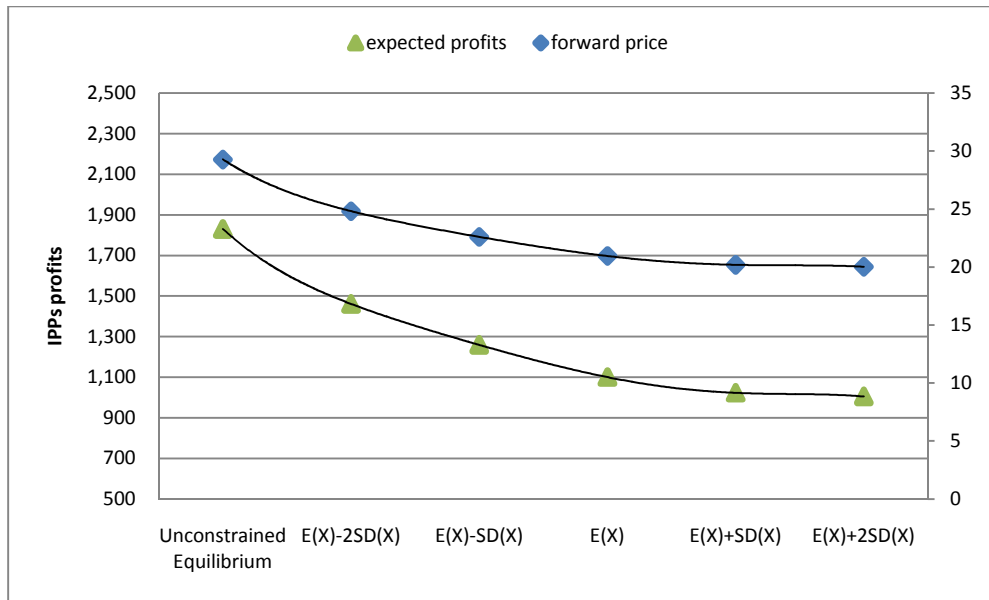


Figure 9: Equilibrium forward price and IPPs expected profits by a capacity withholding constraint

Chapter summary

In this chapter a new theoretical framework for modeling deregulated electricity markets has been developed. The model complies with the desired characteristics we list at the beginning of the chapter. It incorporates firms' behaviors in electricity markets to construct transparent and traceable market equilibrium measures. In addition, we performed computational experiments to demonstrate how the model can be employed in studying applied problems. We presented sensitivity analysis for the impact of parameters describing generation costs, industry structure and uncertainties on market equilibrium. The model showed itself to be flexible and accommodating large arrays of assumptions regarding the characteristics of the delivery period of electricity.

Similar to real-world electricity markets, the distributions of the spot price at different delivery periods in the model diverge greatly. Also, the model generates a wedge between the forward price and the expected spot price. This result is in line with the extensive empirical evidence suggesting the existence of a forward premium. While the literature commonly refers to this wedge as a risk premium, the results presented by this model are not driven by a risk preferences assumption but by the electric industry structure, fundamental properties of electricity production and the design of deregulated electricity markets.

Finally, we show that the deadweight welfare loss associated with a fully liberalized market could be substantial. Having various generation technologies, IPPs have an incentive to substitute away from the more efficient generating units for expensive spot power production. This in turn generates sizeable premiums for forward contracts and supernormal profits. When we add a capacity withholding constraint (also known as a must-offer provision), the welfare loss and premiums are reduced.

In the rest of the study, the model developed here is extended to allow thorough examination of the possible paths and market outcomes for wind power integration. In particular, the required extension of the theoretical model is introduced in chapter 4, and the appropriate numerical methodology for simulating scenarios of wind power integration is developed in chapter 5.

Chapter 3: Wind power

Introduction

Our objective in this chapter is to discuss the technical, statistical and financial principles of wind power capacity. We start with a review of recent developments, current status and challenges of wind power expansion. Then, we make use of Iowa wind speed data to explain and illustrate the basics of wind speed statistics and the estimation of a local wind speed probability distribution density. Next, we give details about the relation among wind speed, wind power resources and usable wind power, by exemplifying the performance of a typical modern large wind turbine. In doing so, we explore spatial differences as well as month to month variability of harvesting wind power at selected sites in Iowa. In the following section, we outline some findings from the literature regarding wind spatial correlation. This is particularly relevant for this study since we are interested in modeling an intermittent regional wind power supply. Lastly, we discuss the implications of uncertain power supply with relation to electricity markets and our economic framework in particular.

Overview

Global installation of wind power capacity has been increasing rapidly during the last two decades. In particular, more than 30% of the world's wind power capacity was added just in 2008 (DOE 2009). The highest penetration rate is experienced by Denmark where wind

power accounts for 20% of overall electricity consumption. Next, Spain followed by Portugal, Ireland and Germany demonstrate penetration rates in the range of 7%-12%. In many other countries wind power capacity has increased recently as well, yet accounts for only up to 5% of overall capacity. When it comes to overall wind power capacity, the ranking is quite different. During 2008 the U.S. overtook Germany to take the lead in cumulative wind capacity with 25,369 MW vs. 23,933 MW in Germany. However, the percentage of wind power consumed in the U.S. accounts only for 2% of overall electricity consumption. Other countries with increasing wind capacity but still low penetration rates are India and China (about 3% and 1%, respectively). This trend suggests that there is room for large increases in wind capacity in many countries.

Several linked forces may explain the growth in wind power capacity in recent years. First, advances in wind harvesting technologies have allowed larger turbines to be installed. The average wind turbine installed in the U.S. in 2008 was rated at 1.67 MW of capacity, which is 133% higher than average rated capacity of turbines in 1998-1999. Nowadays, engineers have completed the design and manufacturing of 3 MW turbines, which are the largest commercial turbines to come online. As we explain in the next section, economies of scale are important in wind power production. Therefore, the ability to transport, install and connect larger turbines to the grid at sites with appropriate wind speed conditions yields increasing returns. Scale effects, technological advances in turbine designs and better transmission lines have significantly lowered the cost of harvesting and delivering wind power over the years.

Government subsidies supporting renewable energy have also increased, reducing the private cost of wind projects further. The main justifications for these subsidies are energy independence and reductions in environmental externalities from the combustion of fossil fuels. Life cycle assessment studies show that the energy payback time of a wind turbine is less than six months over a 20 year life time (Martínez, et al. 2009; Schleisner 2000). Switching from conventional generators that run on coal and natural gas to wind turbines mitigates almost all greenhouse gasses emissions related to the production of electricity. Martínez et al. show that the cradle to grave environmental contamination of wind project may be recovered nearly 31 times during the life of a wind turbine.

Concerns regarding dependency on fossil fuels brought forward the importance to diversify energy portfolios. Employing various renewable energy sources in a portfolio is a practical way to promote energy security. A renewable portfolio standard (RPS) is a state policy in the U.S. and in some other countries that support this goal. RPSs mandate the shares of electricity to be produced from wind, solar, hydro, biomass and other renewable energy sources.

In addition, speculations about fuels reserves and their price behaviors encourage investments in wind power projects. The intrinsic variation of wind speed is uncorrelated with fuel markets. From a risk management point of view, this fact alone may enhance an energy portfolio in a firm level.

Several factors need to be considered and resolved before the installation of significant new wind power capacity becomes feasible. The main challenge with large projects is updating transmission systems. Wind capacity that exceeds local electricity demand requires

additional costs associated with updating the grid and constructing adequate transmission lines. Even so, many wind farms are constructed in rural areas. That is because of two main advantages those areas have over urban areas: land availability for wind projects and the decrease of the potential problems associated with turbines' sound due to relatively low population density. Since power systems in rural areas are not structured to handle electricity flows from large wind farms, integrating new wind capacity to the grid involves substantial planning and investments. The costs of updating transmission lines to deliver energy from distant areas to hubs of electricity are usually governed by the regional system operators.

The physical aspect of setting up wind turbines is another limiting factor. Costs related to transportation and installation of large turbines increase exponentially with size. Therefore, the benefit from scaling up wind projects should be weighed against the cost of the extra logistics involved. For example, on shore turbines used to be generally larger than offshore ones due to ground transportation constraints. Also, the delivery (if applicable) and installation requirements become more complex when dealing with larger components. To be able to overcome the downside of shipping and handling turbine's parts over long distances, factories manufacturing these parts may be constructed in mainland areas. For instance, Iowa and its surrounding states are in the process of creating a conglomeration of plants for turbines, blades and towers.¹⁸ For that reason, it is not surprising that Iowa is ranked second in the U.S. with current wind capacity of 3043.28 MW and first in wind power consumption

¹⁸ For example, during 2008 alone the following facilities came online: Clipper Windpower (Cedar Rapids), Acciona Energy North America (West Branch), Siemens Power Generation (Fort Madison) and TPI (Newton).

of 13.3%.¹⁹ Wind capacity expansion in that region in recent years is explained partly by the availability of locally manufactured parts.

Finally, once adequate infrastructures are established and turbines had been constructed the transmission itself is not cost free. Long distance power transmissions and distributions incur line losses. The costs associated with these losses are particularly relevant for wind farms constructed in rural areas.

Wind speed

Wind is caused by differences in air pressure within the atmosphere. Air tends to flow from regions of high pressure to regions of low pressure. The difference in pressure is the outcome of uneven heating of the earth by solar radiation. Therefore, wind variation may be viewed based on annual, seasonal, diurnal, hourly and inter-hourly differences. These variations need to be acknowledged and evaluated properly for wind energy considerations.

Numerous probability density functions (pdf) have been employed in applications of wind speed studies. Carta, Ramirez and Velazquez (2008) carry out a review based on more than two hundred studies describing wind speed frequency distributions. The most frequently employed is the two-parameter Weibull pdf which has been found to have a series of advantages. Among these are dependency on two parameters only, flexibility, simplicity and a good fit to measured data. The Weibull is generally an appropriate pdf choice for wind speed modeling with one exception. For regions that have frequent occurrences of no wind,

^{18, 19, 21} American Wind Energy Association, <http://www.awea.org/projects/projects.aspx?s=Iowa> (accessed August 09).

other probability distributions may be more suited. The catalog presented by Carta, Ramirez and Velazquez (2008) review the appropriate pdfs in this circumstance as well. However, since the decision on location for wind farms is not random, sites with low wind speeds are unlikely choices for wind projects. Thus we focus on the Weibull pdf in this study. Next, we give some details how to go about employing the Weibull pdf to describe the statistics of wind speed.

Let v (m/s) denote wind speed, c (m/s) and k the scale and the shape parameters of the Weibull pdf respectively, then the wind speed density function can be written as

$$f(v) = \frac{k}{c} \left(\frac{v}{c}\right)^{k-1} \exp\left[-\left(\frac{v}{c}\right)^k\right] . \quad (3.1)$$

Some families of distributions are obtainable as special cases of the Weibull distribution. For example, for $k=1$ the Weibull distribution becomes an exponential distribution. In the case of $k=2$ the distribution is reduced to the Rayleigh distribution, which if applicable simplifies the analysis of wind speed considerably²⁰. For the special case of $k=3.6$ the Weibull distribution is approximately normal (Dubey 1967). It was shown that a simple data transformation can make the relation between the Weibull and the Gaussian distributions very useful for studying wind speed (Torres, et al. 2005). The transformation is based on the fact that a Weibull distribution raised to the power of a is also a Weibull. Let $a = k/3.6$ and raise wind speed data to the power of a , then wind speed data may be analyzed with respect to the normal distribution. In figure 10 we describe the distributions for the case that wind

²⁰ The knowledge of mean wind speed alone is sufficient to employ the Rayleigh distribution. Denote mean wind speed by m , the pdf can be described as $f(v) = \frac{\pi}{2} \left(\frac{v}{m}\right) \exp\left[-\frac{\pi}{4} \left(\frac{v}{m}\right)^2\right]$.

speed has Weibull distribution with the parameters $k=2.2$ and $c=3$. It is shown that an approximation to the Weibull may be obtained by employing one of the other distributions discussed here. The decision on which distribution to apply and the consequent goodness of fit is determined by the particular shape parameter of the Weibull pdf in use.

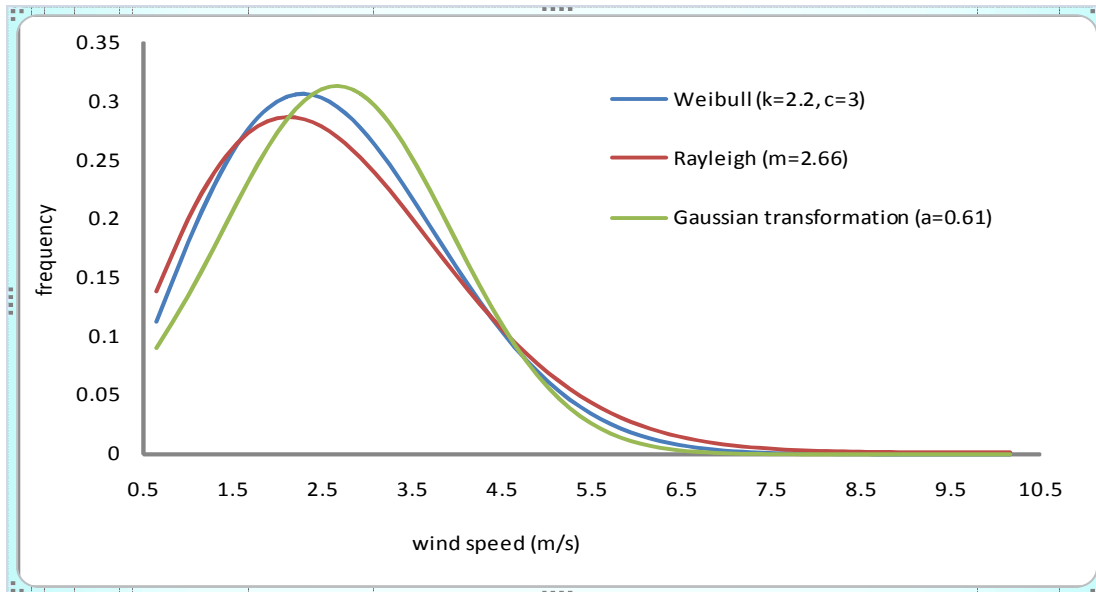


Figure 10: Illustration of a Weibull pdf with relation to other distributions

In the following, we utilize data from Iowa to investigate and exemplify the distributional patterns of wind speed. Long run averages of hourly wind speed data from numerous cities in Iowa are available from the Iowa Energy Center. The data we employ is reported in a frequency distribution format where the number of hours at each wind speed is recorded.

Parameters can be estimated with methods of moments, maximum likelihood, or least squares. In this study we employ a method introduced by Seguro and Lambert (2000). This is a modified maximum likelihood method for analyzing data in a frequency format. Denote the

relative frequency of a particular wind speed v_i by $p(v_i)$ where $\sum_i p(v_i) = 1$. The Weibull pdf parameters are estimated by the expressions

$$k = \left[\frac{\sum_{i=1}^n p(v_i) v_i^k \ln(v_i)}{\sum_{i=1}^n p(v_i) v_i^k} - \sum_{i=1}^n p(v_i) \ln(v_i) \right]^{-1} \quad (3.2)$$

and

$$c = \left[\sum_{i=1}^n p(v_i) v_i^k \right]^{1/k} . \quad (3.3)$$

Equation (3.2) is solved by an iterative process first, and then equation (3.3) is solved directly.

The relation among the Weibull parameters and the moments of the distribution are given by

$$m = c\Gamma(1 + 1/k) \quad (3.4)$$

and

$$v = c^2[\Gamma(1 + 2/k) - \Gamma^2(1 + 1/k)] = c^2\Gamma(1 + 2/k) - m^2 \quad (3.5)$$

where m and v stand for the mean and the variance of wind speed, respectively and $\Gamma(\cdot)$ is the gamma function.

Wind speed is classified on a scale of 1 to 7 and is usually measured at 10 or 50 meters above ground (table 1). Iowa wind speed is ranked 10th in the U.S. for its wind energy potential.²¹

The annual average wind speeds measured 50 meters above ground in Iowa are 5.5-6 m/s at

the northeastern parts of Iowa, and generally increase as one goes from the southeastern to the northwestern parts from 6 m/s to 8 m/s. We choose to examine counties in Iowa which already accommodate a large number of wind power plants (e.g. the northwestern counties) as well as others to demonstrate the distributional differences of wind resources over space.

Table 1: Wind speed classification

| Wind power class | Resources potential | Wind speed at 10 m height (m/s) | Wind power density at 10 m height (W/m ²) | Wind speed at 50 m height (m/s) | Wind power density at 50 m height (W/m ²) |
|-----------------------------------|---------------------|---------------------------------|---|---------------------------------|---|
| 1 | | <4.4 | 0-100 | <5.6 | 0-200 |
| 2 | Marginal | 4.4-5.1 | 100-150 | 5.6-6.4 | 200-300 |
| 3 | Fair | 5.1-5.6 | 150-200 | 6.4-7.0 | 300-400 |
| 4 | Good | 5.6-6.0 | 200-250 | 7.0-7.5 | 400-500 |
| 5 | Excellent | 6.0-6.4 | 250-300 | 7.5-8 | 500-600 |
| 6 | Outstanding | 6.4-7.0 | 300-400 | 8.0-8.8 | 600-800 |
| 7 | Superb | 7.0-9.4 | 400-1,000 | 8.8-11.9 | 800-2,000 |
| Source: U.S. Department of Energy | | | | | |

The demand for electricity is strongly related to temperature. Low temperatures increase electricity demand due to heating appliances while high temperatures increase demand because of the use of air conditioners. Since heating is fueled by many energy sources and cooling is almost exclusively by electricity, the highest demand typically occurs during the summer months. In figure 11 we exemplify the demand for electricity in April and July in two regions in the U.S. during 2007. In both regions demand is roughly 50 percent higher and much more volatile in July. Higher variability in electricity demand is associated with frequent peak load periods which are typically characterized by higher electricity prices. Therefore, one would expect that in these periods wind power will be in higher demand. For that reason, we focus on the distribution of a typical July to demonstrate the spatial Weibull

densities, means and standard deviations in Iowa (table 2). We employ wind speed data measured at 50 meters above ground.

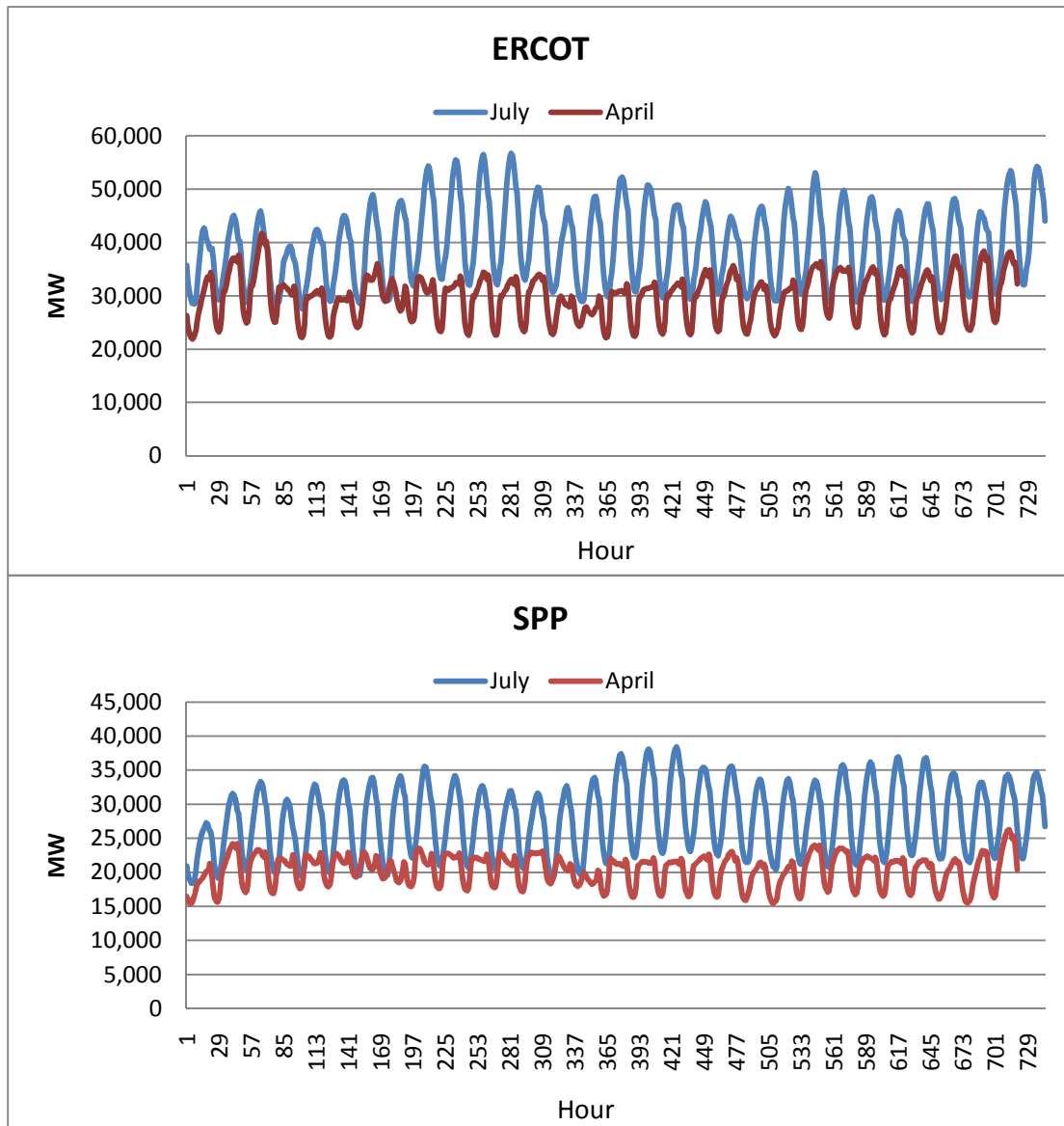


Figure 11: Hourly load in 2007 at the Electric Reliability Council of Texas (ERCOT) and the Southwest Power Pool (SPP) which includes the transmissions to Arkansas, Kansas, Louisiana, Missouri, New Mexico, Oklahoma and Texas.

Table 2: Estimated July wind speed parameters and moments at selected sites in Iowa, U.S.

| County | City | Location | Shape Parameter k | Scale parameter c (m/s) | Mean (m/s) | Std (m/s) |
|------------|--------------|-----------|---------------------------|---------------------------------|---------------|--------------|
| Sac | Scholar | NW | 2.61 | 6.90 | 6.13 | 2.53 |
| Pocahantas | Palmer | NW | 2.62 | 7.16 | 6.36 | 2.61 |
| Hancock | Garner | N Central | 2.60 | 6.88 | 6.11 | 2.53 |
| Carroll | Arcadia | Central W | 2.63 | 7.09 | 6.30 | 2.57 |
| Hamilton | Blairsburg | Central | 2.64 | 7.08 | 6.29 | 2.57 |
| Floyd | Charles City | NE | 2.59 | 6.40 | 5.68 | 2.36 |
| Lee | Argyle | SE | 2.54 | 5.95 | 5.28 | 2.23 |
| Osceola | Harris | NW | 2.64 | 7.41 | 6.58 | 2.68 |
| BuenaVista | Storm lake | NW | 2.59 | 6.98 | 6.20 | 2.57 |
| Worth | Joice | N Central | 2.61 | 6.96 | 6.18 | 2.55 |
| Dickinson | Spirit Lake | NW | 2.63 | 7.09 | 6.30 | 2.57 |
| Greene | Jefferson | Central | 2.58 | 6.45 | 5.73 | 2.38 |
| Allamakee | Churchtown | NE | 2.52 | 5.36 | 4.76 | 2.02 |

The average wind speed is in the range of 4.76 to 6.58 (m/s), and standard deviation is between 2.02 and 2.68 (m/s). The variation of wind speed at different sites cannot be compared by the standard deviations since they are estimates of different Weibull distributions. Thus, for this purpose wind speed coefficient of variation (cv_{ws}) should be computed. We use equations (3.4) and (3.5) to obtain

$$cv_{ws} = \sqrt{v}/m = [\Gamma(1 + 2/k) - \Gamma^2(1 + 1/k)]^{1/2}/[\Gamma^2(1 + 1/k)]. \quad (3.6)$$

It is clear from (3.6) that cv_{ws} is a function of the shape parameter only. Also, it can be shown that cv_{ws} is a decreasing function of k . This result is useful since comparing k of different Weibull distributions alone can provide a standardized index for the fluctuation of wind speed. For example, our results show that counties Hamilton and Osceola have the highest estimated shape parameters (depicted in column 4) therefore, they present the lowest

wind speed variations as well ($cv_{ws} \sim 40.7\%$). Since our estimates suggest that Osceola County also has the highest mean, it is the most preferred site in terms of both average wind speed and coefficient of variation. We depict the fitted distribution of wind speed at Allamakee ($cv_{ws} \sim 42.4\%$) and Osceola counties to demonstrate the differences in wind speed distribution over space (figure 12). These two are selected since they display the minimum and maximum values of both Weibull parameters in our sample respectively. The two fitted distributions are skewed as implied by the magnitude of the shape parameters. The distribution of the northwestern site has higher mean and fatter tails compared to the northeastern site.

Note, however that wind speed distributions by themselves are not sufficient for evaluating returns to wind power projects. As we discuss later, the economic wind potential of a site is actually linked more to the usable power rather than its wind speed. In addition, economic evaluation of wind potential of a site should not be weighted uniformly over all periods. Wind power revenues are subject to the price of electricity at the time of delivery. On periods of higher electricity demand, prices tend to be higher as well. Therefore, higher wind speeds in certain periods are more valuable than in other periods.

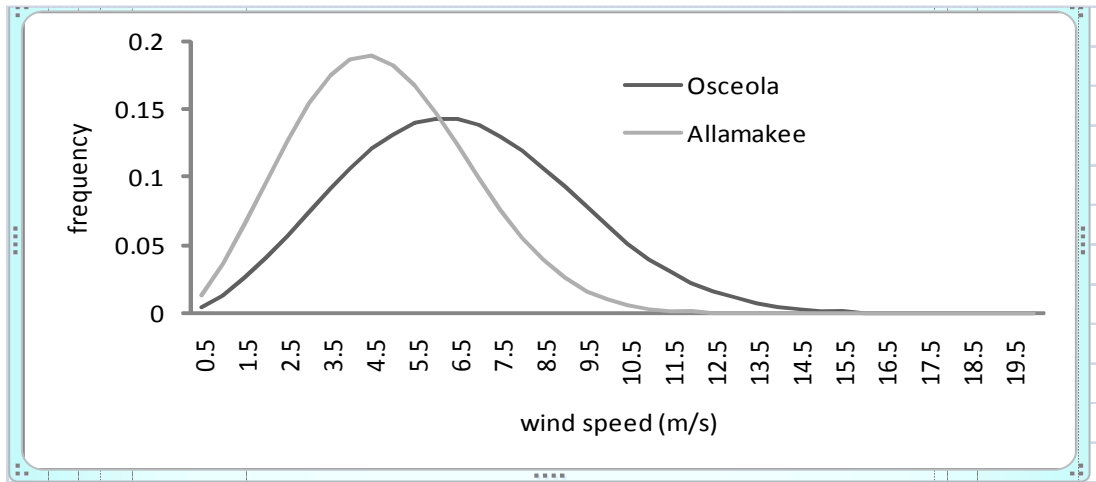


Figure 12: Fitted Weibull pdfs for July wind speed distributions at 50m height for sites at Allamakee and Osceola counties, IA

Next, we examine the month to month variation of wind speed. We carry on with our example and focus on the wind variation at Osceola County (table 3). Our estimation shows that the winter months are windier, peaking in March while summer months are somewhat calmer. The windiest month has roughly 30% higher average wind speed than the lowest. July in particular has the second lowest monthly average wind speed, which stands in conflict with the elevated electricity demand at that time of the year. The coefficient of variation of each month shows non-monotonous trend, peaking in November with 46% and falls below 40% for only a few months in a typical year.

Table 3: Estimated monthly wind speed parameters and moments at Osceola County, IA at 50m

| | Shape parameter k | Scale parameter c (m/s) | Mean (m/s) | Std (m/s) |
|-----------|---------------------------|---------------------------------|---------------|--------------|
| January | 2.73 | 9.07 | 8.07 | 3.19 |
| February | 2.61 | 9.17 | 8.15 | 3.36 |
| March | 2.76 | 9.35 | 8.32 | 3.26 |
| April | 2.50 | 9.37 | 8.31 | 3.55 |
| May | 2.50 | 8.69 | 7.71 | 3.30 |
| June | 2.48 | 8.33 | 7.39 | 3.18 |
| July | 2.64 | 7.41 | 6.58 | 2.68 |
| August | 2.70 | 7.28 | 6.47 | 2.59 |
| September | 2.61 | 8.08 | 7.17 | 2.96 |
| October | 2.67 | 8.85 | 7.87 | 3.18 |
| November | 2.32 | 8.98 | 7.96 | 3.65 |
| December | 2.50 | 9.08 | 8.06 | 3.45 |
| Annual | 2.44 | 8.68 | 7.69 | 3.36 |

Wind power density

The instantaneous input-output relation of wind speed and wind power potential (denoted by P_w) is characterized by the equation

$$P_w(v) = \frac{1}{2} \rho A v^3 \quad (3.7)$$

where ρ is air density (kg/m^3) which depends on altitude and temperature, and v is the wind speed that goes through an area A (m^2). Notice that wind power is an increasing return to scale process of wind speed. Theoretically, if one chooses a twice windier site holding all other factors constant, the wind power potential will be eightfold higher.

Since the density function of wind speed cubed can be represented by a Weibull function as well, mean wind power density of an area of size A can be expressed as (see for example, Jamil 1995):

$$E(P_w) = \int_0^{\infty} P_w(v)f(v)dv = \frac{A}{2}\rho c^3\Gamma(1 + 3/k) . \quad (3.8)$$

Frequently, wind power potential is expressed on a monthly or an annual basis. To arrive at an approximation of the wind power resources per m^2 over a timeframe of a month or a year one could simply multiply (3.8) by 730.48 and 8,765.81 respectively.

The mean wind power density represents the potential of wind resource at a chosen site. Figure 13 portrays mean wind power density per unit square (i.e. $A = 1$) in each month at Osceola County. The required air density data are obtainable from the Iowa Energy Center as well. The estimated figures show that small differences in wind speeds are translated into very large deviations in wind power. The month to month wind power potential varies greatly; from wind classification 2 (marginal) on summer months to classification 5 (excellent) on winter months and early spring.

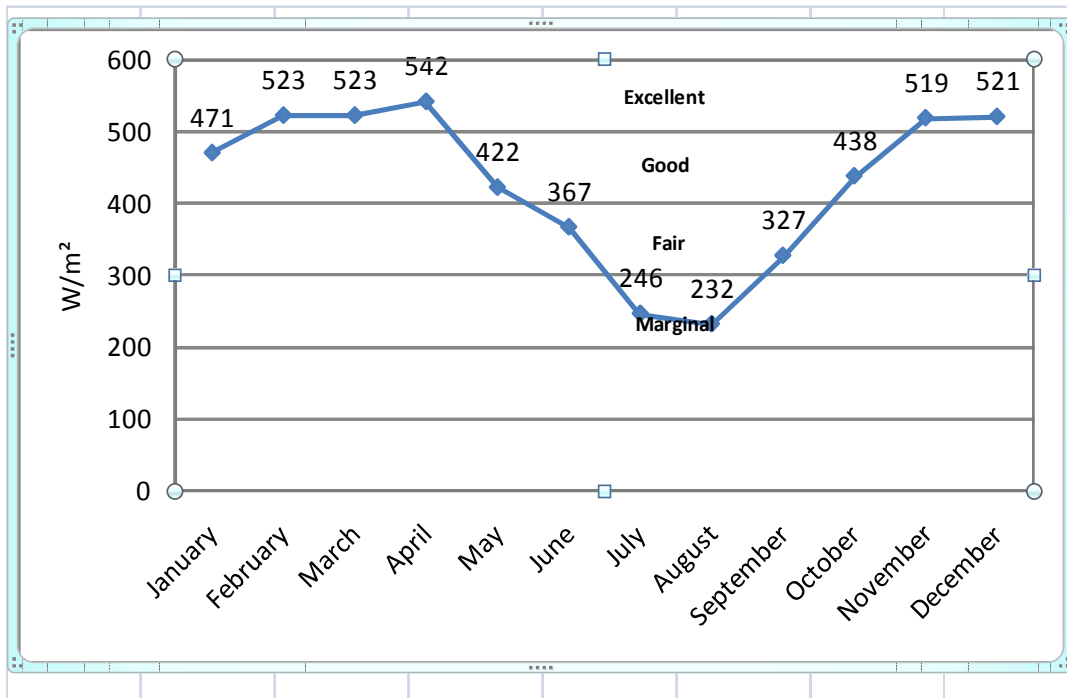


Figure 13: Month to month mean power density at 50m for Osceola County, IA

Usable wind power

When it comes to harvesting wind power, the actual energy that can be extracted by a wind turbine is limited. First, regardless of technology and turbine's design the instantaneous power that can be extracted from wind is bounded. According to Betz Law (Betz 1926) there is an upper limit of 59% for power extraction from air flows²². Secondly, wind turbines impose mechanical limitations as well.

²² Wind turbines extract energy by capturing wind speed. This suggests that for a turbine to be able to gain 100% efficiency, its rotor should be like a brick wall. But in this case it won't spin at all and no kinetic energy would be converted. On the other hand, if there was no rotor at all the wind would have passed through with no impact. In both cases the efficiency of the turbine is 0%.

The capacity of a wind turbine (denoted by P_c) in a given wind speed may be described by the equation

$$P_c(v) = \psi(v) * RP \quad (3.9)$$

where RP is the *rated power* of the turbine. It is generally the maximum power that a wind turbine can generate. $\psi(v)$ is a non-linear function describing the turbine efficiency coefficient. The coefficient measures the rate at which the turbine extracts energy in different wind speeds relative to its rated power. The capacity of wind turbine is commonly characterized by a static power curve. To exemplify, we describe the operation of a typical modern turbine rated 1.5 MW. The minimum wind speed at which the turbine starts generating power at is called *cut in point*. For a 1.5 MW turbine, this point is usually in the range of 3.5-4.0 m/s. Once wind speed is higher than the cut in point, power is generated increasingly with wind speed. The *rated speed* is the speed at which the turbine is intended to achieve its rated power (i.e. RP). In our example, power of 1.5 MW is generated when wind speed is at about 12-14 m/s. At higher speeds, the turbine maintains its rated power or decreases its output gradually, depending on the turbine design and power control. When wind speed exceeds the turbine's *cut out point*, the generator is shut down to avoid exposing the turbine to damage. Cut out point for the described turbine may be in the range of 20-25 m/s.

Estimation of power curves are performed based on field measurements. First, data measuring wind power output is plotted against wind speed. Then, an efficiency coefficient function $\psi(v) \in [0,1]$ is fit to map wind speed into wind power. In doing so one needs to account for the two truncated ranges correspond to the cut in and cut out points. In these

ranges $\psi = 0$ is imposed since no power is generated. At the rated speed of the turbine, its capacity reaches the rated power thus $\psi = 1$.

In figure 14 we depict a power curve of a typical 1.5MW modern turbine against the long averages wind speed distributions of April and July at Osceola county at height of 80m (which is the appropriate hub height of a typical 1.5 MW turbine). The depicted power curve was fitted by eye to the power curve of a particular commercial machine published by the manufacture (details are provided in appendix 3). The illustration magnifies the importance of fitting the right turbine to the wind conditions of the site in question. The monthly average wind speed in typical July and April is 7.05 and 8.95 respectively. Notice that in July, it is not very common for the turbine to run on its rated power. On April, the probability of that to happen is higher. The illustration shows that wind conditions in one month may be more suited than in other months for a turbine of this rate.

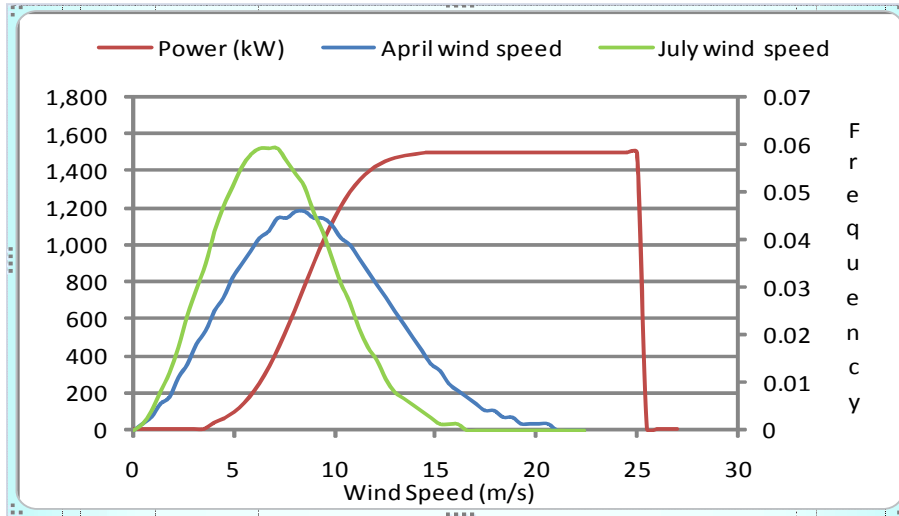


Figure 14: Illustration of July and April wind speed distributions at Osceola County, IA and a power curve of a typical modern 1.5 MW wind turbine

A turbine *capacity factor* (CF) is the ratio between the average power generated over a period of time and the rated power of the turbine. More formally, it can be written as

$$CF = \frac{\int_0^{\infty} P_c(v) f(v) dv}{RP} = \int_0^{\infty} \psi(v) f(v) dv . \quad (3.10)$$

The computation of the capacity factor requires numerical integration techniques. Although the capacity factor is commonly used as an index to indicate the performance of a wind turbine, it should be regarded with caution. The fitted power curve is sensitive to the wind conditions at the specific site and measurement errors. Therefore, the computed capacity factor of a very same wind turbine may be quite different when the turbine is sited and its output is measured at different locations. The anticipated losses of a wind power plant are referred to as a *loss factor*, which accounts (but not limited) to downtime due to maintenance,

line losses, physical conditions and land use (building, trees, crops etc), and a projected decrease in the turbine's efficiency over time²³.

A recent report by the U.S. Department of Energy (2009) indicates that the average U.S. industry capacity factor increased from 22% for projects installed prior 1998 to 35% for projects installed in 2007. Moreover, in the best wind resources areas, wind plants commonly exceed a 40% capacity factor and in some cases the capacity factor is even greater than 50%.

The month to month variation of the computed capacity factor of our 1.5MW turbine at Osceola County is large (figure 15). For instance, the capacity factor attains 40% in a typical July month and 58% in a typical April month. These estimates ought to be adjusted down by the anticipated loss factor.

The capacity factor is considered to be a good measure for the productivity of a wind turbine. However, its variability over time and space and the fact that the hourly price of electricity fluctuates as well, suggest that more inputs are required in order to assess the economic value of a wind turbine.

²³ Iowa Energy Center suggests using a default loss factor of 12%.

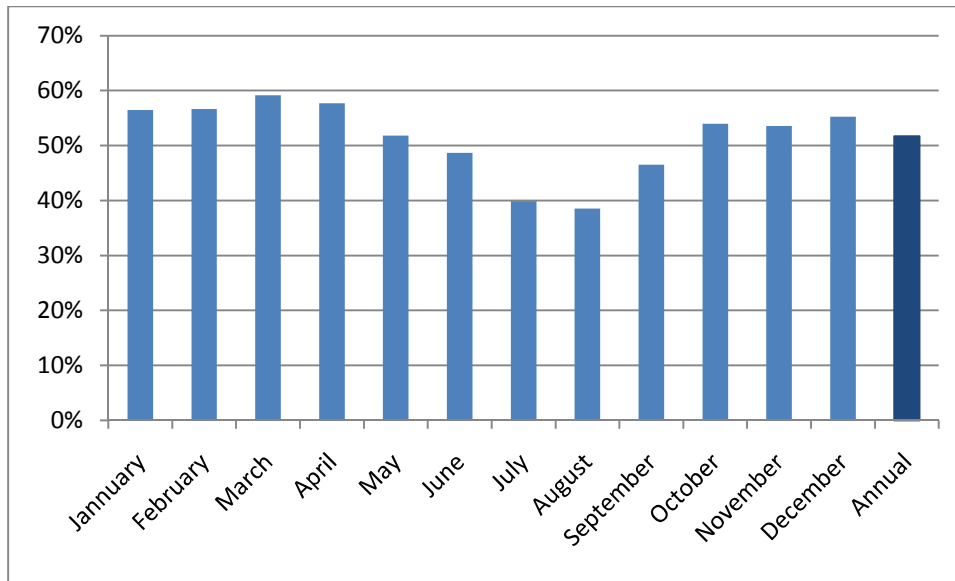


Figure 15: Monthly numerical capacity factors of a 1.5MW wind turbine sited at Osceola County, IA (disregarding loss factor).

Regional wind power supply

Estimating the instantaneous distribution of overall wind power supply to a power system is important from various engineering reasons; frequency control, coordination and operation, and system reserves. From an economic point of view, the expectations regarding overall wind power supply may impact trade in futures markets for electricity and therefore electricity prices.

There are two main approaches to study overall energy flow from wind projects in a region. In the first, the researcher estimates the stochastic nature of the problem by investigating the spatial correlation of wind speed. In the next stage, wind speed data is transformed into wind power according to the technicalities of the specific wind turbines employed in the analysis. In the second approach, recorded data of wind power output produced by wind farms is used

directly in the analysis. The advantage of the first approach is the ability to examine the two stages independently. In doing so, the energy potential in a region may be analyzed according to various scenarios of geographical spreads of wind farms. In addition, this approach is not limited to the specifics of wind turbines in the region in question. Therefore, the researcher has the flexibility to apply a range of assumptions about the future figures of wind energy conversions. On the downside, the estimation in the first approach requires much more data. Long term records of wind speed data from as many sites as possible of the region in question are required to account for a spatial trend in wind speed means. Then, simultaneous wind speed observations from these sites are needed for the spatial modeling. Moreover, even if spatial correlation is ignored, extensive wind speed data is still needed. Since the relation between wind speed and wind power is non-linear (and truncated) the knowledge of average wind speeds alone are insufficient. In effect, for wind power considerations, full description of long-run wind speed distributions are required.

Wind spatial correlation

In a pioneering work, Haslett and Raftery (1989) estimated the daily average wind energy at a new site for which only a short run data was available. In doing so, long term records at twelve meteorological stations in Ireland were utilized. Haslett and Raftery introduced an autoregressive integrated moving average (ARIMA) model for the space-time process of wind speed. The model was constructed based on the assumption that the second order moment of the space–time process is constant. Therefore it is separable and can be written as

a product of the two processes. Particularly, the cross-correlation between every two locations has been fitted by the function

$$r_{ij} = \begin{cases} \alpha e^{-\beta d_{ij}} & \text{if } i = j \\ 1 & \text{if } i \neq j \end{cases} \quad (3.11)$$

where d_{ij} is the distance between the two sites (i, j) , $\alpha \in [0,1]$ and $\beta \geq 0$ are parameters.

The empirical curve displays a strong spatial correlation (figure 16). The correlation of the daily average wind speed was above 0.5 even when reaching a range of 450 km between two locations in Ireland. The correlation level depends on the time interval which wind speeds observations are being averaged on. The study by Haslett and Raftery was based on daily average wind speeds, thus is not detailed enough for the purpose of valuing wind power. Since the price of electricity fluctuates greatly during the day as well, hourly wind speed data is more suitable.

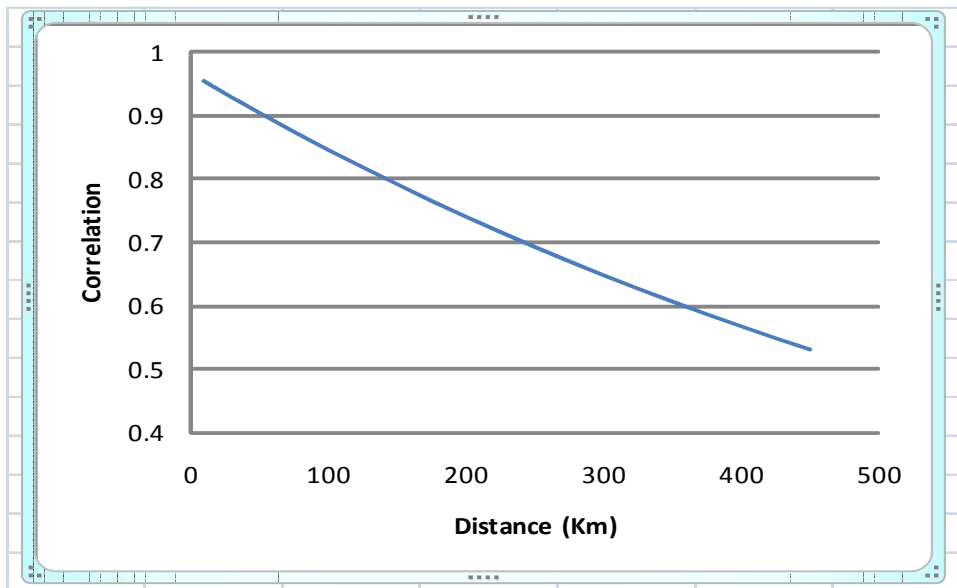


Figure 16: Empirical spatial correlation function of wind speed in Ireland. Source: Haslett and Raftery (1989)

At the second stage of the estimation, Haslett and Raftery approximated wind power output. The energy conversion ratio was oversimplified by assuming that generating wind power is proportion to wind power potential. Assuming that, the authors overestimated the potential output of wind turbines (i.e. ignoring zero output at wind speeds which are lower than the cut in point and higher than the cut out point).

Cellura, et al. (2008) employed hourly data to study the spatial wind speed patterns for energy planning in Sicily. Specific Weibull density functions were fitted for each wind site and a complete geostatistics analysis was performed. The study shows how wind resources in a region may be evaluated taking into account the spatial nature of wind. However, Cellura, et al. did not consider wind power production in their study.

Holttinen (2005) studied the hourly variation of wind power production directly. Real output data from the Nordic countries was utilized to examine wind energy variability in a large geographical scale. The cross-correlation of wind power production was fitted by the correlation function (3.11) for sites in an area where the maximum distance between sites is 2,000 km (figure 17). The spatial correlation of wind power production was found to be strong for sites which are just a few hundred km apart, above 0.35 for sites which are 500 km apart and below 0.1 when the distance is about 1,200 km or more. Sinden (2007) portrayed very similar results studying cross-correlation between 2,080 pairs of wind power sites in the UK. The maximum distance between sites in that study was 1,200 km and at this range the correlation was also slightly under 0.1. Also depicted in figure 18, an extrapolation of spatial correlation functions fitted in studying wind energy in the Netherland (Gibescu, Brand and

Kling 2009; Landberg, et al. 1997), and a spatial correlation function fitted for a spread of 4,500 km over locations in the EU (Giebel 2000).

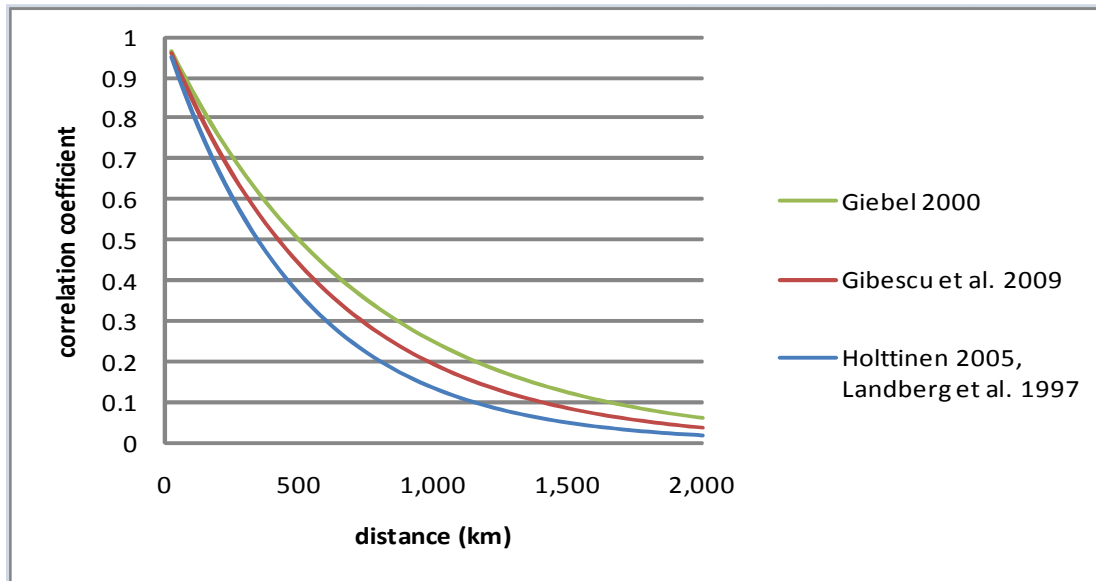


Figure 17: Fitted cross correlation functions of wind power output, various studies

Focken, et al. (2002) studied the effect of spatial distribution of wind farms on forecasting regional wind power. They considered wind power output data of about 9,000 wind turbines in Germany in 1999. Their study shows that the magnitude of the reduction of forecasting error depends only weakly on the number of wind sites and is mainly determined by the size of the region. Similar to the other studies, the spatial correlation of wind power was fitted by equation (3.11). In doing so, Focken, et al. were able to weigh the prediction improvement of aggregate wind power proposed by wind farms diversification. The study compared regions of diameter size of 370 km and 730 km. Interestingly, in both cases prediction error improved and reached a minimum level at around 50 turbines. A larger number of turbines did not enhance prediction precision. Normalizing a single site prediction error to 1,

prediction error in the smaller region was 0.63 while the larger region demonstrated error of size 0.53.

Introduction to a wind-integrated electricity market

Once wind capacity had been installed, the production of wind power is not a choice variable. Similar to electricity demand it is a stochastic process which may be predicted with some precision level. For that reason it is sensible to define the expected amount that needs to be generated by conventional power units as a *net load*. The distribution of the net load depends on the correlation between electricity demand and aggregate wind power production. Wind power output may move in the same direction as the system load in some regions while against it in others. However, there is no reason for the short-term fluctuations of wind power and system load to be related (Holttinen 2005; Wan and Liao 2006). If short-term fluctuations are indeed uncorrelated, expected net load may be expressed as

$$\int_0^{\bar{W}} \int_0^{\infty} (X - W) f_X(X|\hat{X}) f_W(W|\hat{W}) dX dW \quad (3.12)$$

where W is the hourly aggregate regional wind power output, \bar{W} is the rated regional capacity, \hat{W} is the prediction of aggregate wind power and $f_W(\cdot)$ is the conditional probability distribution function of aggregate wind power.

Integration of wind power capacity into deregulated electricity markets has two primary effects. While producers of conventional power face convex cost functions, the marginal cost of wind power is close to zero. Therefore, the regional marginal cost of producing overall

load is higher than the marginal cost of producing net load. Second, prediction of load minus available wind power has different statistical features than the prediction of overall load because it also includes errors in wind power predictions. The task of making correct predictions and balancing load under these terms is more complex since it involves stochastic processes of both demand and supply. Wan and Liao (2006) examine the change in the short term variation of load due to installation of wind power capacity. In their study 74 MW of wind energy (rated power) had been added to a conventional generation capacity of 1,400 MW. This addition has the potential to account for 6% of electricity demand in peak load periods at the particular region of study. It was shown that at this penetration rate the increase in standard deviation of the net load compare to overall load is in the range of 3% in August to 18% in June. Looking at a six month average (June to November) an overall increase of 8% in the standard deviation was computed.

Recent experience of the Electric Reliability Council of Texas (ERCOT) may emphasize the complexity of predicting net load²⁴. On Tuesday evening, February 26th, 2008 an emergency situation was announced when a sharp decline in wind energy production in west Texas occurred at the same time that electricity demand soared due to a sudden decrease in temperature. At that time, ERCOT electricity demand increased from 31,200 MW to a peak of 35,612 MW. Wind power production fell from more than 1,700 MW to only 300 MW. During that event some industrial electricity was curtailed and the emergency situation was ended in three hours (which is a sufficient time to activate most gas turbines).

²⁴ ERCOT manages a region with the largest installed wind power capacity in the U.S. At the first quarter of 2008 Texas had about 5,300 MW wind power capacity installed, and by the end of 2008 this number jumped to 7,118 MW.

In a wind-integrated electricity market, firms need to consider the conditional distribution of the net load in making their financial decisions. Optimization problems should be formulated with respect to the distribution of the spot price, which in turn, is derived from the distribution of net load given the forecasts. These optimization problems are the focus of our next chapter.

Chapter 4: Theoretical framework for modeling wind-integrated electricity markets

Introduction

In this chapter we extend the electricity market model to account for the economic environment of markets with significant amount of wind power capacity. A wind-integrated electricity market model allows us to examine and compare the outcome and welfare distribution subject to various assumptions regarding the path for wind power expansion. In particular, we expand our model to analyze two key economic questions with regard to wind penetration rate. First, if the electric industry experiences market power, the question who invests in wind capacity may be important for welfare distribution and for identifying potential losses caused by a non-competitive behavior. Second, geographical diversification of wind power plants determines the probability distribution of aggregate wind power supply. Hence, one could ask what effect wind power diversification has on market equilibrium.

We examine the situation where wind power is utilized fully by the system operator in real-time whenever it is available. This is similar to the current situation in most deregulated electricity markets. In these markets wind power is not being traded regularly in the day-ahead markets therefore it is not being priced directly. Instead, wind power producers receive the settled spot price which is determined by the price of the marginal MW of electricity

produced by the marginal fossil fuel generator. That way, the ISO utilizes all available wind power in real-time before dispatching power from fossil fuel resources.

The results we derive in this chapter show that even though wind power is not priced directly it may have a substantial impact on how electricity from fossil fuel generators is priced. This is particularly true when market power exists in electricity markets. In addition, the theoretical framework presented in this chapter is developed with accordance to the objective of examining the impact of wind power diversification. We attend this question after introducing the required numerical methodology in chapter 5.

Setup

Wind power output is not a decision variable and it is not traded in the market for forward contracts. Therefore, the residual power that needs to be generated by fossil fuel generators in real-time is a pure probabilistic matter. We denote this amount as *net load*.²⁵

Net load is exogenous to electricity markets but wind power revenues are not. Since these revenues are contingent on the settled spot price, wind power producers would always prefer a higher spot price. For this reason, the presence of market power and the ability to manipulate the spot price make ownership of wind power capacity a key for understanding how electricity is priced in a wind-integrated market.

²⁵ We assume that the net load is always positive. This is reasonable since a wind penetration rate higher than in the range of 20% to 30% (depending on the region) has reliability and other engineering constraints which have not been solved yet.

We start with some useful notation: recall that W is the hourly aggregate regional wind power output and \bar{W} denotes the regional rated wind power capacity. Effectively, this is the upper bound for aggregate wind power output in a region at a specified wind penetration rate (i.e. total wind power nameplate capacity in the region). The prediction of regional wind power at the time of trading forwards is denoted by \widehat{W} , and the conditional distribution of the prediction of regional wind power is given by the conditional probability distribution function $f_W(W|\widehat{W})$.

Similar to the base model presented in chapter 2 (of no wind power), LSEs may choose to lock in (aggregately) X_F units of electricity by purchasing forward contracts for the price P_F . But unlike the base model, the residual amount of energy that LSEs need to balance in real time accounts for the availability of wind power, that is $X - W - X_F$. Whether it is positive or negative, this amount would be settled against the spot price (if negative, a contract for differences is put into effect). After the spot market is cleared LSEs would make a monetary transfer of size $P_S W$ to the owners of wind power capacity.

In the following, we solve for the outcome of the two-settlement process (i.e. forwards and spot markets) assuming wind energy is fully utilized by the system operator in real-time. We compare two cases: wind power capacity is owned by IPPs (*Cournot wind capacity*) or by an independent entity or entities which do not take part in electricity markets otherwise (*fringe wind capacity*). Historically, investments in wind capacity need to be subsidized to become competitive therefore the distribution of revenues generated by wind power is a policy question. We do not analyze in this study the long run incentives to invest in wind power capacity. Therefore, the two cases may be viewed as the outcome of a favorable policy or

mandates for IPPs or other entities to invest in wind power capacity. Next, we give details about the optimization problems in each ownership case and the associated equilibrium outcomes.

Cournot wind capacity

Start by assuming that wind power capacity is part of the generation asset portfolio owned and operated by IPP firms. We keep the symmetric structure of the problem by assuming that wind power capacity is uniformly distributed among IPPs. Yet, we let realizations of wind power output to vary at the firm level. This in turn yields asymmetric profits. An IPP firm that has higher (lower) than average wind power output will have profits which are higher (lower) than average.

Next, we need to acknowledge the difference in the implications of wind power forecasts at the aggregate and at the firm level. First, at the aggregate level, prediction of wind power supply provides information about the distribution of the spot price. Focusing on the symmetric solution, the knowledge of aggregate wind power is sufficient to foretell the spot price. That is because forward positions are identical across firms and competitive behavior in the spot market implies identical marginal costs. Therefore, similar to the base model, the spot price stands for the marginal cost of electricity production from conventional energy resources. Second, at the firm level, wind power prediction helps IPPs making more informed decisions about expected revenues in real-time. More about the importance of firm level prediction is discussed when IPP's optimization problem is detailed.

Since the knowledge of firm level output is not important for the evolution of the spot price we can characterize the LSEs problem in terms of aggregate wind power. The LSEs maximization problem given the predictions of load and aggregate wind power at the time of trading forwards is

$$\begin{aligned}
\mathbb{N} \equiv \max_{x_F^j} E \left(\pi_{LSE}^j \middle| \hat{X}, \sum_{n=1, n \neq j}^N \bar{x}_F^n, \hat{W} \right) &= [P_R - P_F] x_F^j \\
+ \int_0^{\bar{W}} \int_W^\infty \left[P_R - P_S \left(X, \sum_{n=1, n \neq j}^N \bar{x}_F^n, W \right) \right] \\
&\times \left(\frac{X - W}{N} - x_F^j \right) f_X(X | \hat{X}) f_W(W | \hat{W}) dX dW \\
+ \int_0^{\bar{W}} \int_W^\infty \left[P_R - P_S \left(X, \sum_{n=1, n \neq j}^N \bar{x}_F^n, W \right) \right] \\
&\times \frac{W}{N} f_X(X | \hat{X}) f_W(W | \hat{W}) dX dW .
\end{aligned} \tag{4.1}$$

The first two terms are the familiar expressions describing payoffs from trading electricity in forward and spot markets. The third term is the financial payoff for utilizing wind power in real-time. Substituting for the expected spot price and collecting terms we get

$$\begin{aligned}
\mathbb{N} &= [P_R - P_F]x_F^j \\
&+ \int_0^{\bar{W}} \left\{ \int_W^{\sum_{1,n \neq j}^N \bar{x}_F^n + x_F^j + W} \left[P_R - \frac{\alpha_t}{M}(X - W) \right] \times \left(\frac{X}{N} - x_F^j \right) f_X(X|\hat{X}) dX \right. \\
&\quad + \int_{\sum_{1,n \neq j}^N \bar{x}_F^n + x_F^j + W}^{\infty} \left[P_R - \frac{\alpha_t}{M}(X - W) \right. \\
&\quad \left. \left. - \frac{\alpha_s}{M} \left(X - W - \sum_{n=1, n \neq j}^N \bar{x}_F^n - x_F^j \right) \right] \right. \\
&\quad \left. \times \left(\frac{X}{N} - x_F^j \right) f_X(X|\hat{X}) dX \right\} f_W(W|\hat{W}) dW. \tag{4.2}
\end{aligned}$$

Taking the derivative of the objective function with respect to the decision variable and with further algebraic steps we get the following FOC

$$P_F = E[P_S(\cdot)] + \frac{\alpha_s}{MN} \int_0^{\bar{W}} \int_{X_F+W}^{\infty} (X - X_F) f_X(X|\hat{X}) f_W(W|\hat{W}) dX dW. \tag{4.3}$$

LSEs willingness to pay for the marginal forward contract reflects the cost they expect to face in order to purchase the marginal MW for their end-consumers at the spot market. This cost accounts for the expected spot price plus the expected penalty for not scheduling the marginal unit for delivery in advance (associated with turning on the marginal power generator). The optimality condition is integrated over all possible realizations of wind power output. Substituting for the deterministic case where $f_W(W = 0|\hat{W}) = 1$, this FOC coincides with the demand curve of the base model of no wind power. In this sense the demand curves

developed in this section may be seen as a generalization of the one produced by the base model in chapter 2.

As noted earlier, in order to analyze the IPPs problem one should account for both aggregate and a firm's prediction of wind power output. The knowledge of both helps IPPs to make more informed decisions in the forwards market. That is because each IPP's revenues from wind power depend on the distribution of its own output and the distribution of the spot price which in turn depends on the distribution of aggregate wind power.

The prediction of wind power output for the delivery period in question and rated wind power capacity (fixed over all periods) of each IPP firm are denoted by \hat{w} and \bar{w} respectively. We denote the conditional probability distribution function of wind power output of each IPP by $f_w(w|\hat{w})$ with mean μ_w and variance σ_w^2 . Therefore the conditional pdf of the regional aggregate output $f_W(W|\hat{W})$ has mean $M\mu_w$ and notice that the variance is between $M\sigma_w^2$ and $M^2\sigma_w^2$. The lower bound corresponds to the case of uncorrelated wind and the upper bound to the case of a fully correlated wind power output.

If there is an aggregate smoothing effect it improves the prediction of the spot price but does not offer any benefit for the prediction at the firm level output. Therefore, in maximizing profits, each wind power producer needs to consider the statistics of its own expected output as well as the expected aggregate regional output. Finally, the joint conditional probability distribution function of wind power output at the firm level and the output at the aggregate level is denoted by $f_{w,W}(w, W|\hat{W})$.

Each IPP's expected profits are given by

$$\begin{aligned}
\mathcal{M} &\equiv \max_{q_F^i} E \left(\pi_{IPP}^i \middle| \hat{X}, \sum_{m=1, m \neq i}^M \bar{q}_F^m, \hat{W} \right) \\
&= P_F \left(\hat{X}, \sum_{m=1, m \neq i}^M \bar{q}_F^m + q_F^i, \hat{W} \right) \times q_F^i \\
&\quad + \int_0^{\bar{W}} \int_W^\infty \left[P_S \left(X, \sum_{m=1, m \neq i}^M \bar{q}_F^m + q_F^i, W \right) \times (q^i - q_F^i) \right. \\
&\quad \quad \quad \left. - C(q^i, q_F^i) \right] f_X(X|\hat{X}) f_W(W|\hat{W}) dX dW \\
&\quad + \int_0^{\bar{w}} \int_w^{\bar{W}} \int_W^\infty P_S \left(X, \sum_{m=1, m \neq i}^M \bar{q}_F^m + q_F^i, W \right) \times w f_X(X|\hat{X}) f_{w,W}(w, W|\hat{W}) dX dw dW
\end{aligned} \tag{4.4}$$

where the last term stands for the IPPs' expected revenues from owning wind power capacity.

Express \mathcal{M} with respect to the two states of the world (i.e. conventional capacity traded in advance is sufficient or insufficient to meet realized net load)

$$\begin{aligned}
\mathcal{M} &= P_F \left(\hat{X}, q_F^i + \sum_{m=1, m \neq i}^M \bar{q}_F^m, \hat{W} \right) \times q_F^i \\
&+ \int_0^{\bar{w}} \int_{\sum_{1, m \neq i}^M \bar{q}_F^m + q_F^i + W}^{\infty} [P_S(X, W) \times (q^i - q_F^i) \\
&\quad - C(q^i)] f_X(X|\hat{X}) f_W(W|\hat{W}) dX dW \\
&+ \int_0^{\bar{w}} \int_{\sum_{1, m \neq i}^M \bar{q}_F^m + q_F^i + W}^{\infty} \left[P_S \left(X, \sum_{m=1, m \neq i}^M \bar{q}_F^m + q_F^i, W \right) \times (q^i - q_F^i) \right. \\
&\quad \left. - C(q^i, q_F^i) \right] f_X(X|\hat{X}) f_W(W|\hat{W}) dX dW \tag{4.5} \\
&+ \int_0^{\bar{w}} \int_w^{\bar{w}} \int_{\sum_{1, m \neq i}^M \bar{q}_F^m + q_F^i + W}^{\infty} P_S(X, W) \times w f_X(X|\hat{X}) f_{w,W}(w, W|\hat{W}) dX dwdW \\
&+ \int_0^{\bar{w}} \int_w^{\bar{w}} \int_{\sum_{1, m \neq i}^M \bar{q}_F^m + q_F^i + W}^{\infty} P_S \left(X, \sum_{m=1, m \neq i}^M \bar{q}_F^m + q_F^i, W \right) \\
&\quad \times w f_X(X|\hat{X}) f_{w,W}(w, W|\hat{W}) dX dwdW .
\end{aligned}$$

Taking the first derivative

$$\begin{aligned}
\frac{\partial \mathcal{M}}{\partial q_F^i} &= \frac{\partial P_F(\cdot)}{\partial q_F^i} q_F^i + P_F(\cdot) \\
&- \int_0^{\bar{w}} \int_{\Sigma_{1,m \neq i}^M, \bar{q}_F^m + q_F^i + W} P_S(\cdot) f_X(X|\hat{X}) f_W(W|\hat{W}) dXdW \\
&+ \int_0^{\bar{w}} \int_{\Sigma_{m=1, m \neq i}^M, \bar{q}_F^m + q_F^i + W} \left[\frac{\partial P_S(\cdot)}{\partial q_F^i} \times (q^i - q_F^i) + P_S(\cdot) \times \left(\frac{\partial q^i}{\partial q_F^i} - 1 \right) \right. \\
&\quad \left. - C'(q^i, q_F^i) \right] f_X(X|\hat{X}) f_W(W|\hat{W}) dXdW \\
&+ \int_0^{\bar{w}} \int_w^{\bar{W}} \int_{\Sigma_{1,m \neq i}^M, \bar{q}_F^m + q_F^i + W} \frac{\partial P_S(\cdot)}{\partial q_F^i} \times w f_X(X|\hat{X}) f_{w,W}(w, W|\hat{W}) dXdwdW.
\end{aligned} \tag{4.6}$$

Writing explicitly the derivatives of the spot price and the cost function

$$\begin{aligned}
\frac{\partial \mathcal{M}}{\partial q_F^i} &= \frac{\partial P_F(\cdot)}{\partial q_F^i} q_F^i + P_F(\cdot) \\
&- \int_0^{\bar{w}} \int_{\Sigma_{1,m \neq i}^M, \bar{q}_F^m + q_F^i + W} P_S(\cdot) f_X(X|\hat{X}) f_W(W|\hat{W}) dXdW \\
&+ \int_0^{\bar{w}} \int_{\Sigma_{m=1, m \neq i}^M, \bar{q}_F^m + q_F^i + W} \left[-\frac{\alpha_S}{M} \times (q^i - q_F^i) + P_S(\cdot) \times \left(\frac{\partial q^i}{\partial q_F^i} - 1 \right) - \alpha_t q^i \frac{\partial q^i}{\partial q_F^i} \right. \\
&\quad \left. - \alpha_s (q^i - q_F^i) \left(\frac{\partial q^i}{\partial q_F^i} - 1 \right) \right] f_X(X|\hat{X}) f_W(W|\hat{W}) dXdW \\
&- \int_0^{\bar{w}} \int_w^{\bar{W}} \int_{\Sigma_{1,m \neq i}^M, \bar{q}_F^m + q_F^i + W} \frac{\alpha_S}{M} w f_X(X|\hat{X}) f_{w,W}(w, W|\hat{W}) dXdwdW.
\end{aligned} \tag{4.7}$$

Employing symmetry and collecting terms

$$\begin{aligned}
\frac{\partial \mathcal{M}}{\partial q_F^i} &= \frac{\partial P_F(\cdot)}{\partial q_F^i} q_F^i + P_F(\cdot) - E[P_S(\cdot)] \\
&+ \alpha_s \left(1 - \frac{1}{M}\right) \int_0^{\bar{w}} \int_{\sum_{m=1, m \neq i}^M \bar{q}_F^m + q_F^i + W}^{\infty} (q^i - q_F^i) f_X(X|\hat{X}) f_W(W|\hat{W}) dX dW \\
&- \frac{\alpha_s}{M} \int_0^{\bar{w}} \int_w^{\bar{W}} \int_{\sum_{1, m \neq i}^M \bar{q}_F^m + q_F^i + W}^{\infty} w f_X(X|\hat{X}) f_{w,W}(w, W|\hat{W}) dX dwdW \\
&- \int_0^{\bar{w}} \int_w^{\bar{W}} \int_{\sum_{1, m \neq i}^M \bar{q}_F^m + q_F^i + W}^{\infty} \frac{\alpha_s}{M} w f_X(X|\hat{X}) f_{w,W}(w, W|\hat{W}) dX dwdW .
\end{aligned} \tag{4.8}$$

The FOC is

$$\begin{aligned}
P_F(\cdot) &= E[P_S(\cdot)] - \frac{\partial P_F(\cdot)}{\partial q_F^i} q_F^i \\
&- \alpha_s \left(1 - \frac{1}{M}\right) \int_0^{\bar{w}} \int_{\sum_{m=1, m \neq i}^M \bar{q}_F^m + q_F^i + W}^{\infty} (q^i - q_F^i) f_X(X|\hat{X}) f_W(W|\hat{W}) dX dW \\
&+ \frac{\alpha_s}{M} \int_0^{\bar{w}} \int_w^{\bar{W}} \int_{\sum_{1, m \neq i}^M \bar{q}_F^m + q_F^i + W}^{\infty} w f_X(X|\hat{X}) f_{w,W}(w, W|\hat{W}) dX dwdW .
\end{aligned} \tag{4.9}$$

The first derivative of the forward price with respect to quantity is

$$\frac{\partial P_F(\cdot)}{\partial q_F^i} = -\frac{\alpha_s}{M} \left(1 + \frac{1}{N}\right) \int_0^{\bar{w}} \int_{\sum_{1, m \neq i}^M \bar{q}_F^m + q_F^i + W}^{\infty} f_X(X|\hat{X}) f_W(W|\hat{W}) dX dW . \tag{4.10}$$

Solving for the symmetric Cournot-Nash equilibrium where $q_F^1 = q_F^2 = \dots = q_F^M \equiv q_F$ gives the following optimality condition

$$\begin{aligned}
P_F(\cdot) &= [P_S(\cdot)] + q_F^* \frac{\alpha_S}{M} \left(1 + \frac{1}{N}\right) \int_0^{\bar{W}} \int_{X_F^*+W}^{\infty} f_X(X|\hat{X}) f_W(W|\hat{W}) dX dW \\
&\quad - \alpha_S \left(1 - \frac{1}{M}\right) \int_0^{\bar{W}} \int_{X_F^*+W}^{\infty} (q - q_F^*) f_X(X|\hat{X}) f_W(W|\hat{W}) dX dW \\
&\quad + \frac{\alpha_S}{M} \int_0^{\bar{w}} \int_w^{\bar{W}} \int_{X_F^*+W}^{\infty} w f_X(X|\hat{X}) f_{w,W}(w, W|\hat{W}) dX dwdW .
\end{aligned} \tag{4.11}$$

It can be verified that the SOC holds in the same manner it is exemplified in the base model (appendix 2).

Next, by equating aggregate inverse demand with aggregate inverse supply one can show that equilibrium is characterized by the aggregate number of forward contracts that solves (numerically) the following equation

$$\begin{aligned}
X_F^* &= \left(\frac{MN + M - N}{MN + M + 1} \right) \times \frac{\int_0^{\bar{W}} \int_{X_F^*+W}^{\infty} X f_X(X|\hat{X}) f_W(W|\hat{W}) dX dW}{\int_0^{\bar{W}} \int_{X_F^*+W}^{\infty} f_X(X|\hat{X}) f_W(W|\hat{W}) dX dW} \\
&\quad - \left(\frac{MN}{MN + M + 1} \right) \\
&\quad \times \frac{\int_0^{\bar{w}} \int_w^{\bar{W}} \int_{X_F^*+W}^{\infty} w f_X(X|\hat{X}) f_{w,W}(w, W|\hat{W}) dX dwdW}{\int_0^{\bar{W}} \int_{X_F^*+W}^{\infty} f_X(X|\hat{X}) f_W(W|\hat{W}) dX dW} .
\end{aligned} \tag{4.12}$$

Substituting this result back into the inverse demand (or inverse supply) function we get the equilibrium forward price

$$\begin{aligned}
P_F(X_F^*) &= E[P_S(\cdot)] + \frac{\alpha_s}{MN} \left(\frac{N+1}{MN+M+1} \right) \int_0^{\bar{W}} \int_{X_F^*+W}^{\infty} X f_X(X|\hat{X}) f_W(W|\hat{W}) dX dW \\
&+ \left(\frac{\alpha_s}{MN+M+1} \right) \int_0^{\bar{w}} \int_w^{\bar{W}} \int_{X_F^*+W}^{\infty} w f_X(X|\hat{X}) f_{w,W}(w,W|\hat{W}) dX dw dW .
\end{aligned} \tag{4.13}$$

Notice that the first term describing the equilibrium number of forwards traded is identical to the expression describing the equilibrium number in the base model when replacing the statistical properties of net load with these of overall load²⁶. This observation is also true for the first two terms describing the equilibrium forward price²⁷. The additional terms in the RHS of (4.12) and (4.13) are attributed to the fact that IPPs own wind power capacity.

Revenues from wind power output are determined by the realized spot price. When scheduling power for delivery in advance (i.e. forward contracting) the expected spot price decreases due to the availability of more power generation capacity. Therefore, a higher volume of trade in forwards yields a lower expected spot price and thereby reduction in the expected revenues for wind power output. IPPs internalize the linkage between the revenues from the number of forward contracts they sell and the expected revenues from wind power

²⁶ Recall that the equilibrium number of forward contracts in the base model is described by

$$X_F^* = \left(\frac{MN+M-N}{MN+M+1} \right) \times \frac{\int_{X_F^*}^{\infty} X f_X(X|\hat{X}) dX}{\int_{X_F^*}^{\infty} f_X(X|\hat{X}) dX}$$

²⁷ The equilibrium forward price in the base model is described by

$$P_F(X_F^*) = E[P_S(\cdot)] + \frac{\alpha_s}{MN} \left(\frac{N+1}{MN+M+1} \right) \int_{X_F^*}^{\infty} X f_X(X|\hat{X}) dX$$

output. Therefore, IPPs' incentive to withhold capacity in the forwards market in this case is higher than in the case which they do not own wind power capacity. Consequently, the change in the forward premium in this case represents more than just a shift from the statistical attributes of overall load to these of net load. It also accounts for the ability of IPPs to exercise excess market power when they are the owners of wind power capacity.

Fringe wind capacity

In this section we look at the situation where the owners of wind power capacity do not have market power or any flow of income from electricity markets other than compensation for their wind power output. That is to say that wind power is supplied by competitive fringe firms. This is a meaningful case because it includes the examples whereby a government agency or several small private firms invest in wind power capacity and no strategic behavior is involved.

LSEs' maximization problem in this case is similar to the case whereby wind capacity is owned by IPPs. The fact that the recipient of wind power payments is another entity does not change LSEs behavior. Therefore, the demand curve is identical to the previous case, where IPPs own wind capacity.

IPPs revenues in the case of fringe capacity are based on the output of conventional power exclusively. Therefore the maximization problem is

$$\begin{aligned}
\mathcal{M} &\equiv \max_{q_F^i} E \left(\pi_{IPP}^i \left| \hat{X}, \sum_{m=1, m \neq i}^M \bar{q}_F^m, \hat{W} \right. \right) \\
&= P_F \left(\hat{X}, q_F^i + \sum_{m=1, m \neq i}^M \bar{q}_F^m, W \right) \times q_F^i \\
&+ \int_0^{\bar{W}} \int_W^\infty \left[P_S \left(X, q_F^i + \sum_{m=1, m \neq i}^M \bar{q}_F^m, W \right) \times (q^i - q_F^i) \right. \\
&\quad \left. - C(q^i, q_F^i) \right] f_X(X|\hat{X}) f_W(W|\hat{W}) dXdW .
\end{aligned} \tag{4.14}$$

Express \mathcal{M} with respect to the two states of the world

$$\begin{aligned}
\mathcal{M} &= P_F \left(\hat{X}, q_F^i + \sum_{m=1, m \neq i}^M \bar{q}_F^m, \hat{W} \right) \times q_F^i \\
&+ \int_0^{\bar{W}} \int_{\sum_{1, m \neq i}^M \bar{q}_F^m + q_F^i + W}^\infty [P_S(X, W) \times (q^i - q_F^i) \\
&\quad - C(q^i)] f_X(X|\hat{X}) f_W(W|\hat{W}) dXdW \\
&+ \int_0^{\bar{W}} \int_{\sum_{1, m \neq i}^M \bar{q}_F^m + q_F^i + W}^\infty \left[P_S \left(X, q_F^i + \sum_{m=1, m \neq i}^M \bar{q}_F^m, W \right) \right. \\
&\quad \left. \times (q^i - q_F^i) - C(q^i, q_F^i) \right] f_X(X|\hat{X}) f_W(W|\hat{W}) dXdW .
\end{aligned} \tag{4.15}$$

Taking the first derivative

$$\begin{aligned}
\frac{\partial \mathcal{M}}{\partial q_F^i} &= \frac{\partial P_F(\cdot)}{\partial q_F^i} q_F^i + P_F(\cdot) \\
&\quad - \int_0^{\bar{w}} \int_{\sum_{m=1, m \neq i}^M \bar{q}_F^m + q_F^i + W} P_s(\cdot) f_X(X|\hat{X}) f_W(W|\hat{W}) dXdW \\
&\quad + \int_0^{\bar{w}} \int_{\sum_{m=1, m \neq i}^M \bar{q}_F^m + q_F^i} \left[\frac{\partial P_s(\cdot)}{\partial q_F^i} \times (q^i - q_F^i) + P_s(\cdot) \times \left(\frac{\partial q^i}{\partial q_F^i} - 1 \right) \right. \\
&\quad \quad \left. - C'(q^i, q_F^i) \right] f_X(X|\hat{X}) f_W(W|\hat{W}) dXdW.
\end{aligned} \tag{4.16}$$

Writing explicitly the derivatives of the spot price and the cost function

$$\begin{aligned}
\frac{\partial \mathcal{M}}{\partial q_F^i} &= \frac{\partial P_F(\cdot)}{\partial q_F^i} q_F^i + P_F(\cdot) \\
&\quad - \int_0^{\bar{w}} \int_{\sum_{m=1, m \neq i}^M \bar{q}_F^m + q_F^i + W} P_s(\cdot) f_X(X|\hat{X}) f_W(W|\hat{W}) dXdW \\
&\quad + \int_0^{\bar{w}} \int_{\sum_{m=1, m \neq i}^M \bar{q}_F^m + q_F^i + W} \left[-\frac{\alpha_s}{M} \times (q^i - q_F^i) + P_s(\cdot) \times \left(\frac{\partial q^i}{\partial q_F^i} - 1 \right) - \alpha_t q^i \frac{\partial q^i}{\partial q_F^i} \right. \\
&\quad \quad \left. - \alpha_s (q^i - q_F^i) \left(\frac{\partial q^i}{\partial q_F^i} - 1 \right) \right] f_X(X|\hat{X}) f_W(W|\hat{W}) dXdW.
\end{aligned} \tag{4.17}$$

Employing symmetry and collecting terms

$$\begin{aligned}
\frac{\partial \mathcal{M}}{\partial q_F^i} &= \frac{\partial P_F(\cdot)}{\partial q_F^i} q_F^i + P_F(\cdot) - E[P_s(\cdot)] \\
&\quad + \alpha_s \left(1 - \frac{1}{M} \right) \int_0^{\bar{w}} \int_{\sum_{m=1, m \neq i}^M \bar{q}_F^m + q_F^i + W} (q^i - q_F^i) f_X(X|\hat{X}) f_W(W|\hat{W}) dXdW.
\end{aligned} \tag{4.18}$$

The FOC is

$$P_F(\cdot) = E[P_S(\cdot)] - \frac{\partial P_F(\cdot)}{\partial q_F^i} q_F^i$$

$$-\alpha_s \left(1 - \frac{1}{M}\right) \times \int_0^{\bar{w}} \int_{\sum_{m=1, m \neq i}^M \bar{q}_F^m + q_F^i + W}^{\infty} (q^i - q_F^i) f_X(X|\hat{X}) f_W(W|\hat{W}) dX dW .$$
(4.19)

Writing explicitly the IPPs' FOC and imposing clearing market condition

$$P_F(X_F^*) = E[P_S] + q_F^* \frac{\alpha_s}{M} \left(1 + \frac{1}{N}\right) \int_0^{\bar{w}} \int_{X_F^* + W}^{\infty} f_X(X|\hat{X}) f_W(W|\hat{W}) dX dW$$

$$-\frac{\alpha_s(M-1)}{M} \int_0^{\bar{w}} \int_{X_F^* + W}^{\infty} (X - X_F^*) f_X(X|\hat{X}) f_W(W|\hat{W}) dX dW .$$
(4.20)

Equating aggregate inverse demand and inverse supply, the equilibrium number of forward contracts in this case is described by

$$X_F^* = \left(\frac{MN + M - N}{MN + M + 1} \right) \times \frac{\int_0^{\bar{w}} \int_{X_F^* + W}^{\infty} X f_X(X|\hat{X}) f_W(W|\hat{W}) dX dW}{\int_0^{\bar{w}} \int_{X_F^* + W}^{\infty} f_X(X|\hat{X}) f_W(W|\hat{W}) dX dW}$$
(4.21)

and the forward price is

$$P_F(X_F^*) = E[P_S(\cdot)]$$

$$+ \frac{\alpha_s}{MN} \left(\frac{N+1}{MN+M+1} \right) \int_0^{\bar{w}} \int_{X_F^*+w}^{\infty} X f_X(X|\hat{X}) f_W(W|\hat{W}) dX dW . \quad (4.22)$$

Both expressions are identical to these of the base model respectively when taking into account the statistics of net load instead of overall load. Because wind power is owned by a competitive entity, no additional market power is given to IPPs and thus the resemblance between the equilibrium expressions in this case and these of the base model. In the case of fringe capacity, IPPs' incentive to maintain a high spot price is lower than in the case that they are the owners of wind capacity. As a result, more forwards are being traded which brings relatively more conventional capacity online in advance. This in turn, lowers expected marginal cost and the expected spot price.

Chapter summary

In this chapter we expanded the theoretical framework to allow the modeling of wind-integrated electricity markets. In doing so, we accounted for the decrease in the employment of conventional energy resources due to the availability of wind power capacity. Also, we modeled risk management behavior in the forwards market, which are strongly influenced by the new uncertainty introduced from the supply side of the market. Our analytical work provides transparent, traceable and robust results for equilibrium measures of electricity markets with wind energy. The question who invests in wind power capacity is important as the electric industry structure has an effect on the amount of conventional generation

capacity that is traded in advance, thereby impacts equilibrium prices and premiums as well. Our main result is that IPPs have a higher incentive to withhold capacity in the forwards market in the case which they are the owners of wind power capacity. Consequently, in this case prices of electricity in both spot and forward markets are higher compared to the case where wind power capacity is owned by fringe firms.

Employing high frequency historical data, one can calibrate this model and obtain testable empirical results. Since the research question is about the future expansion of wind capacity, the required data for this purpose does not exist yet. Instead, we need to introduce the appropriate numerical methodology to simulate the possible paths for wind power expansion. This is the objective of the next chapter.

Chapter 5: A numerical method for simulating the conditional distribution of regional wind power output for modeling trade of short-term electricity forwards

Introduction

Information about future availability of overall wind energy at the power system is valuable for both technical and economic reasons. In this chapter we are interested in simulating the information that is accessible to firms for the purpose of modeling their behavior in futures markets for spot power. To carry out this task we need to look at the short-term distributional patterns of wind power forecasting because that is the timeframe for the operation of the day-ahead markets. By that time, low resolution outputs from numerical weather prediction models (NWP), as well as downscaling tools (which make use of physical conditions to obtain higher resolution forecasting) are already accounted for. Then, statistical models take these predictions as inputs for shorter forecasting horizons, which is the forecasting time framework we are interested in simulating in this chapter.

The initial step is attaining wind speed forecasts at the locations where wind power capacity is installed. Yet, simulating wind speed forecasts is not easy because one should account for wind speed variability and the need to predict wind speeds at several locations simultaneously. In addition, errors in wind speed forecasts translate into errors in wind power forecasting, which are translated into large errors in energy output. These forecasting errors

may be substantial because of the non-linear nature of the power curve. For all these reasons wind speed forecasts is an important part of the simulations.

In the following we propose a novel methodology for the simulations of the uncertainty regarding the availability of wind power in the day-ahead market. For that purpose, we use the joint distribution of wind speed and wind speed forecasting, their conditional and marginal probability density functions, and the specifications of a wind power curve. To model aggregate regional wind power, we make use of a method first proposed by Iman and Conover (1982) to impose spatial wind correlation in the simulated region.

Simulating wind speed forecasts at one location

Consider the joint probability distribution function (pdf) of wind speed and a short-term wind speed forecast (e.g. day-ahead) for a particular location. Denote this pdf by $f_{w,\hat{w}}(w, \hat{w})$ where w is wind speed and \hat{w} is wind speed forecast. By the laws of probability this may be written as

$$f_{w,\hat{w}}(w, \hat{w}) = f_{w|\hat{w}}(w|\hat{w})f_{\hat{w}}(\hat{w}) \quad (5.1)$$

where $f_{w|\hat{w}}(w|\hat{w})$ is the conditional pdf of wind speed given wind speed forecast, and $f_{\hat{w}}(\hat{w})$ is the marginal pdf of wind speed forecast. Then, the marginal pdf of wind speed is given by

$$f_w(w) = \int_{\hat{w}} f_{w|\hat{w}}(w|\hat{w})f_{\hat{w}}(\hat{w})d\hat{w} . \quad (5.2)$$

Next, assume a particular (Weibull) pdf $f_{\hat{w}}(\hat{w})$ for wind speed forecast. The assumption regarding the particular conditional pdf to employ in the experiment is not important for the

purpose of implementing the proposed method. Therefore, in line with the findings from the relevant literature (e.g. Giebel 2001, Landberg 1994 and Lange 2005) we assume that this conditional pdf is normally distributed and centered at the forecasted value. (That is, forecasts are unbiased). Also, we need to account for the pronounced heteroscedasticity in wind speeds. To be precise, we assume the variance of wind speed forecast errors is non-decreasing in the magnitude of the forecasted value. Formally

$$w|\hat{w} \sim N(\hat{w}, \sigma^2(\hat{w})) \quad (5.3)$$

where $d\sigma^2/d\hat{w} \geq 0$

Then, we generate values of wind speed and wind speed forecasts by means of the following Monte-Carlo simulation:

1. Make draws directly from the pdf $f_{\hat{w}}(\hat{w})$.
2. Use (5.3) to construct a numerical conditional pdf of wind speed $f_{w|\hat{w}}(w|\hat{w})$. Notice that during this process negative values of wind speed may appear. We show later how to avoid this problem when we parameterize the variance of $w|\hat{w}$.
3. Use (5.2) to integrate over wind speed forecasts and compute the marginal pdf of wind speed $f_w(w)$.
4. Adjust the parameters of $f_{\hat{w}}(\hat{w})$ and repeat the process till the resemblance between the simulated $f_w(w)$ and the desired wind speed pdf for the experiment is within an acceptable range. (More details are provided in the example below).

Simulating wind power forecasts at one location

We assume that all turbines in a given location experience the same wind speed. Therefore, wind power output at this location increases linearly in the number of turbines installed. This is a reasonable simplification because the correlation in wind speed within large wind farms is likely very high. Considerations of the aerodynamics interaction between turbines for maximizing power production in wind farms are discussed elsewhere (e.g. Mosetti, Poloni and Diviacco 1994).

We proceed with the Monte Carlo simulation as follows:

5. Specify a power curve of a modern wind turbine to be employed in the experiment.
6. Use the turbine's power curve to translate the draws of wind speed forecasts into draws of wind power output of each turbine.
7. Multiply wind power output of a single turbine by the number of turbines installed to arrive at the aggregate output in the simulated location.

Simulating wind power forecast errors at one location

8. Draw from $f_{w|\hat{w}}(w|\hat{w})$ once again to specify a particular wind speed realization in each simulated delivery period.
9. Use wind speed realization to compute realized wind power output in each simulated period using the power curve and the number of wind turbines installed at the simulated location.

10. Integrate over wind power realizations to compute numerical capacity factor of the employed wind turbine.
11. Calculate prediction error in each realization to compute mean absolute error (MAE) of wind power forecast across all delivery periods.

Calibration and verification

1. The performance of wind power forecasting systems is measured generally by MAE.

This is computed as

$$MAE = \frac{1}{N} \sum_{i=1}^N |Actual_i - Forecast_i| . \quad (5.4)$$

This statistic is usually reported as a percentage of total installed wind capacity or as a percentage of actual energy produced. Adjust the parameterization of $\sigma^2(\hat{w})$ such that the numerical MAE of wind power forecast in the experiment and the empirical MAE reported by the literature are the same.

2. Verify that the numerical capacity factor of the simulated wind turbine matches the reports on the empirical performance of the assumed commercial wind turbine employed in the experiment (capacity factor is discussed in chapter 3).

An example of wind power simulation at one location

Start by assuming the following pdf for the short-term wind speed forecast²⁸

$$\hat{w} \sim Wei(9.35, 2.76) . \quad (5.5)$$

The first and second moments of this distribution are 8.33 and 10.68 respectively.

We parameterize $\sigma^2(\hat{w}) = \sigma^2 \hat{w}^2$ and let $\hat{\sigma}^2=0.05$ (illustrated in figure 18)²⁹. Setting the variance that way serves two purposes; first, it is realistic to assume that the variance increases monotonously in the magnitude of wind speed forecast, secondly, this parameterization produces very small errors in the case that the forecasted value is low and by that diminishes the likelihood of the algorithm to generate negative values of wind speed while constructing the conditional pdf.

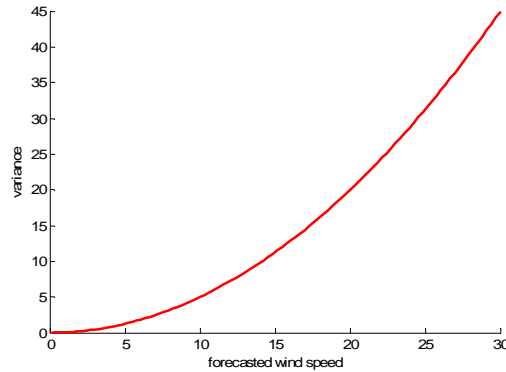


Figure 18: Variance of the conditional wind speed in the experiment

The numerical marginal pdfs of wind speed and wind speed forecast were generated by 5,000 draws and depicted in figure 19.

²⁸ See table 3, this is the distribution of wind speed we fitted at Osceola County, IA in a typical March.

²⁹ The assumption $\hat{\sigma}^2=0.05$ is made only for illustration purposes at this point. However, we use this particular value in the numerical experiment in chapter 6 to generate a desired MAE.

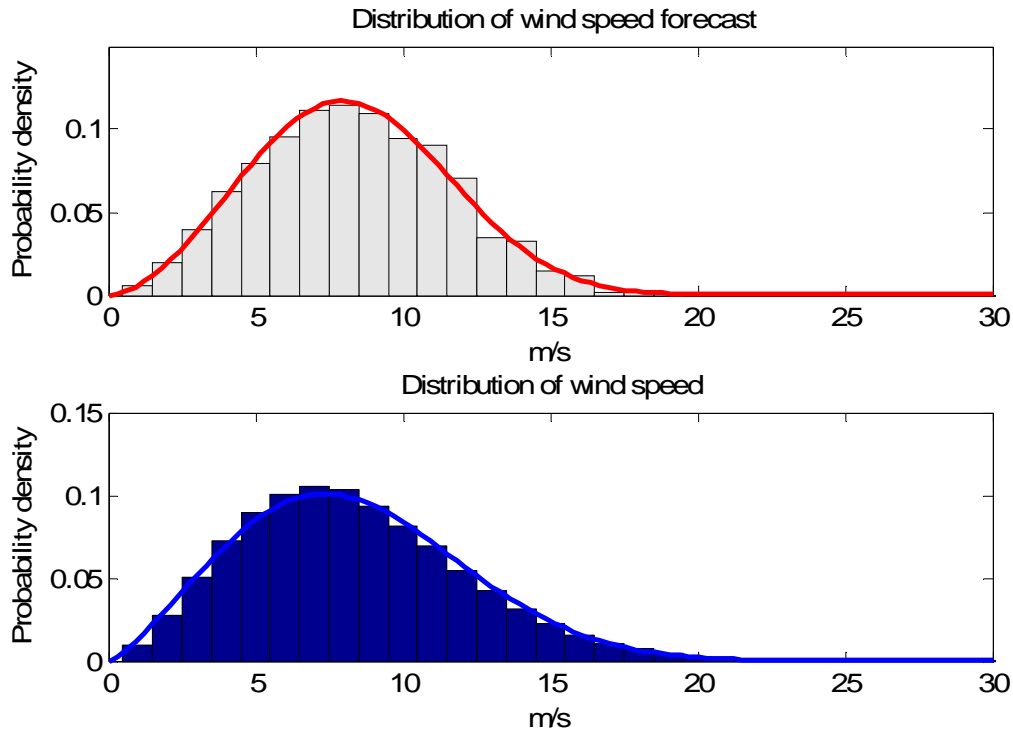


Figure 19: Numerical marginal pdf of wind speed forecast (top) and wind speed (bottom)

Table 4: Moments and parameters of the numerical marginal pdfs of wind speed and wind speed forecast

| | Mean | Variance | Fitted Weibull scale parameter | Fitted Weibull shape parameter |
|---------------------|------|----------|-----------------------------------|-----------------------------------|
| Wind speed forecast | 8.33 | 10.68 | 9.35 | 2.76 |
| Wind speed | 8.32 | 14.67 | 9.40 | 2.31 |

The illustration and the point estimates (table 4) show that assuming wind speed forecast is distributed Weibull provide a good fit for a Weibull distribution of wind speed. The means of the pdfs are approximately the same. This result is expected since we employ an unbiased

wind speed forecast in the experiment. However, the variance of the assumed pdf for wind speed forecast is smaller than the variance of the pdf for wind speed. This is due to the introduction of the disturbance term associated with forecasting error. Our goal is to find values for the parameters of the Weibull function describing the forecasts, which will generate the desired moments of wind speed for the experiment. Notice that wind speed and wind speed forecast have the same mean, thus the two parameters of the Weibull pdf for wind speed forecasts should be a pair that generates the mean of the desired wind speed pdf. Since we have two parameters there is infinite number of pairs that qualify. Recall that the mean value of a random variable distributed Weibull is

$$m = c\Gamma(1 + 1/k) \quad (5.6)$$

where c and k are the scale and shape parameters respectively, and $\Gamma(\cdot)$ is the gamma function.

The total differential is

$$dm = \frac{\partial m}{\partial c} dc + \frac{\partial m}{\partial k} dk . \quad (5.7)$$

By linear approximation, we may write

$$\Delta m = \Gamma(1 + 1/k)\Delta c - ck^{-2}\Gamma'(1 + 1/k)\Delta k . \quad (5.8)$$

Since wind speed forecasting is unbiased, we impose $\Delta m = 0$ and get the following expression

$$\frac{\Delta c}{\Delta k} = \frac{c}{k^2}\psi(1 + 1/k) \quad (5.9)$$

where $\psi(1 + 1/k) = \frac{\Gamma'(1+1/k)}{\Gamma(1+1/k)}$, is the Psi function (also known as the *digamma function*).

Equation (5.9) provides an expression for the relation between the pairs of Weibull parameters that approximate the same mean as that of the particular pair k and c . As long as we change c and k with accordance to condition (5.9) we know that the mean of the two marginal distributions remains approximately the same. The next step is to pick a pair that provides us with the desired variance for the target pdf of wind speed. This is not a difficult task, which may be accomplished by a standard numerical search technique. For example, a simple computation shows that if we wanted to generate a pdf of wind speed which is similar to the estimated March hourly wind speed distribution in Osceola County (eq. 5.5), we should start the Monte Carlo simulation by assuming $\hat{w} \sim Wei(9.26, 3.51)$.

To convert simulated values of wind speed to wind power output a power curve of a modern 1.5 MW turbine is used. This curve is depicted in chapter 3 (figure 14). A wind turbine of this rate is chosen as it is a fairly large machine which is appropriate for regions with excellent conditions of wind resources (wind speed between 7.5 and 8 m/s at 50 m height). Larger commercial machines which are suited for outstanding (8-8.8 m/s) or superb (>8.8 m/s) wind conditions may be considered as well. However, study on the penetration rate of wind power capacity requires that the employed turbine size in the experiment should be with accordance to the availability of spatial wind power resources. Regions of outstanding and superb wind conditions in the U.S. are scarce and many of them do not provide any certainty of delivering stable large flow of wind power during most months and for a large geographical dispersion.

Next, we want to examine how the magnitude of wind speed forecast influences the distribution of wind power forecast (figure 20). While the conditional pdfs of wind speed in

all cases are Gaussian by assumption, the shape of the conditional pdf of wind power is far from being Gaussian. It varies by the magnitude of the forecasted value and has no recognizable form. The reason for that is the nonlinear nature of the power curve. For example, wind power output is truncated on both sides. Namely, for periods with wind speed forecasts from the tails of the distribution, the probability of zero wind power output is high. If the forecasted value is sufficiently low, it is expected that wind speed would not exceed the *cut-in* point and therefore it is most likely that no power would be generated. This is described in figure 20 by the case that the wind speed forecast is 2 m/s. Likewise, a high forecasted value entails higher probability that the turbine may attain its *cut-off* point, and cease power generation to protect itself from damage. That is depicted in figure 20 in the case of wind speed forecast of 25 m/s. Recall that 25 m/s is the *cut-off speed*, therefore it is shown that about half of the time the turbine generates its rated power and in the rest nothing. For wind speeds between the *cut-in* point and 14 m/s which is the *rated-speed* (wind speed at which the turbine generates its rated power) the power curve is convex, which implies that small deviations in wind speed in this segment yields large asymmetric deviations of wind power. Those are reflected by the depicted graphs for wind speed forecasts of 5, 8, 12 and 16 m/s in figure 20.

Our results show that the conditional pdfs of wind power forecasting error are not Gaussian. However, integrating out the forecasts, the unconditional distribution of forecasting error seems like a dense normal distribution (figure 21). This result is in line with several empirical studies that show that wind power prediction errors may be represented (at least) loosely by a

Gaussian distribution (see Blatchford and Zack 2004, Loutan and Hawkins 2007, Madsen et al. 2004, and Pinson and Kariniotakis 2004).³⁰

For modeling trading decisions, it is the conditional distribution of wind power forecasting errors that is important. That is because financial consequences of trading decisions in futures markets are drawn from the distribution of wind power given a short-term forecast.

Averaging over the 5,000 draws (periods) in the experiment, we compute wind power plants' capacity factor of 51% and mean absolute error as percentage of installed capacity of 14%.

³⁰ Blatchford and Zack (2004) and Loutan and Hawkins (2007) studied the predictions of the central wind forecasting system in California ISO. Pinson and Kariniotkais (2004) presented forecast errors for a case study of a single wind farm in Ireland. Finally, Madsen et al. (2004) studied the performances of more than 10 prediction systems in Europe as part of a project of the European Union Commission.

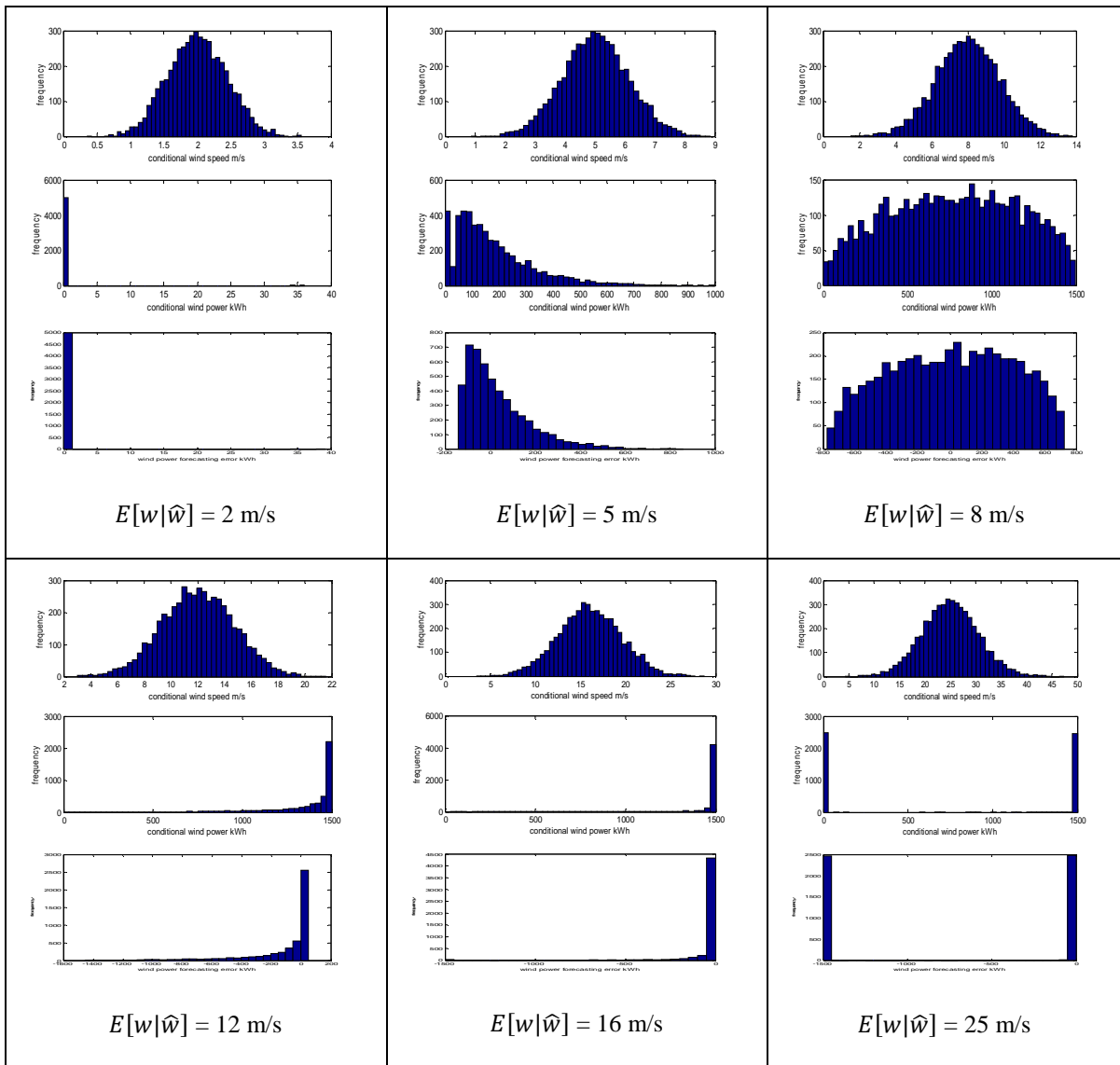


Figure 20: Conditional wind speed, the associated conditional wind power distributions and the distributions of wind power forecasting error given wind speed forecasts of 2, 5, 8, 12, 16 and 25 m/s

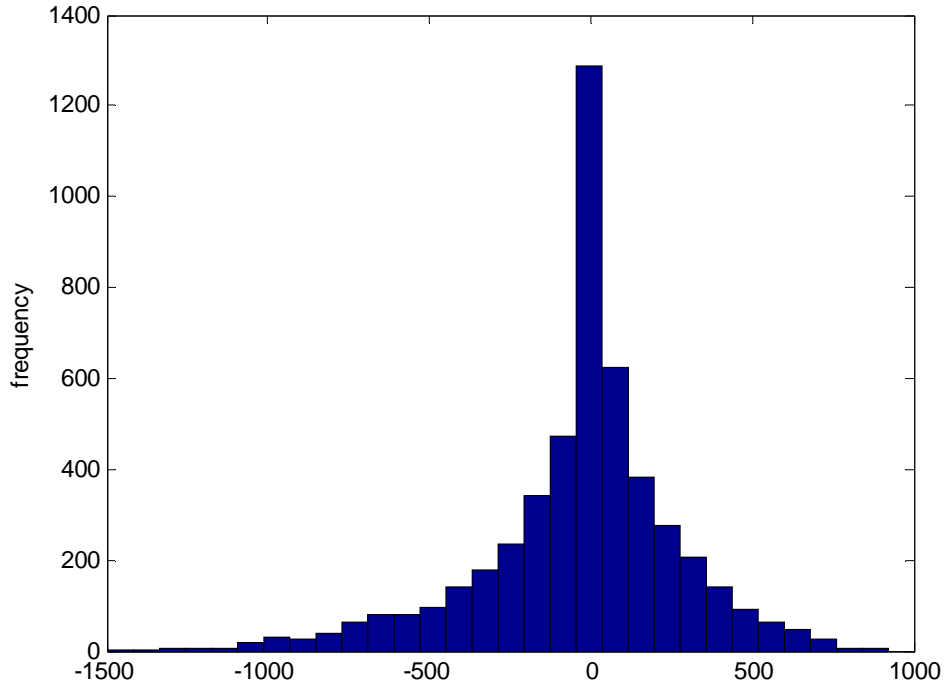


Figure 21: The unconditional distribution of wind power forecasting error at one location (kW)

Aggregate regional wind power output

In the following we consider a study region composed of several wind site locations where there is a short-term wind speed forecast available at each location. The goal is to simulate wind speed forecasts and realizations that are consistent with correlated forecasts and the spatial nature of wind speed.

In general, the forecasting error of wind power output from several sites is lower than forecasting errors from a single site. How fast and to what extent these errors are reduced with the addition of wind capacity depends primarily on the size of the region and how spatially correlated wind is in the region. The geographical distribution of wind farms in a region determines the distribution of regional wind power output.

For the purpose of imposing spatial correlation we employ a method that was introduced by Iman and Conover (IC) in 1982. The method is used in a large variety of applications where there is a need to generate correlated random numbers (see for example, Brus and Jansen 2004, Hart, Hayes and Babcock 2006, Maia and Neto 2004, and Wu and Tsang 2004). The technique is distribution free, preserves the exact form of the marginal distributions on the input variables and simple to use. The theoretical basis of the IC method is that independent random numbers drawn from independent marginal distributions can be sorted to comply with any desired rank correlation matrix.

Let A be a k by n matrix corresponded to k draws from n independent marginal distributions. If C is a target correlation matrix for A then we know that since C is positive definite and symmetric, there exists a lower triangular matrix P such that $PP' = C$ and AP' has the target correlation matrix C . This is the theoretical basis for the IC method.

The objective is to find a rank correlation matrix M that is sufficiently close to the desired correlation matrix C . In order to do so, the IC method requires defining a *score matrix*. For the score matrix, Iman and Conover (1982) suggest using ranks, random normal deviates or van der Waerden scores. We adopt the latter method which is employed in the original paper.

Let R be a k by n score matrix where each of its columns comprise from a random mix of the

van der Waerden scores. That is $a(i) = \Phi^{-1}(i/(N + 1))$ for $i = 1 \dots N$, where Φ^{-1} is the inverse function of the standard normal distribution. Then, find a lower triangular P , which is associated with the target correlation matrix C . Two common ways to compute P are through Cholesky factorization and singular value decomposition. The score matrix R is multiplied by P' to transform its columns such that the transformed matrix, denoted by R^* , has a rank correlation M which is close to C .

To improve the similarity between the matrices M and C , Iman and Conover (1982) suggests proceeding as follows. The difference between M and C is explained partially by R not having a sample correlation equal to the identity matrix I . The goal is to decrease the variance of the transformation matrix in order to reduce the dissimilarity. For that purpose, a matrix S should be found such that $STS' = C$ where T is the sample correlation of R . First, compute a lower triangular Q such that $T = QQ'$. Then, recall that $C = PP'$, so we can write $SQQ'S' = PP'$. From that we know that $SQ = P$ or $S = PQ^{-1}$. Therefore, the matrix denoted by $R_B^* = RS'$ has the exact correlation matrix C and a rank correlation M^* , which is closer to C than M is.

While the implementation of the IC method for our purpose is straightforward, we need to explain how to derive the matrix C to simulate spatial correlation in our application. Start, by defining a study region for the experiment. In theory, the shape of the study region is relatively unimportant as long as it is not too small to capture the full range of spatial variation in the underlying process (Diggle and Ribeiro 2007). Let L be a square lattice which is divided into n by n symmetric locations

$$L = \begin{bmatrix} L_{1,1} & \cdots & L_{1,n} \\ \vdots & \ddots & \vdots \\ L_{n,1} & \cdots & L_{n,n} \end{bmatrix} \quad (5.10)$$

Denote by Δ the side length of each location. Notice that Δ is also the Euclidean distance between the centers of any two orthogonal nearest neighbor locations (likewise, $\sqrt{2}\Delta$ is the Euclidean distance between the centers of any two diagonal nearest neighbor locations).

The next step is to specify the stochastic nature of the spatial process. For example, if wind speed experiences the same distribution at all locations, and spatial correlation depends only on the distance between locations then the process is stationary. Conversely, wind speed may experience spatial trend. For instance, differences in the mean may be explained by the coordinates of the location on the study region. Another example for non-stationarity is due to the existence of directional effects on the correlation structure. Notice that our theoretical framework does not put any restrictions on the structure of the spatial correlation to be employed in the numerical experiment. Spatial correlation may be described by any function of the Euclidean distance, the coordinates of L or other factors affecting the n^2 by n^2 correlation matrix C .

Next, we make n^2 draws from the pdf $f_{\hat{w}}(\hat{w})$ in each simulation. These are the (unsorted) wind speed forecasts at n^2 locations. Each draw is used as row entries in a matrix denoted as A . Suppose we make k draws in the experiment, A 's dimensions are k by n^2 .

Once matrices A and C are defined, the IC method can be applied for imposing spatial correlation among local wind speed forecasts. The imposition of spatial correlation on the forecasts is reasonable because forecasting systems run on low resolution models as first step

and therefore use predictions of regional scale events as inputs before physical downscaling tools³¹ are being implemented.

After we generate local wind speed forecasts, we proceed with the Monte Carlo simulation in each location as elucidated earlier. That way, we obtain local and aggregate conditional pdfs of the short-term wind power forecasting. Those are valuable for us as they will be used as inputs for modeling traders' decision making in the next chapter.

An example of simulating spatially correlated wind

Generally, wind speed should be considered as a non-stationary spatial process because of the physical conditions which are never entirely homogenous over a geographical region. However, since our experiment does not relate to a specific region, we would not want to put restrictions at this stage on the analysis. As argued earlier, for applied purposes, one can impose any specific spatial wind structure to this framework without adding complexity to the analysis.

Assuming stationarity, the Euclidean distances alone are sufficient to construct the desired correlation matrix C . We carry on our example with an exponential correlation function since this is the one that is commonly chosen to describe wind spatial correlation (see references in chapter 3). Ignoring a nugget effect, the correlation function is

³¹ Physical downscaling tools refer to the utilization of high resolution spatial data such as topography and roughness to refine forecasting at the site level.

$$r_{ij} = e^{-\beta d_{ij}} \quad (5.11)$$

where d_{ij} is the Euclidean distance between any two locations i and j , and the value of the parameter β (known as the *characteristic distance*) needs to be calibrated.

Let $n = 10$ and $\Delta = 100$ km, with a region of size 1,000 km², which is divided into 100 wind locations. The literature regarding wind spatial correlation is quite limited and the few empirical studies reviewed earlier, are about wind statistics in European countries (see chapter 3). In line with this literature we set $\beta = 0.002$. The spatial correlation of wind speed for the experiment is illustrated in figure 22.

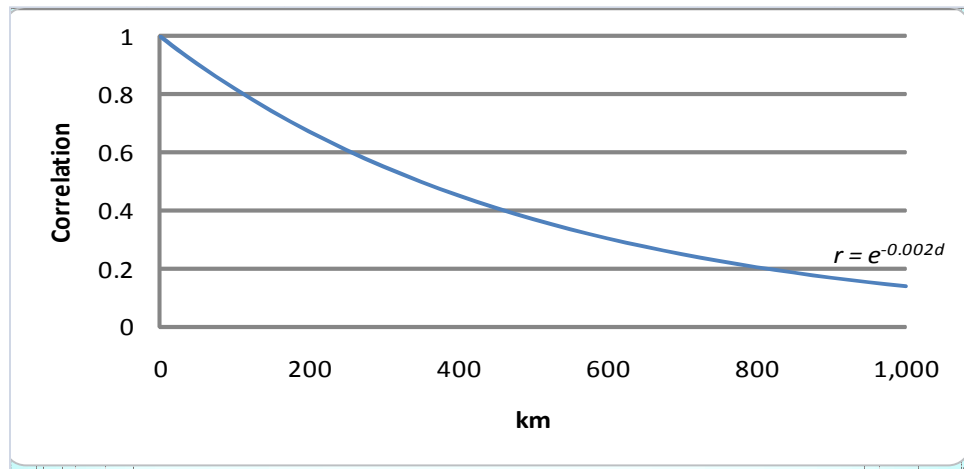


Figure 22: Wind spatial correlation in the experiment

Making use of the spatial correlation function while accounting for the coordinates of wind locations we compute the correlation matrix C . That is the correlation to be imposed while simulating wind speed forecasts in the region study.

The Monte Carlo experiment consists of 5,000 draws. We draw independently for all wind locations from the pdf of wind speed forecast that is used in previous example (eq. 5.5). That gives us a matrix A of 5000 by 100 random draws. To generate the score matrix R we randomize the van der Waerden scores in each column. The required lower triangular matrices P and Q are computed by Cholesky factorizations. Deriving the matrix denoted by R_B^* we get the exact correlation matrix C and a rank correlation M^* . Finally, each column of A is resorted according to the ranks in the columns of R_B^* . Doing so, we generate rank correlation M^* among the columns of A while preserving the marginal distributions of the forecasts in each wind location.

The top entry in each cell in table 5 shows the target correlation matrix C for (randomly depicted) locations 31 to 41. For instance, looking at the first row we see how the correlation dies slowly as we go from left to right (or west to east with regard to the study region L). The correlation of locations 31 and 41 is high again since they are located on top of each other in L . The second entry in each cell of the table is the correlation we get by imposing rank correlation on wind speed forecasts. The difference between the target and the simulated correlations of forecasts shows that the IC method provides a practical approximation for the desired spatial correlation. The third entry in each cell is the correlation between the marginal pdfs of local wind speed. This correlation is lower than the correlation of the forecast because we impose the spatial correlation on the forecasts. As explained earlier, this is realistic because forecasting systems make predictions that are drawn from the forecasting of regional scale events.

In table 6 we depict the results for wind power spatial correlations. The relation between the correlations of wind power forecast and wind power realization is similar to the corresponding relation between the correlations of wind speed. However, due to the non-linearity of the conversion rate of the power curve the spatial correlations of wind power forecasts and realizations are lower than these of wind speed respectively.

Finally, we look at the conditional distribution of aggregate regional wind power output. This distribution depends on the spatial smoothing effect in the region. Since wind statistics and other characteristics of a particular region are specifications which may vary greatly, we employ a broader approach in our analysis. The illustrations include the particular spatial correlation assumed so far in the experiment (figure 22) and two boundary cases. One is a

fully diversified wind case which refers to a zero correlation of wind power in any level of output. It may describe a region which is sufficiently large to accommodate wind power capacity so it is not influenced by spatial correlation. The second is an *undiversified wind* case. This is parallel to scaling up the capacity of a single wind farm since in this case the region does not offer any spatial smoothing effects.

While most likely no real-world region complies with either of the two boundary cases, observing the range of results spanned by these two is practical. It provides an indication of the importance of diversifying wind power production and demonstrates the impacts of spatial correlation that can provide insights into particular regions.

Geographical diversification of wind power may reduce the productivity of wind turbines if less windy areas are developed. In our simulations we do not account for a potential decrease in a capacity factor due to wind diversification. Doing so, we are able to observe all possible outcomes with no prior restrictions. More applied work ought to take this factor into consideration but we do not impose it. In this sense the fully diversified wind case represent the most efficient expansion path possible for regional wind capacity.

We assume a single 1.5 MW wind turbine in every location, thus the rated regional wind capacity in our illustration is 150 MW. The marginal pdf of wind power forecast is depicted in figure 23. Looking at the illustrated distributions it is clear that spatial correlation has a significant impact on the statistical properties of aggregate regional wind power. In the case that wind is uncorrelated the forecast is normally distributed. For the particular correlation imposed in the experiment (figure 22) we see that a smoothing effect takes place but not to the extent that the marginal distribution becomes Gaussian. Particularly, the variance of the

forecast is much higher than the previous case. Finally, if the region does not offer any smoothing effects the distribution of the forecast is very uneven. To be precise, the likelihood of getting values that are not from the tails of the distribution is relatively small. Because wind is fully correlated, the distribution in this case reflects the relatively high probabilities of local wind speed being below the cut in point or above the turbine's rated speed.

Looking at the conditional distribution of wind power we get an interesting result. In figure 24 we depict selected conditional pdfs to exemplify low, intermediate and high wind power forecasts (recall that we generate 5,000 conditional pdfs in the experiment). While all three distributions are Gaussian-like, it seems that using the wind power value implied by the forecasted values of wind speed introduces bias in wind power forecasting. This is especially true in the cases of low and high forecasted values. A forecast in the case of wind speed between the extremes is more dependable since the transformation of speed to power is less likely to be truncated by the power curve at this range. When we integrate over all forecasts we find that transforming expected wind speed to wind power generates a relatively small prediction bias (the average error in the experiment is about 3 MW, which is less than 2.5% of installed capacity). This result is due the fact that wind power output is truncated from both sides.

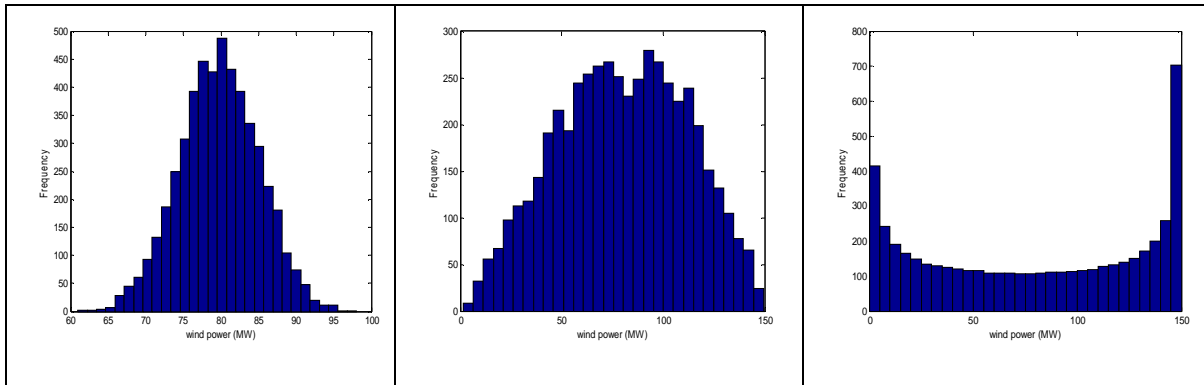


Figure 23: Marginal pdfs of wind power forecast; no correlation (left), some correlation (center) and full correlation (right)

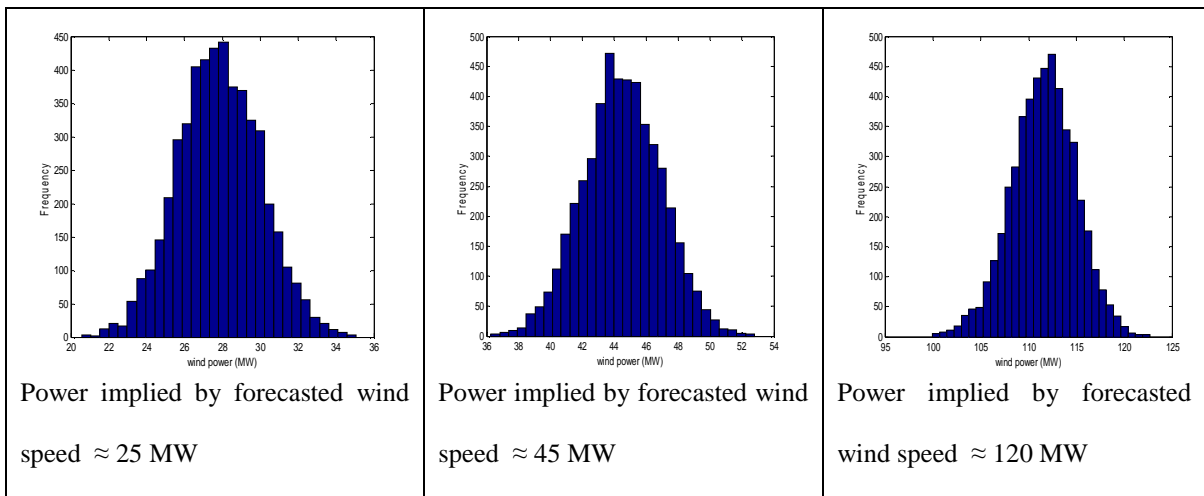


Figure 24: Conditional pdf of wind power, imposing some correlation; low (left), intermediate (center) and high wind power forecasts (right)

Chapter summary

In this chapter, we develop a numerical methodology to simulate the uncertainty regarding future wind power availability at the time of trading short-term electricity forwards. The methodology is relatively simple and independent of any specifications of wind speed conditions, spatial correlation, wind energy conversion, and wind power penetration rate.

Thus, it can accommodate a large array of assumptions regarding the paths for wind power expansion. The IC method, which is commonly applied to construct rank correlation among random variables, is used in this study for the purpose of inducing spatial correlation. Since geographical regions are very different and no concrete wind speed data is available to us at this time, the method is exemplified avoiding any subjective assumptions.

The conditional distribution of wind power derived from wind speed forecasts at one location has no identifiable form. Moreover, the technical nature of the power curve makes it necessary to examine every wind speed forecast individually because some wind speed forecasts are associated with higher wind power variability than others. In periods of very low wind speeds it is almost certain that the turbines will generate zero output. Forecasts that are higher than the turbine's rated speed but not too close to the cut-off point are very likely to generate the rated power. Other values of wind speed forecasts generate peculiar conditional distributions of wind power as well. This result is consequential; it means that in some trading periods traders face more uncertainties than in others. We show that spatial correlation is a main factor determining the uncertainty in aggregate wind power forecasting. The distribution of aggregate output may be U-shaped in the case of no smoothing effects, normal in the case of highly correlated wind or with no conforming shape in the case of some degree of spatial correlation. Therefore, the particular densities of aggregate wind power created by a short-term wind forecasting must be accounted for in modeling electricity markets with wind power capacity. The numerical work developed in this chapter, coupled with the theoretical economic framework introduced earlier, complete the required state of knowledge to model wind-integrated electricity markets.

Chapter 6: Modeling equilibrium in wind-integrated electricity markets

Introduction

The theoretical framework and the numerical methodology developed in previous chapters enable the analysis of various scenarios of wind power integration. In this chapter we generate and discuss results which are based on a particular set of assumptions. The assumptions regarding the structure of the electric industry and load are the ones we used earlier for the illustration of the base model in chapter 2. Assumptions regarding the features of the study region, wind speed statistics, wind power technology and forecasting quality are drawn from the related literature, recent technical reports and the analysis of wind speed data in Iowa.

Since the specifics of electricity markets in different regions vary greatly, the results presented in this chapter should not be seen as a general guideline but rather an example of how to go about modeling equilibrium outcomes in the new economic environment of wind-integrated electricity markets. A more applied work should use this theoretical framework while employing the characteristics of a particular region in question. For instance, assuming a particular industry structure refines the modeling of market power in the associated region. Second, the cost parameters of generating power in the model can be calibrated to fit a particular regional supply curve. Third, for concrete predictions it will be required to evaluate empirically and employ the specifics of wind resources as well the precision of the central

forecasting system in the region in question. While the theoretical framework developed here is flexible to accommodate various applied questions regarding wind power integration, we focus in our simulations on two key questions. The first is the impact that ownership of wind power capacity has on market equilibrium. The second is what role wind power diversification plays on equilibrium prices.

Simulation setup

Overall load

The integration of wind power is our main interest therefore we fix the forecasted value of overall load across all simulations. This allows us to control for variations in the predictions of the model caused by the variations of overall load. The conditional pdf of overall load employed in the experiment is $X|\hat{X} \sim N(10,000, 500^2)$ i.e. the expected load for the modeled delivery period is 10,000 MW with standard deviation of 5%. This amounts to a mean absolute error (MAE) of 4% of total power when forecasting overall load at the day-ahead market.

Industry structure

There are five IPP firms and five LSE firms in the study region, i.e. $M = N = 5$.

Production costs

The cost parameters of generating power are $\alpha_t = 1$ and $\alpha_s = 2$. It is useful to compute the cost of generating power in our experiment before wind power is introduced. In particular,

we look at the marginal cost in the event that load is fully hedged by forwards contracts. This is relevant because it stands for the most efficient production scheme of one hour power supply in the simulated economy. Employing the cost function and symmetry, the expected marginal cost is 20 \$/MWh and total short-run generation costs of each IPP is \$40,000.

Wind power

A careful modeling of the expansion of wind power capacity demands that the probability distribution function of aggregate wind power output in the experiment would not overestimate the potential of wind power in the study region. As penetration rate increases it is only expected that less windy areas would be developed. For that reason we choose a location in center Iowa to generate a representative wind speed pdf for our study region. It is shown in chapter 3 that wind power resources in Iowa increases as one goes North-West therefore the fitted pdf of wind speed in center Iowa is a sensible choice for modeling wind power potential. More specifically, we estimate wind speed pdf at Zearing, where a large wind farm has been constructed in portions of Story and Hardin Counties in Iowa. When fully developed, this wind farm is planned to have the potential of generating 150 MWh³². Making use of data published by Iowa Energy Center we estimate the annual hourly pdf of wind speed at hub height of 80 m at Zearing as $w \sim Wei(8.28, 2.41)$. The mean and the standard deviation of this pdf is 7.34 and 3.25 m/s respectively (depicted in figure 25).

In order to simulate the marginal pdf of wind speed in Zearing in our experiment we make use of the numerical methodology developed in chapter 5. Recall that in doing so we need to

³² At this time, bilateral contracts are signed to deliver 30 MWh to the city of Ames and 6 MWh to Iowa State University. The purchase represents roughly 15% and 10% shares of overall electricity consumption respectively.

parameterize the conditional pdf of wind speed $w|\hat{w}\sim N(\hat{w},\sigma(\hat{w}))$ and to solve for the parameters of the marginal pdf of wind speed forecast, which in turn generates the desired marginal pdf of wind speed.

To construct the conditional pdf of wind speed we need to look at the precision of modern wind forecasting systems. Nowadays, wind power forecasting models are able to provide unbiased forecasts (Madsen, et al. 2004). On the other hand, MAE at one wind site location for a prediction horizon of day-ahead is still substantial. For instance, for wind farms participating in California ISO's central forecasting system³³ MAE is 17.5% of installed capacity (Blatchford and Zack 2004). MAE in different locations in Europe is about 13% of installed capacity (Madsen, et al. 2004). The most recent report available at this time indicates 10%-12% MAE of installed capacity for a single site (Smith 2008). Considering the particularities employed in these studies, e.g. wind farms technology, geographical characteristics of wind and more the results do not diverge dramatically.

Taking these figures into consideration, we set $w|\hat{w}\sim N(\hat{w},0.05\hat{w}^2)$ and generate the marginal pdf of local wind speed by a particular marginal pdf of wind speed forecasts, which is $\hat{w}\sim Wei(8.24,2.93)$. Recall that by employing the Iman-Conover method we are able to impose any degree of spatial correlation while preserving the exact marginal pdf of wind speed forecast across all simulations. Therefore, we are able to draw sample of wind speed forecasts only once and use the very same one in all simulations. That way, we avoid the intrinsic variation related to the sampling of wind speed forecasts.

³³ The central forecasting system Participating Intermittent Resources Program (PIRP) was created by California ISO in 2003.

The chosen wind turbine in the experiment is similar to the 1.5 MW turbines installed in the wind farm in Zearing. The particular power curve of the employed machine is portrayed in figure 25. Finally, wind turbine output in the experiment are discounted by a loss factor of 12%, which is the figure proposed by the Iowa Energy Center (see chapter 3 for details). Taking the particular wind conditions and the loss factor into consideration, the capacity factor of the illustrated turbine in the experiment is 36.74%. The computed MAE at the day-ahead for a single wind site in our simulations is 14%.

Study region and spatial correlation

We simulate a square lattice which is similar to the one exemplified in chapter 5: a grid of 10 by 10 wind site locations with side length of 100 km each to form a region study of 1,000 km². Spatial correlation is assumed to be stationary and modeled as an exponential function of the Euclidian distance between locations (see eq. 5.11). We simulate three cases of wind spatial correlation: no correlation, some degree of positive correlation and full correlation. This is accomplished by setting the value of the parameter β (the *characteristic distance*) appropriately and imposing rank correlation accordingly.

Regional wind power capacity and wind power penetration rate

Rated wind capacity specifies the upper bound for the hourly output of wind energy in the study region. The expansion of wind power capacity is performed in the experiment by a symmetric increase in the number of wind turbines in each location. In particular, we focused on the following figures: 5, 10, and 20 turbines in each location which correspond to simulating wind capacity that account for 7.5%, 15%, and 30% of the expected load. We

illustrate and discuss in details only the results for the case of 30% since our key findings can be observed when simulating wind capacity at this scale.

Wind power penetration rate is defined here as the share of forecasted wind power of the expected load in a particular delivery period. Notice that the actual share may be higher than the rated capacity if realized load is lower than expected. If realized load is higher than expected, wind penetration rate is always lower than the rated capacity.

General

In line with the empirical studies discussed in chapter 3, we assume that the hourly distributions of wind power and load are uncorrelated. All the numerical results consist of 500 draws of 100 local wind speed forecasts (i.e. 500 delivery periods). Conditional pdfs of load and local wind speed for each delivery period consist of 500 draws as well.

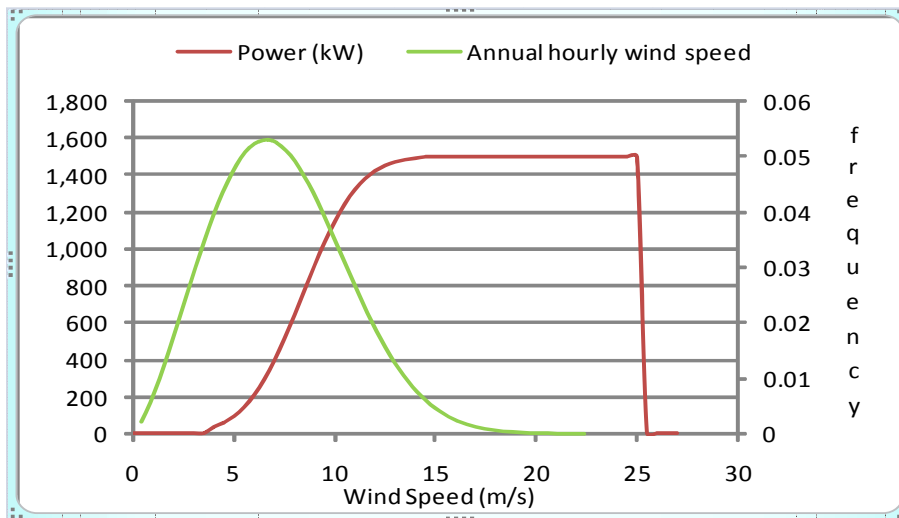


Figure 25: Fitted annual hourly wind speed pdf in Zearing, IA and the power curve of a 1.5 MW turbine employed in the experiment

Results

The following are the results of a computational experiment that examine the market equilibrium which arises from modeling regional rated wind power capacity of 3,000 MW (i.e. wind power capacity accounts for 30% of the expected load). Recall that for presentation purposes, we denote wind power capacity in the case that it is owned by IPPs as a *Cournot capacity* and in the case that wind is owned by competitive firms as a *fringe capacity*.

The results by ownership of wind capacity and for the three cases of wind diversification are depicted in figure 26-28. It is shown that in all three cases of wind diversification fewer contracts are being traded if wind capacity is owned by IPPs. Looking at the illustration for the case of undiversified wind (figure 26, top), the two series reflect similar trend. The only difference is that the Cournot capacity case demonstrates a slight reduction in the equilibrium number of forwards before a sharp increase takes place. The increase happens at the region where net load approaches the volume of power hedged by forwards contracts. This is because the probability of starting up generators in real-time decreases fast in wind penetration rate in this region. For the fringe case, at about 19% wind penetration rate the number of forwards hit a saturation point. For the Cournot case this point is reached only at about 23% wind penetration rate. The saturation points are related to the fact that at these wind penetration rates the expected forward premiums are exhausted respectively (discussed further below).

When we look at the case that wind experiences some spatial correlation (figure 26, center) the saturation point in the case of fringe capacity is reached at about 21% wind penetration

rate. On the other hand, for the Cournot capacity the number of forwards has not reached a saturation point in the experiment. Moreover, the increase in the number of forwards in this case is less obvious than in the case of the fringe capacity. Finally, if there is no spatial correlation there is a noticeable increase in the share of forwards for the fringe capacity case but for the Cournot capacity case there is no clear trend (figure 26, bottom). The fully diversified case enjoys smoothing effects hence is less likely to generate extreme realizations of regional wind power output. The 500 wind speed forecasts at 100 wind site locations in the experiment are translated into a relatively narrow range of 9.1% to 13.3% wind penetration rate. As a result, there is not much variability in the volume of trade in forwards contracts in both cases of ownership.

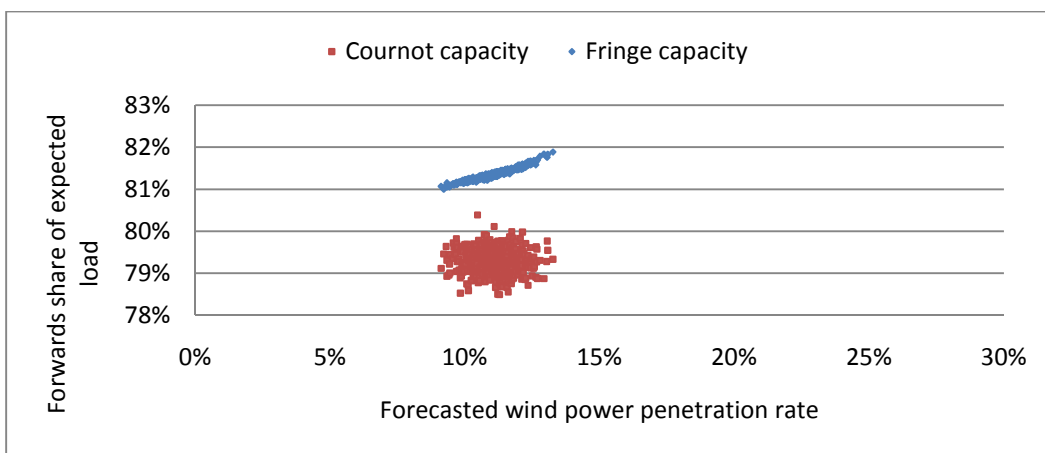
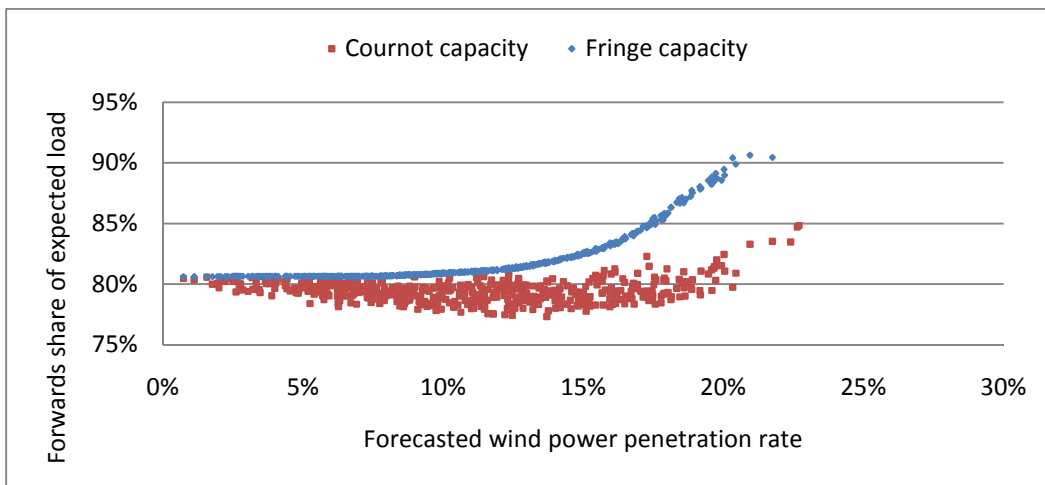
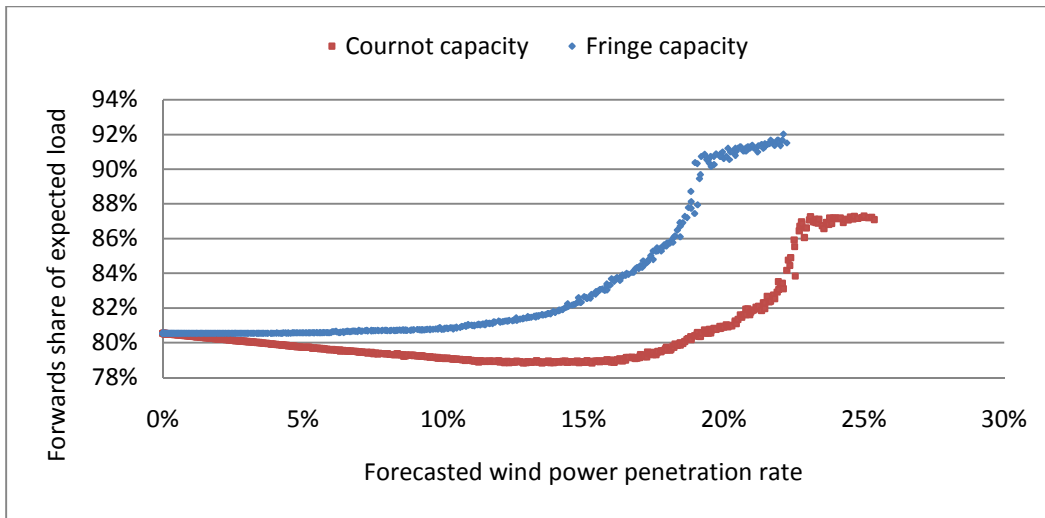


Figure 26: Forecasted wind power penetration rate and the share of forwards of expected load; full correlation (top) some correlation (middle) and zero correlation (bottom)

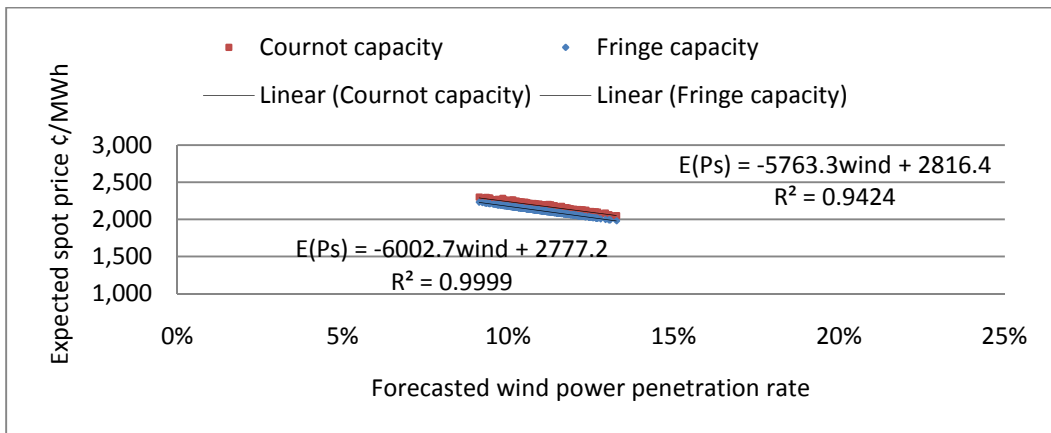
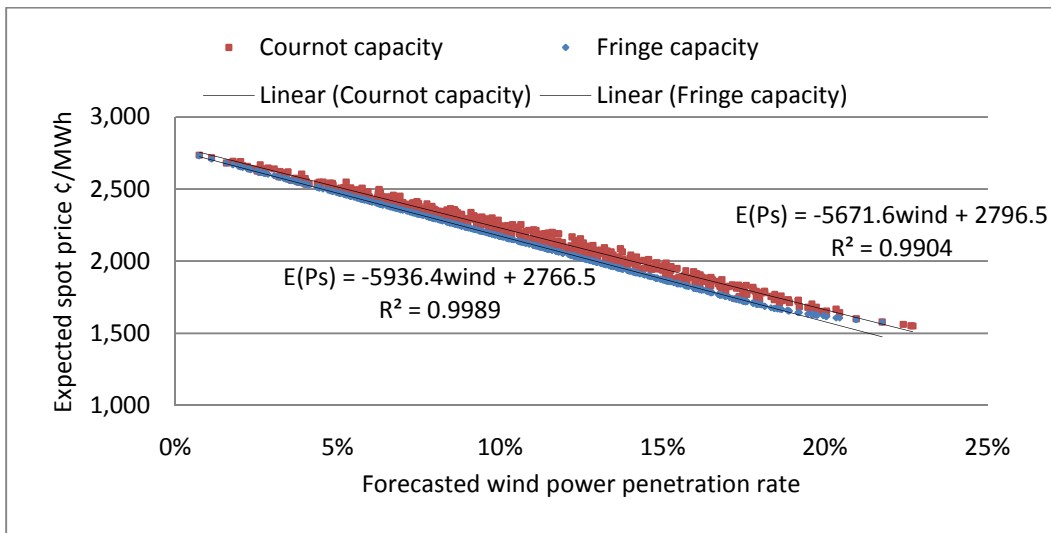
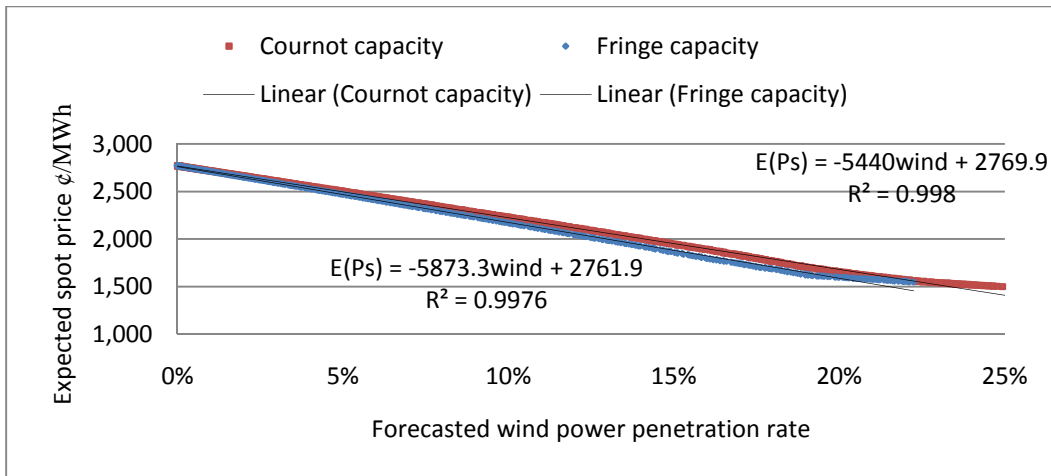


Figure 27: Forecasted wind power penetration rate and expected spot price; full correlation (top) some correlation (middle) and zero correlation (bottom)

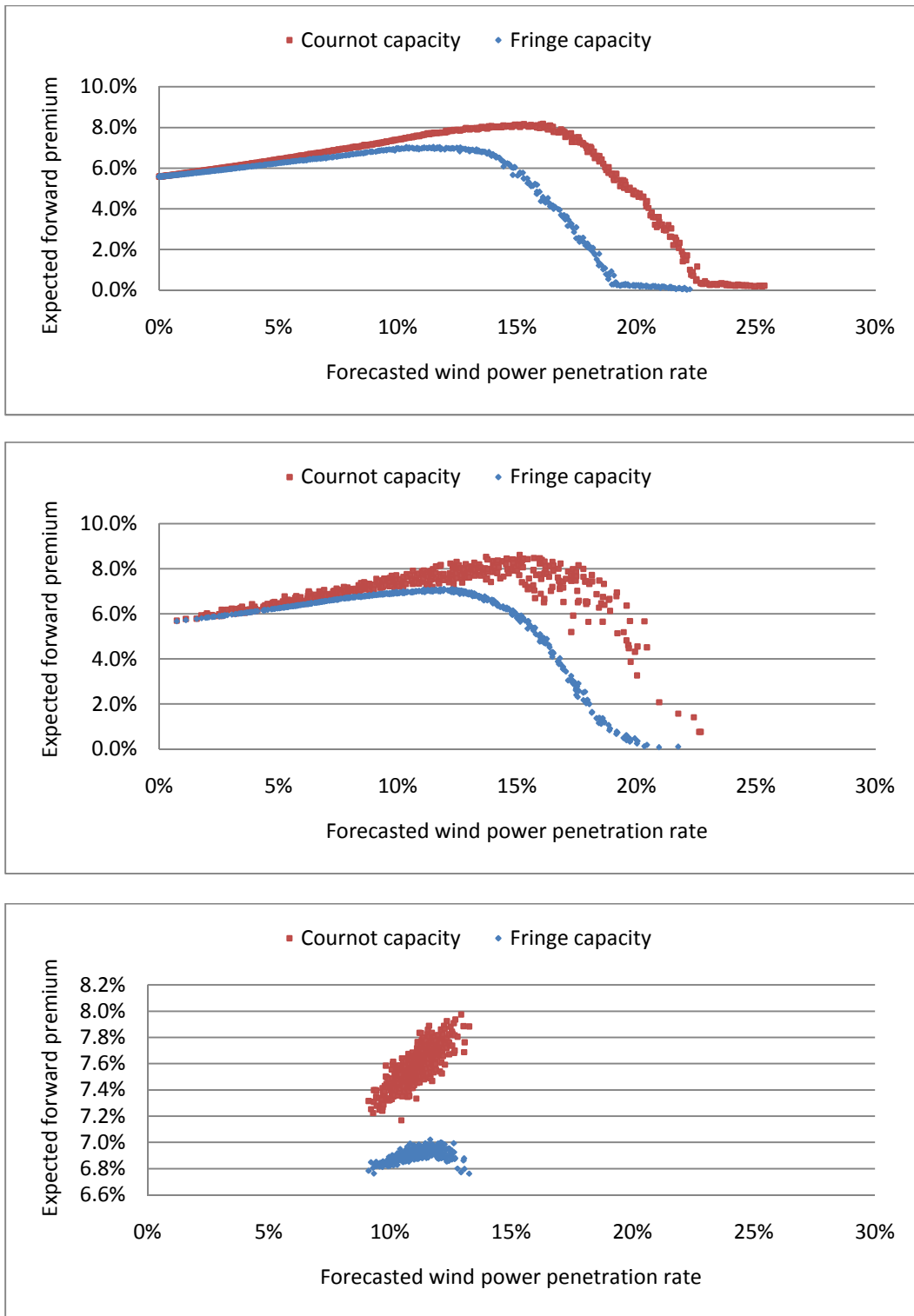


Figure 28: Forecasted wind power penetration rate and expected forward premium; full correlation (top) some correlation (middle) and zero correlation (bottom)

The graphs in figures 27-28 depict the prices associated with the quantities presented in the graphs in figure 26 respectively. We plot forecasted wind penetration rate against expected spot price (figure 27) and against expected forward premium (figure 28). Starting with the spot price, the linear curves in the graphs are fitted to describe the relationship between the expected spot price and the expected wind penetration rate (denoted in the equations as *wind*). In periods that forecasted wind penetration rate is zero the expected spot price is 27.71 \$/MWh. The difference between this price and the marginal cost of 20 \$/MWh computed earlier is explained by the fact that the higher figure corresponds to the actual forwards positions taken in equilibrium.

The trend in the spot price caused by wind penetration rate is very similar across all three levels of wind diversification: first, the expected spot price decreases in wind penetration rate rapidly since the availability of wind energy reduces the marginal cost of generating power in the region. In our illustration, an increase of 1% in wind penetration rate causes a decrease of about 0.6 \$/MWh in the expected spot price. Second, the expected spot price is higher in the case of Cournot capacity than in the case of the fringe capacity because the number of forwards traded is higher in the latter. The coefficients of the spot price equations imply that the price is more responsive to wind penetration rate in the case of fringe capacity. This means that the spot price decreases in the share of wind power faster if the owners of wind power capacity behaves competitively. In our example, integrating over all wind penetration rates the expected spot price is about 3% higher in the case of Cournot capacity compare to the case of fringe capacity. That is true for all three cases of wind diversification.

The role of spatial correlation can be examined by looking at the range spanned by the expected spot price in each case of wind diversification. While the average expected spot price is relatively comparable across all three cases, the coefficient of variation varies greatly; it is 0.02 for the case of fully diversified wind and 0.2 for the case of undiversified wind. Our result suggests that wind diversification is a significant factor in modeling the variance of the expected spot price in the day-ahead market. This is especially true considering the fact that we control for forecasted load and we use the same marginal pdf of local wind speed in all three cases of wind spatial correlation in our experiment.

Premiums for electricity forward contracts are depicted in figure 28. The expected premium before the integration of wind power is 5.58% and diverge greatly afterwards. First, at relatively low wind penetration rates we observe a premium increase across all cases of ownership and wind diversification. Premiums for the Cournot capacity are larger than these under fringe capacity for all three levels of wind diversification. In particular, the maximum premiums for each ownership case are 8.6% and 7.1% respectively (figure 28, center). The difference in premiums becomes noticeable at about 10% wind penetration rate and exceeds a 5% gap at about 18.5% penetration rate for the cases of correlated wind.

When the number of forwards traded becomes sufficiently high, the forward price converges to the expected spot price. This can be observed at the top graph in figure 28. When that happens the marginal forward contract provides no added value in expectations. On the other hand, in the case of fully diversified wind there is an interior solution for the number of forwards even when simulating 30% wind power capacity because high realizations of aggregate wind power are very unlikely (figure 28, bottom). For that reason, in this case IPPs

are more certain regarding the outcome of withholding capacity because high premiums are guaranteed with higher probability.

Two main factors impact the change in electricity forward premiums due to an expansion of wind power capacity. These are the change in the probability of extreme realizations and the fact that IPPs compete for a smaller share of residual demand. First, the uncertainty regarding the availability of wind power preserves high prices because in the case of low wind additional generators would be turned on, driving spot price up. Second, the availability of wind power shifts production level downward, therefore at some point it becomes less profitable to withhold capacity.

This increase in premiums takes place until wind power share is large enough to diminish IPPs ability to manipulate market prices. When this takes place more forwards are being traded (see figure 26) and the forward premium changes direction and starts declining (figure 28). In the case of no spatial correlation the uncertainty introduced by wind is relatively small because aggregate wind forecasts are mapped into a small range of expected premium. On the other hand, for some degree of wind correlation the expected premium is sparse and depends on the aggregation of a particular set of local wind sites forecasting.

Ownership of wind power capacity, generation costs and welfare distribution

We seek to examine differences in outcomes for the case in which IPPs own wind power capacity and the case that wind capacity is owned by fringe firms. The two outcomes of interest are the costs of power generation and IPPs profits from non-wind power generation

units. We motivate the direct comparisons of equilibrium outcomes across cases on two grounds. First, the decision to invest in wind power capacity in the model is predetermined thereby seen as a sunk cost³⁴. Also, the addition of ancillary services associated with the variability in wind power supply is administrated by the system operator and supplied by generators which do not take part in the markets for spot power. Therefore, investments and other costs related to the expansion of wind power capacity should not affect our comparison. Second, the demand for electricity in real-time is inelastic and does not respond to changes in prices. Therefore, the change in expenditure is the only parameter required for measuring changes in consumer surplus. Thus, we relate to the first outcome of interest as measuring how much the economy pays for generating power while the second stands for the changes in welfare distribution in electricity markets due to the integration of wind power capacity.

For the cases that wind is correlated, the difference in the cost of generating power demonstrates a parabolic trend (figure 29, top and center). This trend also reflects how IPPs' ability to exercise market power changes in wind penetration rate. IPPs' market power initially rises due to the increase in LSEs' financial risk and then decreases rapidly where generators compete for a smaller share to be produced by their conventional units. The average excess generation cost in the case of IPPs ownership of wind is 0.48% and 0.75% for the undiversified wind and for some degree of wind correlation, respectively. If wind is uncorrelated the range for forecasted wind penetration rate is between 11% and 14% and the

³⁴ Recent global trend of setting mandates along with various government financial supports for renewable energy made wind power production viable. A model of investments should take into consideration the fact that wind power capacity expansion is paid partly by consumers.

average excess cost is 0.90% compare to the fringe capacity case. These seemingly minor deviations may be substantial when considering energy efficiency in a regional scale.

Looking at IPPs' profits from non-wind power generation units the differences between the two cases of wind power ownership may be remarkable (figure 30). The average difference in the expected profits is 18.58%, 18.08% and 16.88% for full correlation, some correlation and zero wind correlation, respectively. In addition, the volatility of the difference in profits is very high if wind is undiversified and relatively dense in the case of fully diversified wind. If wind is correlated it is more likely that available wind power will account for a larger portion of regional power supply. When this happens, IPPs profits in the case that they own wind power capacity may be 40% above the fringe capacity case. The reason for that is the following: at a relatively high penetration rate the forward premium approaches zero in the fringe capacity case while it is still high in the Cournot capacity case. In periods when the expected share of wind power is above 20%, the difference decreases in wind penetration rate due to the decrease in IPPs ability to exercise market power at this range.

Lastly, we performed further simulations to examine the sensitivity of our results to the possibility that the cost of generating power is higher than assumed in our experiments. When we employ $\alpha_s = 3$ (instead of 2) in the simulations the results are scaled up otherwise, they do not change much (figures 31-32). In this experiment, the costs of electricity in the case of Cournot capacity are higher by 0.73% to 1.30%, subject to wind diversification compare to the fringe capacity case. The difference in IPPs profits is on average about 18.23% to 22.42% higher in the Cournot capacity case, subject to wind diversification. For periods where forecast approaches 20% wind penetration rate, the IPPs profits in the case

that IPPs own wind capacity may be more than 60% higher than the case of a fringe capacity (figure 32, center). Similar to previous results, this gap decreases at higher forecasted wind penetration rate.

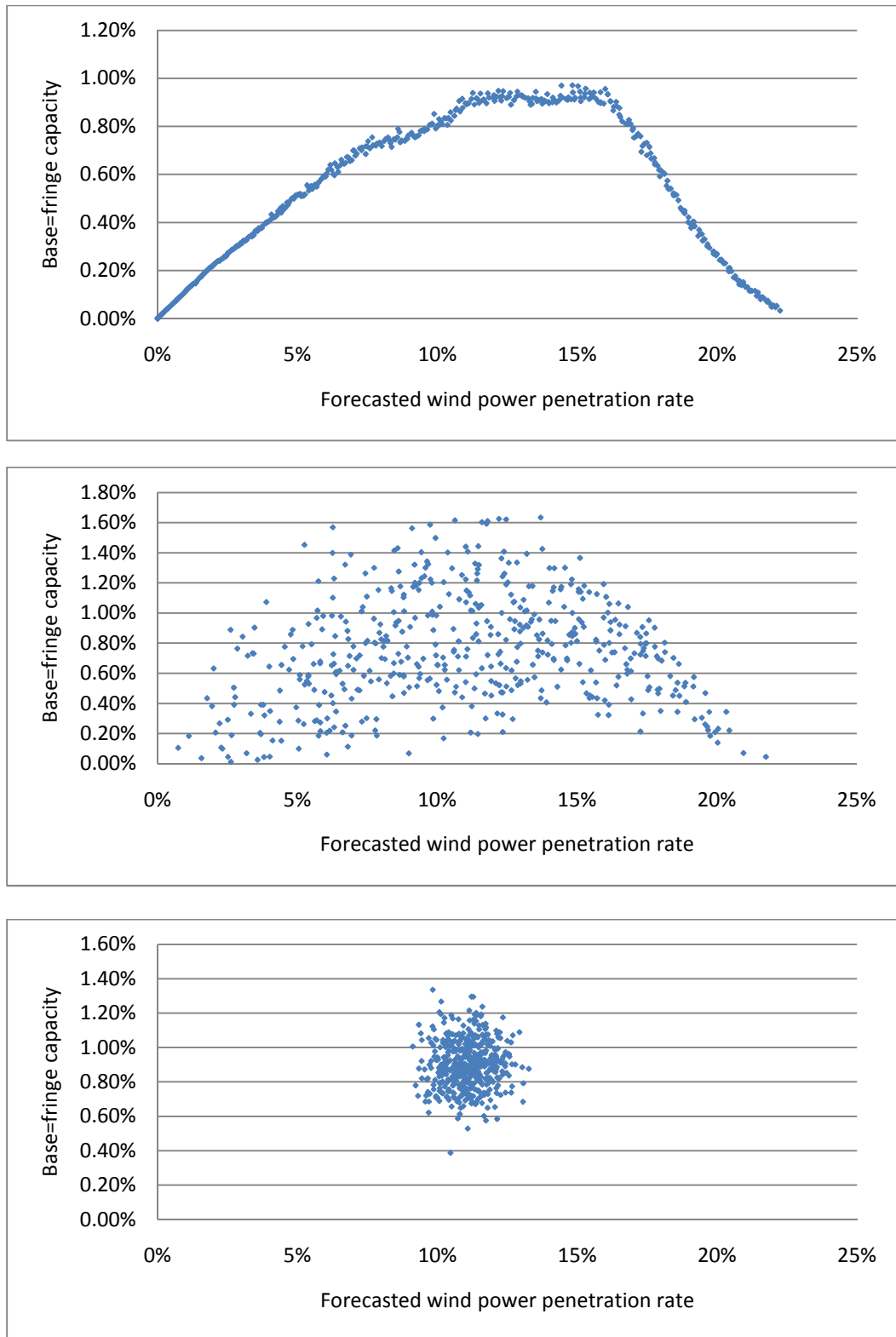


Figure 29: Ratio between total short-run generation costs in the Cournot capacity case and fringe capacity case; full correlation (top) some correlation (middle) and zero correlation (bottom)

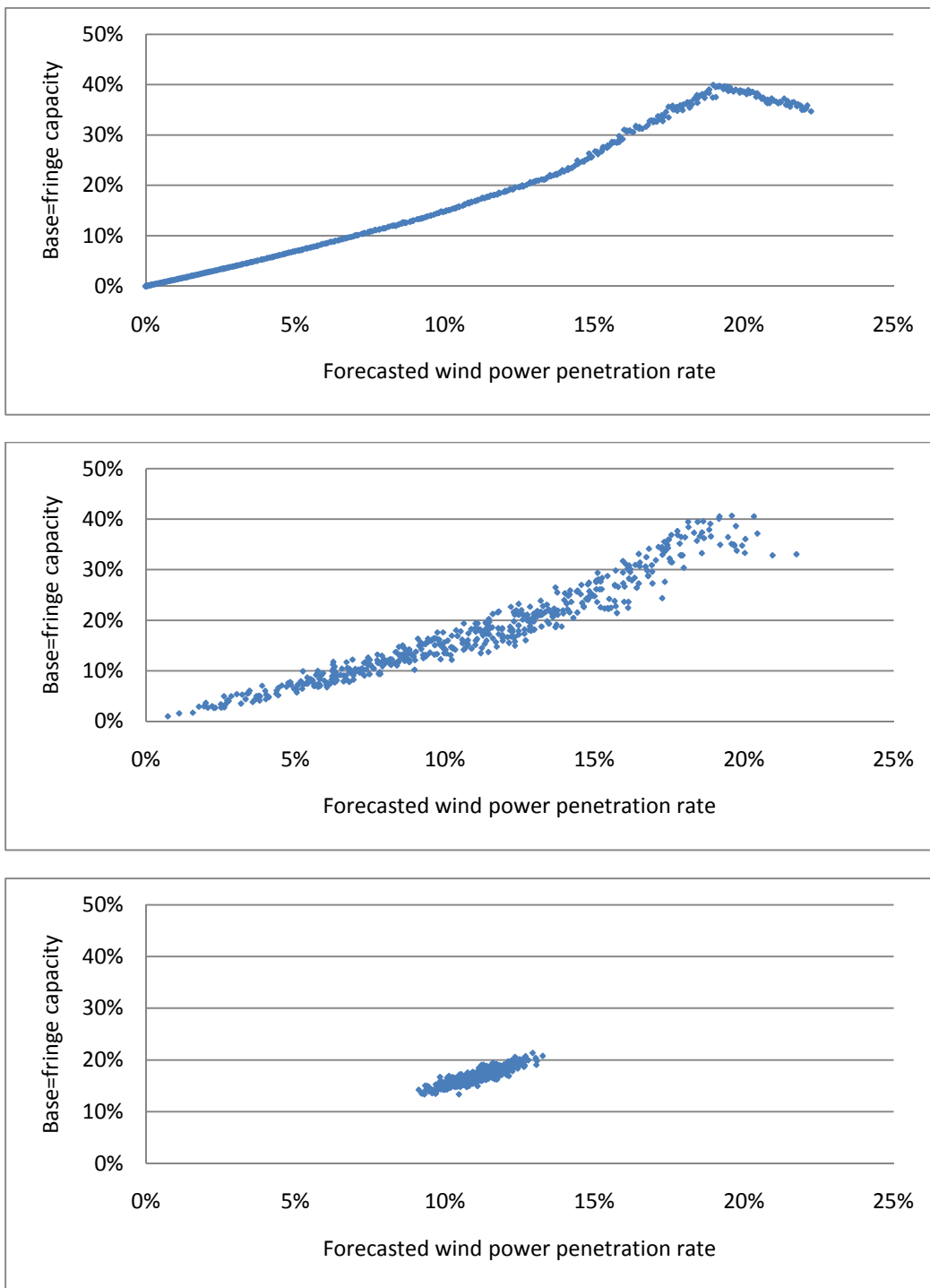


Figure 30: Ratio between IPPs' profits from non-wind power generation units in the Cournot capacity case and fringe capacity case; full correlation (top) some correlation (middle) and zero correlation (bottom)

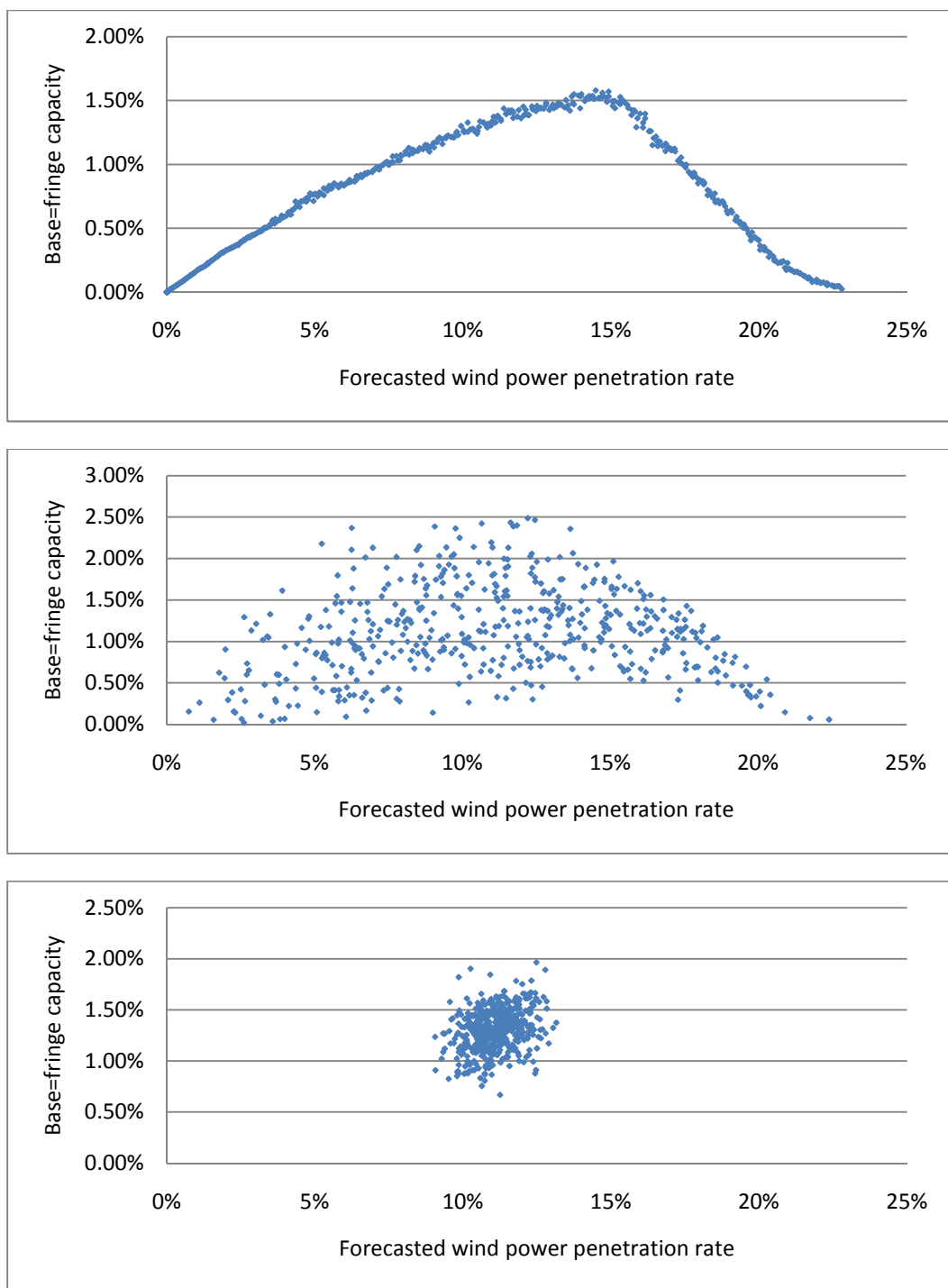


Figure 31: Ratio between total short-run generation costs in the Cournot capacity case and fringe capacity case, $\alpha_s = 3$; full correlation (top) some correlation (middle) and zero correlation (bottom)

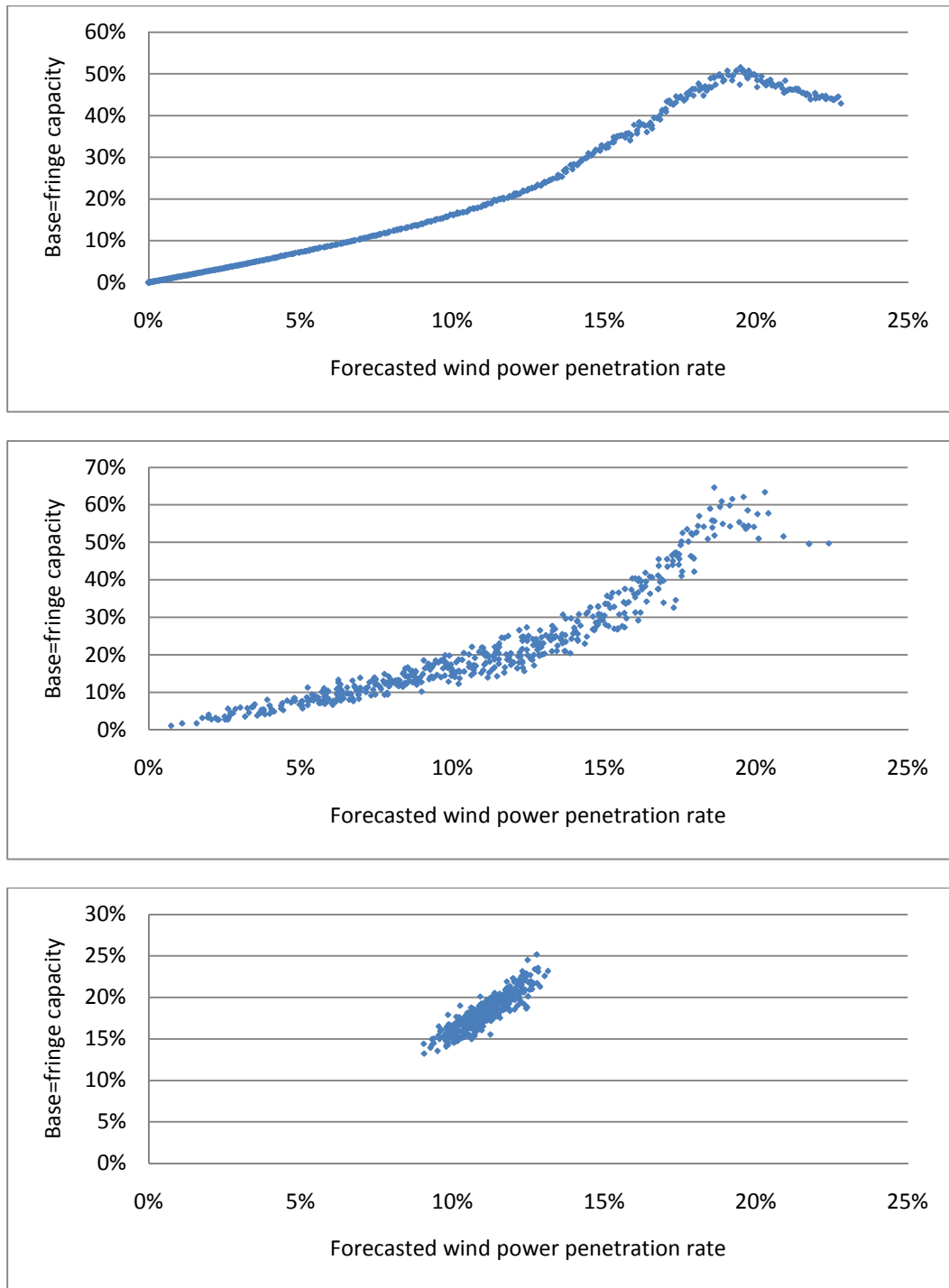


Figure 32: Ratio between IPPs' profits from non-wind power generation units in the Cournot capacity case and fringe capacity case, $\alpha_s = 3$; full correlation (top) some correlation (middle) and zero correlation (bottom)

Chapter summary

Our simulations predict a large impact of wind power expansion on deregulated electricity markets. Our results depend on assumptions regarding ownership of wind power capacity and geographical diversification of wind power, but some model predictions are consistent through all scenarios. First, as wind penetration rate increases a substantial decrease in electricity spot price is expected. The parameters employed in our experiment imply that the decrease in the spot price due to wind power penetration rate is in the ratio of two to one (e.g. at 10% wind penetration rate we estimate about 20% decrease in the expected spot price). Notice however that this decrease is not translated into a net increase in consumer welfare. In fact, the expansion of wind power requires investments in wind capacity and additional ancillary service, which we do not model as we take the decision to expand wind power capacity as a predetermined policy in our short-run model. Second, we find that the forward premium increases in penetration rate due to the intermittent nature of wind power supply. However, when wind energy reaches a considerable share of regional power supply the forward premium starts to decline dramatically. This is because at some point net load is sufficiently small thus it is less profitable for IPPs to withhold capacity.

When we examine the role of wind diversification we see that the smoothing effect in the region determines the range of possible realizations for the expected spot price, the number of forward contracts and the predictability of the forward premiums. Perhaps the most significant result with regard to wind spatial correlation is related to the notion that if wind is diversified (completely uncorrelated) it is with relatively low probability that aggregate wind

power supply meets its regional rated capacity. Consequently, production levels from conventional sources of energy almost never falls to the range where IPPs compete more aggressively in forward markets. Therefore, when wind power is diversified, the model predicts that IPPs profits from their non-wind power generators are higher than in the case of undiversified wind. Looking at the case where IPPs own wind power capacity these conclusions are even stronger. In this case it is in producers' interest to withhold more conventional generation capacity compared to the case when they do not own wind power capacity. As a result, in this case less power is traded via forward contracts, expected spot price is higher and positive premiums sustain even when wind power accounts for more than 20% of electricity consumption in expectations. Moreover, since with diversified wind it is almost for certain that wind power will never account for more than 15% of electricity consumption, the profits for IPPs in this case are substantially higher than the case that wind power is owned by competitive firms or if wind is spatially correlated. Our example shows excess profits for IPPs in the range of up to 40% when they own wind power capacity compare to the case that wind capacity is owned by competitive firms. In addition, we estimate expected losses of energy resources in the region in the range of 0.5%-0.9% (subject to wind diversification) if IPPs are the owners of wind power capacity. Finally, a sensitivity analysis show that if the cost of starting up generators is higher than assumed in our base case experiment the differences in IPPs profits and losses of energy resources between the two cases of ownership are even more substantial.

Chapter 7: General conclusions

The overall objective of this dissertation is to develop a theoretical framework for analyzing deregulated electricity markets with wind energy. This is relevant since the state of knowledge for modeling electricity markets is insufficient for our purpose. While doing so, we are able to propose three main contributions. The first is the introduction of a novel equilibrium approach for modeling deregulated electricity markets. We develop a double-sided auction model that explains for the first time, to the best of our knowledge, the coexistence of forward premiums and spot market mark-ups. That is a significant contribution since the two have been explained so far separately, by two conflicting modeling approaches. The body of literature explaining forward premiums is based on the assumptions of perfect competition and risk aversion. The main downside of this approach is that electric industries are concentrated by nature therefore it overlooks potential market failure caused by market power. In contrast, the expected outcome of taking an oligopoly modeling approach is spot market mark-ups. This is explained by producers' incentive to withhold generation capacity. The drawback of this approach is the partial representation of the demand side in electricity markets, in particular, a lack of distinction between real-time load and the demand for forwards at the day-ahead market. Therefore, although this approach accounts for exercising market power it does not relate to the existence of forward premiums.

The fact that both mark-ups and forward premiums are well documented in the empirical literature implies that the state of knowledge regarding modeling electricity markets is

incomplete. Our approach relies on two additional features describing the reality of deregulated electricity markets. First, the supply curve of electricity is dynamic due to ramping costs; frequent start-ups and shut-downs of generators increase the costs of generating power. Therefore, it is an important aspect of electricity pricing. Second, adequate regulation of the power system requires that scheduling power for future delivery relies on designated generators and their locations. This makes the market for short-term forwards illiquid since traders cannot make commitment to supply future power in the day-ahead market and secure the required amount only in the spot market. We show that by accounting for these fundamental elements of electricity markets our theoretical framework is capable of modeling oligopolistic competition, spot prices which are higher than the marginal costs of generating power and the existence of positive premiums in expectations. Moreover, we show that when we disregard ramping costs the predictions of our model coincide with the outcome that one would expect to see under perfect competition and the assumption of risk neutrality.

Secondly, we expand the theoretical framework to account for the new economic environment of deregulated electricity markets with wind power. The integration of intermittent sources of energy introduces uncertainty from the supply side. This is an important addition to the model because it enables for the first time to integrate the characteristics of a renewable source of energy into an equilibrium modeling approach of electricity markets. In so doing, we also discuss the implications of a change in the industry structure due to the expansion of wind power capacity and geographical diversification of

wind power. The theoretical part of the study suggests that both issues may be fundamental for modeling wind-integrated markets.

Our third contribution is related to the fact that wind power forecasting provides essential information for traders. The information of future availability of wind power is used to form expectations regarding spot market and risk management decisions. The ability to simulate this information is necessary for modeling traders' behavior accurately in the day-ahead markets. We introduce a novel methodology that accounts for the joint distribution of wind speed and wind speed forecast for modeling the conditional distribution of regional wind power at the time of trading forwards. The simulation of regional wind power requires consideration of wind speed spatial correlation. Local wind speed raw data is described best by a Weibull distribution. However, so far researchers were using only approximations of the Weibull distribution in simulating the distribution of regional wind power. This is mainly because there is no a natural way to extend the case of a univariate Weibull to the multivariate case. For the purpose of imposing spatial correlation we make use of a technique introduced by Iman and Conover (1982). This technique is distribution free. Therefore it has a clear advantage for considerations of simulating regional wind speed. Our example in chapter 5 shows how to go about modeling the distribution of regional wind power supply starting with a fitted Weibull distribution to describe the distribution of local wind speed.

The computational experiment in chapter 6 provides intuition regarding future expansion of wind power capacity. The outcomes in wind-integrated electricity markets depend to a great extent on the industry structure and the distribution of wind power output in the region. Relatively more concentrated electric industries are expected to generate higher profits for

IPPs as wind penetration rate increases. In the case that IPPs are also the owners of wind power capacity the integration of wind power would enhance their profits significantly compare to the case that wind capacity is owned by competitive firms. Also, we show that these excess profits are generated by inefficient employment of energy resources. In periods that wind penetration rate approaches the rated capacity IPPs are less likely to withhold capacity. This is true because in this case IPPs compete on a smaller residual demand. The main impact of wind diversification is the ability of wind energy, as an uncontrolled source of power, to reduce IPPs market power. Our results show that in the extreme case that wind power is fully correlated realizations of high wind power supply have relatively high probability. Under this circumstance, IPPs compete more aggressively because their ability to manipulate market prices is relatively low. If wind is less spatially correlated the likelihood of high wind penetration rate is lower therefore residual demand is relatively higher which in turn allows IPPs to exercise more market power.

Future research

A possible extension of the model would examine the impact of developing better batteries for energy storage. Making the storage of electricity economically viable will have two significant impacts. First, from regulation perspective the power system would be able to handle the variation of wind energy better therefore it would be possible to integrate more wind power capacity to the system. Second, storage would have a direct impact on electricity pricing. It is expected that the batteries would not be used in all times but only when the spot price is high enough to justify the cost of storage. In order for our model to account for this,

one would need to incorporate a truncated distribution for the spot price. This corresponds to the idea that expected spikes in demand can be met by power produced in base load periods when the cost of generating power is relatively low. With an upper bar on the spot price, demand for hedging risk via forward contracts is reduced. As a result, it is not just that the expected spot price of electricity is lower, but producers facing lower demand curve for forwards would have less incentive to withhold generation capacity.

Another extension for our model may include investments decisions in wind power capacity. This would allow performing a full welfare analysis of the problem in hand. Our results make it obvious that there are large welfare implications for policy that support wind power capacity. Nowadays, wind energy enjoys considerable public support. The fact that global expansion of wind power is being subsidized by consumers makes this question most relevant. Our study shows that in addition to lowering electricity prices, wind power may help diminish market power. A complete welfare analysis may define the conditions under which public support is required to correct for a market failure and what are the circumstances in which subsidizing wind power becomes only a question of income redistribution.

Lastly, the current design of electricity markets is based on the two-settlement process (i.e. day-ahead and spot markets). With considerable amount of wind power capacity it may be required to reconsider the time for trading forward contracts. Forecasting load at the day-ahead market is relatively accurate, but it is still inefficient to forecast the availability of wind power for more than several hours ahead. Therefore, in markets that accommodate a large share of wind power it may be better to consider a new gate closure for trade in electricity

forwards. Our model can be used for this purpose as long as forecasting precisions of load and wind power at the proposed time of trading forwards are known. However, such an analysis should take into consideration the system constraints and the costs of scheduling conventional generators closer to the time of the delivery period. These should be added to the model as it is beyond the scope of our study.

Appendix

Appendix 1: Contract For Differences

The stochastic nature of load gives rise to realizations where actual electricity demand is lower than the amount settled for delivery via forward contracts. In this case the excess amount cannot and will not be produced for physical and economical reasons. Physically, the excess amount causes transmission and reliability problems in the power system. These and the associated costs are not treated in this study. Economically, surplus of electricity cannot characterize equilibrium in electricity markets. Therefore, one would expect that a financial settlement which enables the buy-out of surplus be part of electricity market operation. Next, we show why a Contract for Differences (CFD) in particular may be an instrument to solve for the missing market problem and eliminate surplus of power supply.

LSE's willingness to resell excess forward contracts is obvious since electricity cannot be economically stored. For an IPP firm, we compare the economic payoff from generating the volume traded via forward contracts versus generating the exact realized load with accordance to a CFD settlement. Recall that in the event that load happens to be lower than the amount scheduled in advance the supply curve corresponds to the cost of a more efficient production regime. This curve is depicted in figure 33 by S_F . The less efficient production regime of a higher load realization is depicted by the portion of the supply curve denoted

as S_S . Also in the figure, x^* and x denote the amounts of power traded via forward contracts and a (lower) realized amount which a particular LSE responsible to deliver respectively.

Generating the entire amount traded in advance, the IPP is paid the forward price P_F . In figure 33 we depicted P_F as the competitive price, assuming for now that there are no forward premiums in expectations (we relax that assumption later). Notice that regardless of the existence of a CFD, the illustrated realization provides the IPP with an extra producer surplus of $P_F A C P_S$ (compare to the standard surplus created by the spot price P_S). If load is produced up to the entire volume traded via forward contracts, P_F coincides with the marginal cost and the area ABC is added to the producer surplus. On the other hand, if the IPP can buy back the excess contracts for the (expected) spot market price³⁵, the added producer surplus is the area $ABCD > ABC$.

For the case of positive forwards premium, simply increase P_F to show that for the same level of x^* the producer surplus will be larger than in the case of zero premiums in expectations. In solving the model we showed that negative premiums in expectations are not possible in this market. Therefore, it is clear that both LSEs and IPPs benefit from trading a CFD. Thus we establish that a financial settlement such as a CFD is expected to be part of a market clearing condition.

³⁵ Assuming that the spot price is a benchmark for trading excess supply is appropriate since in reality market participants balance quantities in the spot markets.

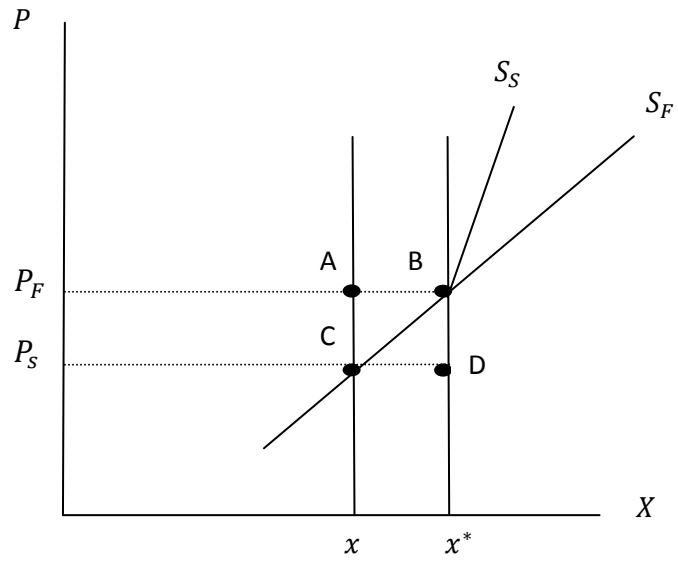


Figure 33: The two-settlement process in the case of over-trading forward contracts

Appendix 2: SOC for the IPPs problem

The second derivative of \mathcal{M} with respect to the number of forward contracts is

$$\begin{aligned}
\frac{\partial^2 \mathcal{M}}{\partial q_F^{i^2}} &= \frac{\partial^2 P_F(\cdot)}{\partial q_F^{i^2}} q_F^i + 2 \frac{\partial P_F(\cdot)}{\partial q_F^i} - \int_0^{\sum_{m=1, m \neq i}^M \bar{q}_F^m + q_F^i} \frac{\partial P_s(\cdot)}{\partial q_F^i} f_X(X|\hat{X}) dX \\
&+ \int_{\sum_{m=1, m \neq i}^M \bar{q}_F^m + q_F^i}^{\infty} \left\{ -\frac{\alpha_s}{M} \times \left(\frac{\partial q^i}{\partial q_F^i} - 1 \right) + \frac{\partial P_s(\cdot)}{\partial q_F^i} \times \left(\frac{\partial q^i}{\partial q_F^i} - 1 \right) \right. \\
&+ P_s(\cdot) \left(\frac{\partial^2 q^i}{\partial q_F^{i^2}} \right) - \alpha_t \left(\frac{\partial q^i}{\partial q_F^i} \right)^2 - \alpha_t q^i \left(\frac{\partial^2 q^i}{\partial q_F^{i^2}} \right) \\
&\left. - \alpha_s \left[\left(\frac{\partial q^i}{\partial q_F^i} - 1 \right)^2 + (q^i - q_F^i) \left(\frac{\partial^2 q^i}{\partial q_F^{i^2}} \right) \right] \right\} f_X(X|\hat{X}) dX. \tag{2.35}
\end{aligned}$$

Notice that

- 1) $\frac{\partial^2 P_F(\cdot)}{\partial q_F^{i^2}} = 0$ and $\frac{\partial^2 q^i}{\partial q_F^{i^2}} = 0$,
- 2) $\int_0^{\sum_{m=1, m \neq i}^M \bar{q}_F^m + q_F^i} \frac{\partial P_s(\cdot)}{\partial q_F^i} f_X(X|\hat{X}) dX = 0$, which is to say that in the event that no

additional generators are turned on after the forwards market is cleared the spot price is not affected by the marginal forward contract.

Therefore we can write

$$\begin{aligned}
\frac{\partial^2 \mathcal{M}}{\partial q_F^{i^2}} &= 2 \frac{\partial P_F(\cdot)}{\partial q_F^i} \\
&+ \int_{\sum_{m=1, m \neq i}^M \bar{q}_F^m + q_F^i}^{\infty} \left[\left(-\frac{\alpha_s}{M} + \frac{\partial P_s(\cdot)}{\partial q_F^i} \right) \times \left(\frac{\partial q^i}{\partial q_F^i} - 1 \right) \right. \\
&\quad \left. - (\alpha_t + \alpha_s) \left(\frac{\partial q^i}{\partial q_F^i} \right)^2 + \alpha_s \left(2 \frac{\partial q^i}{\partial q_F^i} - 1 \right) \right] f_X(X|\hat{X}) dX .
\end{aligned} \tag{2.36}$$

Substitute for $\frac{\partial P_s(\cdot)}{\partial q_F^i} = -\frac{\alpha_s}{M}$, and $\frac{\partial q^i}{\partial q_F^i} = \frac{M-1}{M} \times \frac{\alpha_s}{\alpha_t + \alpha_s}$ we get

$$\begin{aligned}
\frac{\partial^2 \mathcal{M}}{\partial q_F^{i^2}} &= 2 \frac{\partial P_F(\cdot)}{\partial q_F^i} \\
&+ \int_{\sum_{m=1, m \neq i}^M \bar{q}_F^m + q_F^i}^{\infty} \left[\frac{2\alpha_s(\alpha_t M + \alpha_s)}{M^2(\alpha_t + \alpha_s)} - \left(\frac{M-1}{M} \right)^2 \times \frac{\alpha_s^2}{\alpha_t + \alpha_s} \right. \\
&\quad \left. + \frac{\alpha_s(\alpha_s M - 2\alpha_s - \alpha_t M)}{M(\alpha_t + \alpha_s)} \right] f_X(X|\hat{X}) dX
\end{aligned} \tag{2.37}$$

$$\begin{aligned}
&= 2 \frac{\partial P_F(\cdot)}{\partial q_F^i} \\
&+ \int_{\sum_{m=1, m \neq i}^M \bar{q}_F^m + q_F^i}^{\infty} \frac{2\alpha_s(\alpha_t M + \alpha_s) - \alpha_s^2(M-1)^2 + \alpha_s M(\alpha_s M - 2\alpha_s - \alpha_t M)}{M^2(\alpha_t + \alpha_s)} \\
&\times f_X(X|\hat{X}) dX
\end{aligned} \tag{2.38}$$

$$= 2 \frac{\partial P_F(\cdot)}{\partial q_F} + \alpha_s \int_{\sum_{m=1, m \neq i}^M \bar{q}_F^m + q_F^i}^{\infty} \left\{ \frac{\alpha_s + \alpha_t M(2 - M)}{M^2(\alpha_t + \alpha_s)} \right\} f_X(X|\hat{X}) dX . \quad (2.39)$$

Substituting for the derivative of the forward price

$$\begin{aligned} \frac{\partial^2 \mathcal{M}}{\partial q_F^i{}^2} &= -2 \frac{\alpha_s}{M} \left(1 + \frac{1}{N} \right) \int_{\sum_{m=1, m \neq i}^M \bar{q}_F^m + q_F^i}^{\infty} f_X(X|\hat{X}) dX \\ &\quad + \alpha_s \int_{\sum_{m=1, m \neq i}^M \bar{q}_F^m + q_F^i}^{\infty} \left[\frac{\alpha_s + \alpha_t M(2 - M)}{M^2(\alpha_t + \alpha_s)} \right] f_X(X|\hat{X}) dX \end{aligned} \quad (2.40)$$

$$= \alpha_s \int_{\sum_{m=1, m \neq i}^M \bar{q}_F^m + q_F^i}^{\infty} \left[\frac{-2M(\alpha_t + \alpha_s) \left(1 + \frac{1}{N} \right) + \alpha_s + \alpha_t M(2 - M)}{M^2(\alpha_t + \alpha_s)} \right] f_X(X|\hat{X}) dX \quad (2.41)$$

$$= \alpha_s \int_{\sum_{m=1, m \neq i}^M \bar{q}_F^m + q_F^i}^{\infty} \left[\frac{-2M\alpha_s \left(1 + \frac{1}{N} - \frac{1}{2M} \right) - \frac{2M\alpha_t}{N} - \alpha_t M^2}{M^2(\alpha_t + \alpha_s)} \right] f_X(X|\hat{X}) dX \quad (2.42)$$

$$= -\alpha_s \int_{\sum_{m=1, m \neq i}^M \bar{q}_F^m + q_F^i}^{\infty} \left\{ \frac{2\alpha_s(N(2M - 1) + 2M) + M\alpha_t(2 + MN)}{M^2N(\alpha_t + \alpha_s)} \right\} f_X(X|\hat{X}) dX \quad (2.43)$$

which is negative for any positive integers of N and M . Therefore, \mathcal{M} is strictly concave in q_F^i , thus we know that if there is an interior symmetric solution it has to be unique.

Appendix 3: Wind turbine used in this study

The power curve of a wind turbine used throughout this study is modeled in attempt to mimic the characteristics of a particular commercial 1.5 MW wind turbine.

Table 7: Wind turbine technical data

| | |
|--------------------|----------|
| Rated power (RP) | 1,500 kW |
| Cut-in wind speed | 3.5 m/s |
| Rated wind speed | 14 m/s |
| Cut-out wind speed | 25 m/s |
| Rotor diameter | 77 m |
| Hub height | 80 m |

The turbine's output is expressed as

$$P_c(v_i) = \begin{cases} 0 & \text{if } 3.5 \geq v_i \\ \psi(v_i) * RP & \text{if } 25 \geq v_i > 3.5 \\ 0 & \text{if } v_i > 25 \end{cases} \quad (3.13)$$

where the function describing the efficiency coefficient is

$$\psi(v_i) = \begin{cases} \tilde{\Phi}(v_i) & \text{if } 14 \geq v_i > 3.5 \\ 1 & \text{if } 25 \geq v_i > 14 \\ 0 & \text{else} \end{cases} \quad (3.14)$$

and $\tilde{\Phi}(v_i)$ is a normal cumulative density function (cdf) to be fitted by eye to the power curve of the desired wind turbine.

In figure 19 we depict a power curve generated by using a normal cdf with mean 7.9 and variance 2.2. This fitted power curve is depicted in chapter 3 and also being used for numerical purposes in the rest of this study.

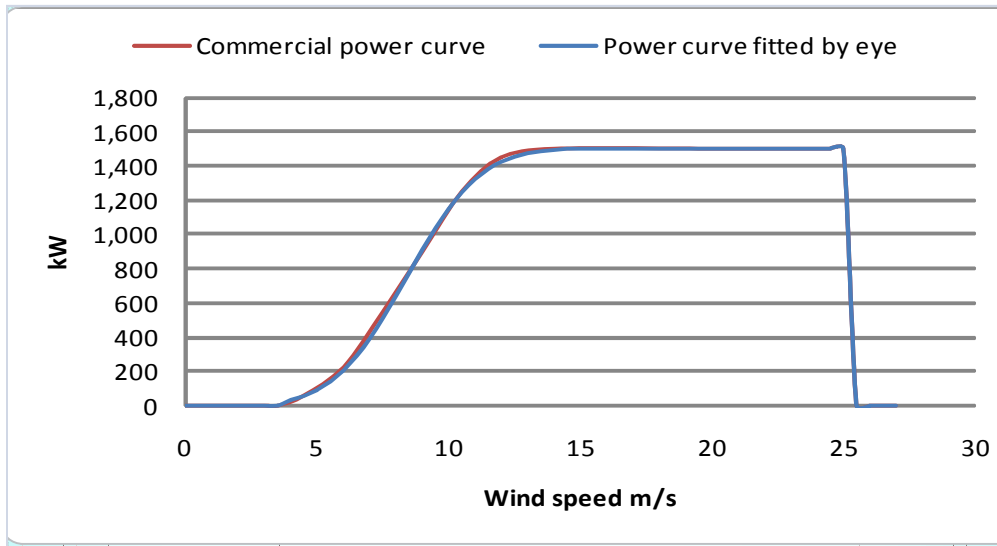


Figure 34: Fitted power curve of a 1.5MW wind turbine to be used in this study

References

Allaz, Blaise, and Jean-Luc Vila. "Cournot competition, forward markets and efficiency ." *Journal of Economic Theory*, 1993: 59(1): 1-16.

Bakos, George C. "Feasibility study of a hybrid wind/hydro power-system for low-cost electricity production." *Applied Energy*, 2002: 72(3-4):599-608.

Barlow, M. T. "A diffusion model for electricity prices." *Mathematical Finance*, 2002: 12(4):287-298.

Benth, Fred Espen, Álvaro Cartea, and Rüdiger Kiesel. "Pricing forward contracts in power markets by the certainty equivalence principle: Explaining the sign of the market risk premium." *Journal of Banking & Finance*, 2008: 32(10):2006-2021.

Bessembinder, Hendrik, and Michael L. Lemmon. "Equilibrium Pricing and Optimal Hedging in Electricity Forward Markets." *The Journal of Finance*, 2002: 57(3):1347-1382.

Betz, A. *Windenergie und ihre Ausnutzung durch Windmühlen Vandenhoeck und Ruprecht*. Göttingen, Germany: Vandenhoeck & Ruprecht, 1926.

Bjorgan, Roger, Chen-Ching Liu, and Jacques Lawarree. "Financial risk management in a competitive electricity market." *IEEE Transactions on Power Systems*, 1999: 14(4):1285-1291.

Blatchford, J., and J. Zack. "California ISO's Participating Intermittent Resource Program (PIRP): Description and initial results." *Global Windpower*. 2004.

Borenstein, Severin, and James Bushnell. "An Empirical Analysis of the Potential for Market Power in California's Electricity Industry ." *The Journal of Industrial Economics*, 1999: 47(3): 285-323.

Borenstein, Severin, James B. Bushnell, and Frank A. Wolak. "Measuring Market Inefficiencies in California's Restructured Wholesale Electricity Market." *The American Economic Review*, 2002: 92(5): 1376-1405.

Brus, D. J., and M. J.W. Jansen. "Uncertainty and sensitivity analysis of spatial predictions of heavy metals in wheat." *Journal of Environmental Quality* , 2004: 33: 882–90.

Byström, Hans N. E. "Extreme value theory and extremely large electricity price changes." *International Review of Economics & Finance*, 2005: 14:41-55.

Carta, J.A., P. Ramirez, and S. Velazquez. "A review of wind speed probability distributions used in wind energy analysis. Case studies in the Canary Islands." *Renewable and Sustainable Energy Reviews*, 2008.

Cartea, Alvaro, and Marcelo G. Figueroa. "pricing in electricity markets: a mean reverting jump diffusion model with seasonality." *Applied Mathematical Finance*, 2005: 12(4):313-335.

Cartea, Álvaro, and Pablo Villaplana. "Spot price modeling and the valuation of electricity forward contracts: The role of demand and capacity." *Journal of Banking & Finance*, 2008: article in press.

Cellura, M., G. Cirrincione, A. Marvuglia, and A. Miraoui. "Wind speed spatial estimation for energy planning in Sicily: Introduction and statistical analysis." *Renewable Energy*, 2008: 33(6):1237-1250.

Clewlow, L., and C. Strickland. *Energy derivatives: pricing and risk management*. London: Lacima Publications, 2000.

Deng, Shijie, and Shmuel S. Oren. "Electricity Derivatives and Risk Management." *Energy*, 2006: (31) 940–953.

Deng, Shijie. "Stochastic models of energy commodity prices and their applications: Mean-reversion with jumps and spikes." *POWER working paper, University of California Energy Institute, Berkeley* (POWER working paper, University of California Energy Institute), 2000: PWP-073.

Denton, Michael, Adrian Palmer, Ralph Masiello, and Petter Skantze. "Managing market risk in energy." *IEEE Transactions on Power Systems*, 2003: May 18(2):494-502.

Diggle, J. Peter, and Paulo J. Jr. Ribeiro. *Model-based Geostatistics*. New York, NY: Springer, 2007.

DOE. *2008 Wind Technologies Market Report*. U.S. Department of Energy, Energy Efficiency and Renewable Energy, 2009.

Doherty, Rona, and Mark O'malley. "A new approach to quantify reserve demand in systems with significant installed wind capacity." *IEEE Transactions on Power Systems*, 2005.

Douglas, Stratford, and Julia Popova. "Storage and the electricity forward premium." *Energy Economics*, 2008: 30(4):1712-1727.

Dubey, Sat Ya D. "Normal and weibull distributions ." *Naval Research Logistics Quarterly*, 1967: 14(1):69-79.

El-Fouly, Tarek H. M., Ehab F. El-Saadany, and Magdy M. A. Salama. "One Day Ahead Prediction of Wind Speed and Direction." *IEEE Transactions on Energy Conversion*, 2008: 23(1):191-201.

Elliott, Robert J., Gordon A. Sick, and Michael Stein. "Modelling electricity price risk." *Preprint, University of Calgary*, 2003.

Available at <http://www.ucalgary.ca/~sick/Research/markovElectricity14.pdf>.

Focken, Ulrich, Matthias Lange, Kai Mönnich, Hans-Peter Waldl, Hans Georg Beyer, and Armin Luig. "Short-term prediction of the aggregated power output of wind farms - a statistical analysis of the reduction of the prediction error by spatial smoothing effects." *Journal of Wind Engineering and Industrial Aerodynamics*, 2002.

Garcia, Reinaldo C., Javier Contreras, Marco van Akkeren, and João Batista C. Garcia. "A GARCH forecasting model to predict day-ahead electricity prices." *IEEE Transactions on Power Systems*, 2005: 2(2):867-874.

Geman, Hélyette, and Andrea Roncoroni. "Understanding the fine structure of electricity prices." *The Journal of Business*, 2006: 79(3):1225-1261.

Gibescu, Madeleine, Arno J. Brand, and Wil L. Kling. "Estimating of variability and predictability of large-scale wind energy in the Netherlands." *Wind Energy*, 2009: 12:241-260.

Giebel, G. *On the benefits of distributed generation of wind energy in Europe*. PhD Dissertation, Oldenburg, Germany: Carl von Ossietzky University, 2000.

Goto, Mika, and George Andrew Karolyi. "Understanding Electricity Price Volatility Within and Across Markets." *Dice Center Working Paper No. 2004-12* , 2004.

Green, Richard J., and David M. Newbery. "Competition in the British electricity spot market." *Journal of Political Economy*, 1992: 100(5): 929-953.

Green, Richard. "The Electricity Contract Market in England and Wales ." *The Journal of Industrial Economics*, 1999: 47(1): 107-124 .

Griffin, James M, and Steven L Puller. *Electricity Deregulation: Choices and Challenges*. University of Chicago Press, 2005.

Hart, Chad E., Dermot J. Hayes, and Bruce A. Babcock. "Insuring eggs in baskets: should the government insure individual risks?" *Canadian Journal of Agricultural Economics* , 2006: 54(1):121-137.

Haslett, John, and Adrian E. Raftery. "Space-time modeling with long-memory dependence: Assessing Ireland's wind power resources." *Applied Statistics*, 1989.

Holttinen, H. "Optimal electricity market for wind power." *Energy Policy*, 2005: 33(16): 2052-2063 .

Holttinen, H. "Impact of hourly wind power variation on the system operation in the Nordic Countries." *Wind Energy*, 2005: 8(2):173-195.

Holttinen, Hannele, and Ritva Hirvonen. "Power system requirements for wind power." In *Wind Power in Power Systems*, by T. Ackermann. John Wiley and Sons Ltd, pp 143–167., 2005.

Holttinen, Hannele. "Hourly wind power variations in the Nordic countries." *Wind Energy*, 2005.

Huang, Yun-Hsun, and Jung-Hua Wu. "A portfolio risk analysis on electricity supply planning ." *Energy Policy*, 2008: 36(2):627-641.

Huisman, Ronald, and Ronald Mahieu. "Regime jumps in electricity prices." *Energy Economics*, 2003: 25:425-434.

Iman, Ronald L., and W. J. Conover. "Communication in Statistics - Simulation and computation." *A distribution-free approach to inducing rank correlation among input variables*, 1982: 11(3): 311-34.

IRC. "Increasing renewable resources, how ISOs and RTOs are helping meet this public policy objectives." October 16, 2007.

Jamil, M., S. Parsa, M. Majidi. "Wind power statistics and an evaluation of wind energy density." *Renewable Energy*, 1995.

Jauch, Clemens, Julija Matevosyan, Thomas Ackermann, and Sigrid Bolik. "International comparison of requirements for connection of wind turbines to power systems." *Wind Energy*, 2005: 8(3):295-306.

Kian, Ashkan R., Jose B. Jr. Cruz, and Robert J. Thomas. "Bidding strategies in oligopolistic dynamic electricity double-sided auctions." *IEEE Transactions on power systems*, February 2005: 20(1):50-58.

Klemperer, Paul D., and Margaret A. Meyer. "Supply Function Equilibria in Oligopoly under Uncertainty ." *Econometrica*, 1989: 57(6): 1243-1277 .

Knittel, Christopher R., and Michael R. Roberts. "An empirical examination of restructured electricity prices." *Energy Economics*, 2005: 27:791-817.

Landberg, L. *Short-term prediction of local wind conditions* . Technical Report No. Risø-R-702(EN) , Risø: Risø National Laboratory, 1994.

Landberg, L., M.A. Hansen, K. Vesterager, and W. Bergstrøm. *Implementing wind forecasting at a utility*. Laboratory Technical Report No. Risø-R-929(EN), Risø National Laboratory, 1997.

Lange, Matthias. "On the Uncertainty of Wind Power Predictions—Analysis of the Forecast Accuracy and Statistical Distribution of Errors." *Journal of Solar Energy Engineering*, 2005: 127(2): 177–184.

Longstaff, Francis A., and Ashley W. Wang. "Electricity Forward Prices: A High-Frequency Empirical Analysis." *The Journal of Finance*, 2004: 59(4):1877-1900.

Loutan, Clyde, and David Hawkins. *Integration of Renewable Resources*. California: California ISO, 2007.

Lucia, Julio J., and S. Eduardo Schwartz. "Electricity prices and power derivatives: Evidence from the Nordic Power Exchange." *Review of Derivatives Research*, 2002: 5(1):5-50.

Madsen, H., G. Kariniotakis, Nielsen H.Aa., and T.S.l Pinson, P. Nielsen. "A protocol for standardizing the performance evaluation of short-term wind power prediction models." *Global wind power*. Chicago, 2004.

Maia, A. H. N, and D. D. Neto. "Probabilistic tools for assessment of pest resistance risk associated to insecticidal transgenic crops." *Scientia Agricola* , 2004: 61:481–85.

Mansur, Erin T. "Measuring welfare in restructured electricity markets." *Review of Economics & Statistics*, 2008: 90(2):369-386.

Martínez, E., F. Sanz, S. Pellegrini, E. Jiménez, and J. Blanco. "Life cycle assessment of a multi-megawatt wind turbine." *Renewable Energy*, 2009: 34(3):667-673 (available online since July 7th 2008).

Mosetti, G., C. Poloni, and B. Diviacco. "Optimization of wind turbine positioning in large windfarms by means of a genetic algorithm." *Journal of Wind Engineering and Industrial Aerodynamics*, 1994: 51(1): 105-116.

Mount, Timothy D., Yumei Ning, and Xiaobin Cai. "Predicting price spikes in electricity markets using a regime-switching model with time-varying parameters." *Energy Economics*, 2006: 28:62-80.

Newbery, David M. "Competition, Contracts, and Entry in the Electricity Spot Market ." *The RAND Journal of Economics*, 1998: 29(4): 726-749 .

Oum, Yumi, Shmuel Oren, and Shijie Deng. "Hedging quantity risks with standard power options in a competitive wholesale electricity market." *Naval Research Logistics*, 2006: 53(7):697-712.

Paravan, D., G.B. Sheble, and R Golob. "Price and volume risk management for power producers." *8th International Conference on Probabilistic Methods Applied to Power Systems*. Ames, IA: Iowa State University, 2004. 699-704.

Pinson, P., and G. Kariniotakis. "On-line assessment of prediction risk for wind power production forecasts." *Wind Energy*, 2004: 7 (2):119-132.

Puller, Steven L. "Pricing and firm conduct in California's electricity market." *The Review of Economics and Statistics*, 2007: 89(1):75-87.

Sánchez, Ismael. "Short-term prediction of wind energy production." *International Journal of Forecasting*, 2006: 22(1):43-56.

Schleisner, L. "Life cycle assessment of a wind farm and related externalities ." *Renewable Energy*, 2000: 20(3):279-288.

Seguro, J.V., and T.W. Lambert. "Modern estimation of the parameters of the Weibull wind speed distribution for wind energy analysis." *Journal of Engineering and Industrial Aerodynamics*, 2000.

Sinden, Graham. "Characteristics of the UK wind resource: Long-term patterns and relationship to electricity demand." *Energy Policy*, 2007: 35:112-127.

Smith, J. Charles. "The 20% wind energy scenario system operation: and transmission needs." Pittsburgh, PA: IEEE PES Meeting, 2008.

Söder, Lennart, Lutz Hofmann, Claus Stefan Nielsen, Antje Orths, and Hannele Holttinen. "A comparison of wind integration experiences in some high penetration areas." *Nordic Wind Power Conference*. Espoo, Finland, 2006.

Suenaga, Hiroaki, and Jeffrey Williams. "The Natural Number of Forward Markets for Electricity." *University of California Energy Institute. Policy & Economics.*, 2005: Paper EPE-015, available at <http://repositories.cdlib.org/ucei/policy/EPE-015> .

Sun, Junjie, and Leigh S. Tesfatsion. " Dynamic testing of wholesale power market designs: An open-source agent-based framework." *Computational Economics*, 2007: 30:291–327.

Torres, J. L., A. Garcia, M. De Blas, and A. De Francisco. "Forecast of hourly average wind speed with ARMA models in Navarre (Spain)." *Solar Energy*, 2005: 79:65-77.

Tseng, Chung-Li, and Graydon Barz. "Short-term generation asset valuation: A real options approach." *Operations Research*, 2002: 50(2):297-310.

Vehviläinen, Iivo, and Tuomas Pyykkönen. "Stochastic factor model for electricity spot price—the case of the Nordic market." *Energy Economics*, 2005: 27:351-367.

Wan, Y., and J. R. Liao. *Analyses of wind energy impact on WFE system operations*. Journal article NREL/JA-500-39583, NREL National Renewable Energy Laboratory, 2006.

Wolfram, Catherine D. "Measuring Duopoly Power in the British Electricity Spot Market." *The American Economic Review*, 1999: 89(4) 805:826.

Woo, Chi-Keung, Rouslan I. Karimov, and Ira Horowitz. "Managing electricity procurement cost and risk by a local distribution company." *Energy Policy*, 2004: 32(5):635-645.

Woo, C-K, I., Horii B. Horowitz, and R.I. Karimov. "The efficient frontier for spot and forward purchases: an application to electricity ." *Journal of the Operational Research Society*, 2004: 55(11):1130-1136.

Wu, F. C., and Y. P. Tsang. "Second-order Monte Carlo uncertainty/variability analysis using correlated model parameters: Application to Salmonid embryo survival risk assessment." *Ecological Modelling*, 2004: 177: 393–414.